‘BLACK BOX’ MEETING AT SÁROSPATAK EDITORIAL PREFACE TO AM 2008/1

KATALIN T. BIRÓ

Hungarian National Museum, Budapest, Hungary
Email: tbk@ace.hu

KEYWORDS: ANCIENT CHARM PROJECT, NEUTRON BASED IMAGING ANALYSIS, EXPERIMENT

KULCSSZAVAK: ANCIENT CHARM PROGRAM, NEUTRON ALAPÚ KÉPALKOTÁSI TECHNIKÁK, KÍSÉRLETEK

Abstract

*In the framework of the Ancient Charm Project (*Analysis by Neutron resonant Capture Imaging and other Emerging Neutron Techniques: new Cultural Heritage and Archaeological Research Methods, http://ancient-charm.neutron-eu.net/ach), *imaging potentials of non-destructive neutron analytical methods are evaluated for archaeological applications. Prior to working on real archaeological specimens, so-called 'black boxes' were constructed (and characterised) for tests of the various methods. This issue of Archaeometry Workshop is dedicated to the study of these experimental test objects on the basis of a workshop held in November 2007 at Sárospatak.*

Kivonat

*Az Ancient Charm Program keretében (*Analysis by Neutron resonant Capture Imaging and other Emerging Neutron Techniques: new Cultural Heritage and Archaeological Research Methods, http://ancient-charm.neutron-eu.net/ach), *különféle neutron analitikai vizsgálatok képalkotási lehetőségeit vizsgáljuk a kulturális örökség körébe tartozó tárgyakon. Mielőtt a régészeti műtárgyakat vizsgálnánk, a különféle vizsgálatok lehetőségeinek felmérésére kísérleti tárgyakat, úgynevezett "fekete dobozokat" készítettünk, amelyeken a módszereket kipróbálhattuk. Az Archeometriai Műhely / Archaeometry Workshop jelen számát ezeknek a próbatestek a vizsgálatáról állítottuk össze, egy 2007. novemberében tartott kisebb konferencia (Sárospatak) anyagára alapozva.*

Introduction

Ancient Charm (Analysis by Neutron resonant Capture Imaging and other Emerging Neutron Techniques: new Cultural Heritage and Archaeological Research Methods) is a multi-national project launched among the EU-FP 6 NEST (New and Emerging Science and Technology) programmes. It addresses problems and challenges related to neutron-based imaging techniques and their possible use in the study of cultural heritage materials (Gorini 2007).

In order to present the aims of the projects precisely, let us quote from the project central webpage:

’The idea of developing an imaging technique based on epithermal neutron absorption is totally new and presents a number of scientific and technical challenges which are best addressed by the joint development of two related 3D imaging methods:

• Prompt Gamma Activation Imaging combined with cold Neutron Tomography (PGAI/NT) and

• Neutron Diffraction Tomography (NDT).

Developing the ‘Neutron Resonant Capture Imaging’ combined with ‘Neutron Resonance Transmission’ (NRCI/NRT) as a non-invasive technique for 3D tomographic imaging and its use in cultural heritage research is the ultimate aim of the ANCIENT CHARM project.

The three new imaging methods will provide a new, comprehensive neutron-based imaging approach, which will be applied here for the 3D imaging of elemental and phase composition of objects selected as a result of a broad scope archaeological research.’

Hungary is represented in this project by a team from the Hungarian National Museum, working in charge of WP-1 (‘*Cultural heritage foundations of neutron-based imaging*’), and a team from the Isotope Institute of the HAS working on PGAI and technical problems concerning measurements such as sample support construction.

Black boxes

Prior to the useful application of these leading edge technologies to archaeological objects, it seemed imperative to test potentials of the methods on objects of controlled geometries and materials, known to the constructors but unknown to the analysts.

Archaeologists taking part in the project planned a test series of possible complex materials likely to occur together in an archaeological context (Hajnal 2008). A series of 40*40*40 mm metal cubes were made, of iron plates (Hungarian boxes, Dúzs 2008) and another series of cubes, 50x50x50 mm large, made of aluminium sheets (German boxes, Kirfel 2008). The contents and the construction of these boxes were carefully documented, the raw materials used analysed by standard material testing procedures.

HU ISSN 1786-271X; urn:nbn:hu-4106

The boxes were sealed, and circulated among the Ancient Charm participants. A 3D coordinate system (x,y,z) was attached to the external parts of the cubes for clear orientation and reproducibility.

The analysts had no clue as to the contents of the closed boxed. However, the analysts could exchange information among themselves. For instance, neutron radiographies and X-ray radiographies were available at the time of the diffraction and PGAA measurements. The first time, the analysts had information on the actual planning, construction and the results of the other teams was at a small workshop held at Sárospatak, Hungary.

In this way we could test the potentials of the methodologies applied and define an optimal sequence of proper analysis for the archaeological objects to be analysed in the framework of the project.

The present issue of *Archeometriai Műhely / Archaeometry Workshop / Archaeometry Workshop* is dedicated to the results of this experimental work.

References

DÚZS K. (2008): Realisation of the planned 'Black Boxes' in the Hungarian National Museum. *Archeometriai Műhely / Archaeometry Workshop* **2008/1**. 7-20

FESTA et al. (2008): Festa, G., Kockelmann, W., Kirfel, A., Neutron Diffraction Analysis of 'Black Boxes'. *Archeometriai Műhely / Archaeometry Workshop* **2008/1** 61-72.

GORINI, G. and the Ancient Charm Collaboration (2007): Ancient Charm: A research project for neutron-based investigation of cultural-heritage objects. In: Mando et al. eds., Workshop on RICH 2005 IlNC. *Il Nuovo Cimento Bologna Societa Italiana di Fisica* **30/1** 47-58

HAJNAL Zs. (2008): Test objects for developing 3D material analysis on Cultural Heritage objects: Plans for the 'Black Boxes' to be analysed in the Ancient Charm Project. *Archeometriai Műhely / Archaeometry Workshop* **2008/1** 3-6

KASZTOVSZKY Zs. & BELGYA T. (2006): 'Non-Destructive Investigations of Cultural Heritage objects with Guided Neutrons: The Ancient Charm Collaboration', *Archeometriai Műhely / Archaeometry Workshop* **2006/1** 12-17

KIRFEL, A. (2008): Construction and description of the UNIBONN 'Black Boxes'. *Archeometriai Műhely / Archaeometry Workshop* **2008/1** 21-34.

KIS et al. (2008): Kis, Z., Belgya, T., Szentmiklósi, L., Kasztovszky, Zs., Kudejova, P. & Schulze, R., Prompt Gamma Activation Imaging on 'Black Boxes' in the 'Ancient Charm' Project. *Archeometriai Műhely / Archaeometry Workshop* **2008/1** 41-60.

KUDEJOVA, P. (2008): Neutron and X-Ray imaging of the 'Black Boxes' for the Ancient Charm project. *Archeometriai Műhely / Archaeometry Workshop* **2008/1** 35-40.

*

Sárospatak, Rákóczi Museum –of the HNM - http://www.spatak.hu/

HU ISSN 1786-271X; urn:nbn:hu-4106 © by the author(s)

DEVELOPING NON-DESTRUCTIVE 3D MATERIAL ANALYSIS OF CULTURAL HERITAGE OBJECTS: PLANS FOR 'BLACK BOXES' AS TEST OBJECTS TO BE ANALYSED IN THE ANCIENT CHARM PROJECT

ZSUZSANNA HAJNAL

Hungarian National Museum, Budapest, Hungary
Email: hajnal.zsuzsa@hnm.hu

Abstract

*In the framework of the Ancient Charm Project (*Analysis by Neutron resonant Capture Imaging and other Emerging Neutron Techniques: new Cultural Heritage and Archaeological Research Methods, http://ancient-charm.neutron-eu.net/ach), *imaging potentials of non-destructive neutron analytical methods are evaluated for archaeological applications. Prior to working on real archaeological specimens, so-called 'black boxes' were constructed (and characterised) for tests of the various methods. This paper is about the planning of the test boxes.*

Kivonat

*Az Ancient Charm Program keretében (*Analysis by Neutron resonant Capture Imaging and other Emerging Neutron Techniques: new Cultural Heritage and Archaeological Research Methods, http://ancient-charm.neutron-eu.net/ach), *különféle neutron analitikai vizsgálatok képalkotási lehetőségeit vizsgáljuk a kulturális örökség körébe tartozó tárgyakon. Mielőtt a régészeti műtárgyakat vizsgálnánk, a különféle vizsgálatok lehetőségeinek felmérésére kísérleti tárgyakat, úgynevezett "fekete dobozokat" készítettünk, amelyeken a módszereket kipróbálhattuk. Az alábbi cikk a próbatestek tervezéséről szól.*

KEYWORDS: NEUTRON BASED IMAGING ANALYSIS, EXPERIMENT PLANNING

KULCSSZAVAK: NEUTRON ALAPÚ KÉPALKOTÁSI TECHNIKÁK, KÍSÉRLETEK, TERVEZÉS

Purpose and aim of the constructions

In the framework of the Ancient Charm Project, several European research institutes cooperate in developing new non-destructive methods for 3-dimensional elemental composition and phase analyses (PGAI/NT and NRCI/NRT with NDT) to be applied on cultural heritage objects. In a first step of the collaboration of physicists and engineers, objects were needed that should be characterised by,

i) simple geometrical forms and

ii) simple elemental compositions in order to provide easily controllable situations fit to help with designing, setting up and exploring the new technologies.

The second step of work concerns testing the kind of archaeological and art objects that *in praxi* qualify for the new analyses. This means that it should at least be recognised to which extent the measurements require special care and how to conduct them without danger to the precious original objects. Besides studying these important questions it is also intended to test the kind of additional new data provided by the new methods as compared to conventional composition analyses.

In order to tackle these complex problems it was decided in the course of an early Ancient Charm project meeting (2006) to construct series of suitable calibration objects, so called 'black boxes'. This task was declared part of the work package responsible for the cultural heritage aspect.

Considerations in planning the constructions

The discussions about the 'black box' arrangements commenced with referring to a list of the most frequently encountered elements prepared by Tamás Belgya and Zsolt Kasztovszky. This table summarised detailed information about which elements are easily visible by means of gamma radiation spectroscopy and for thermal neutrons, how these elements affect the visibility of other sample components as well as to which sample thickness (in cm) measurements are feasible. The 'black box' elements were then chosen according to the Belgya & Kasztovszky absorption and scattering data and on their abundance in archaeological and art objects. 10-12 boxes were asked by the physicists and engineers. 2 or 3 of them should be open ones in order to improve and calibrate the respective methods. Another 8 or 9 pieces should be sealed for ensuing 'blind tests'.

HU ISSN 1786-271X; urn:nbn:hu-4106

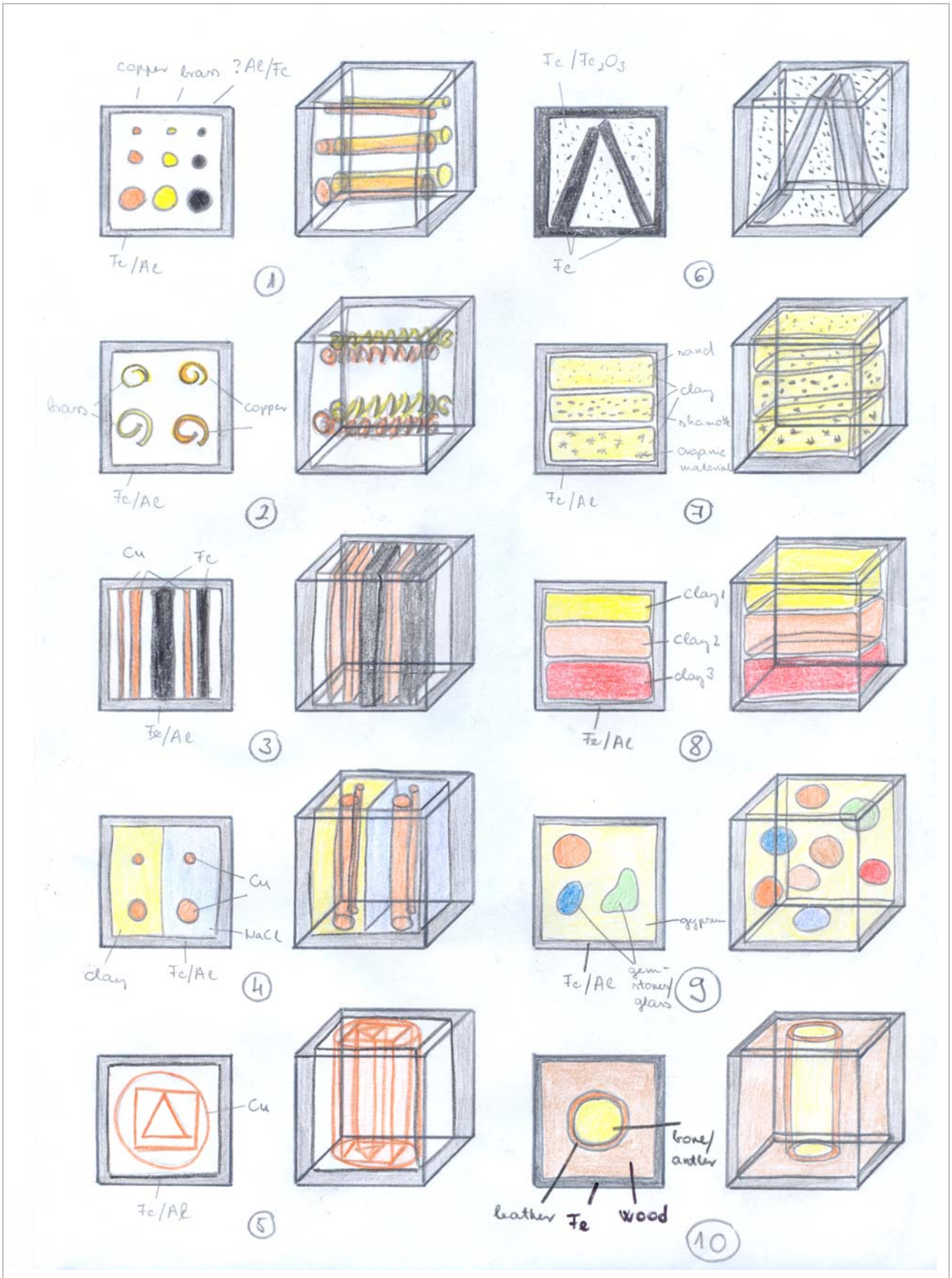

Fig.1. Plans for the test objects (‘black boxes’)

HU ISSN 1786-271X; urn:nbn:hu-4106

Since it was also decided to produce for the last phase of testing, elaborate and noble copies of the chosen historic objects, with elemental compositions similar to those of the originals, some boxes were already planned to offer the same difficulties that the future measurements on the original objects would probably hold.

Plans of the boxes

In the plans (**fig. 1.**), the boxes were designed as cubes with 40 – 50 mm edge length and about 1 mm wall thickness. Apart from these constraints, they were mostly defined in terms of general types, leaving some liberty of using available raw materials. The number of each box correlates roughly with the expected difficulties met in the characterisation of the box content with respect to element detection, material identification and spatial arrangement of the components. The first group of boxes (Nrs. 1-5.) contains simple elements and simple geometrical forms; the second group (Nrs. 6-10.) includes boxes approximating archaeological objects, i.e. boxes with more complex compositions and/or arrangements of more complex materials with different geometrical forms.

Individual descriptions of the planned boxes

Nr. 1.

Fe or Al plate box (bent, soldered or glued) with 2 sides remaining open. Inside: cylindrical rods of different diameter made of 2 or 3 different materials (like brass/copper or iron/copper, or bronze/copper).

Nr. 2.

Fe or Al plate closed box (bent, soldered or glued). Inside: 4 spirals made of cylindrical wires of 2 different materials (brass/copper or Fe/copper, or Fe/Al) and with different diameters.

Nr. 3.

Fe or Al plate box (bent, soldered or glued) with 2 sides remaining open. Inside: several parallel, but separate metal plates of different thickness made of 2 different metals (brass/Fe or Fe/copper, or Fe/Al).

As an additional or alternative box of this type a closed version was suggested with the rest volume filled with rock salt (NaCl) or sand (SiO_2). This was with the intention to see the difference between air and other materials that surround the objects, i.e. the effect on the clearness and/or resolution of the image.

Nr. 4.

Fe or Al plate closed box (bent, soldered or glued). Inside: 2 pairs of cylindrical metal rods of different diameter and made of 2 different metals (brass/Fe or Fe/copper, or Fe/Al). Each pair of rods occupies one half of the cube which is divided into two parts, one filled with salt, the other with sand or dry clay. Thus, Nr. 4 is a variant of box Nr. 1. allowing for assessing the effect of a solid rod environment on the imaging.

Nr. 5.

Fe or Al plate closed box (bent, soldered or glued). Inside: a concentric arrangement of 2 or 3 hollow objects with axial symmetry (cylinder, prisms with triangular and square cross sections) made from metal (copper, brass or Fe) plates. No filling material.

Nr. 6.

Fe or Al plate closed box (bent, soldered or glued). Inside: 2 rectangular iron plates forming a ’Λ’ with one cube face as basis. The rest volume is filled with iron rust (Fe-oxides) or iron powder. The intention of this design concerns the questions: can the metal bulk and rust be observed and distinguished, what is the effect of the weathering products on the core object image and can the new methods help with ’fresh’ archaeological objects and possibly support conservation?

Nr. 7.

Fe or Al plate closed box (bent, soldered or glued). Inside: 3 equally thick layers of burnt or dried clay containing different materials, traditional slimming materials: ground organic matter, ground chamotte and added minerals (sand and small stones) in order to test the possibility of distinguishing and identifying different ceramics and defining corresponding archaeological questions to be answered.

For the Hungarian National Museum realisation process discarded small original pieces of ancient ceramics could be used.

Nr. 8.

Fe or Al plate closed box (bent, soldered or glued). Inside: 3 or 4 layers of burned clay bricks of different mineral and chemical compositions taken from ancient ceramic waste of different origins and periods. As for box Nr. 7, it is aimed to study the methods with respect to ceramic findings, their analyses and definitions of related archaeological questions. Nr. 7 is for the small inclusions and

HU ISSN 1786-271X; urn:nbn:hu-4106 © by the author(s)

additional materials and Nr. 8 is for the original chemical and mineralogical composition of the clays.

Nr. 9.

Fe or Al plate closed box (bent, soldered or glued). Inside: embedded in a filling of gypsum or salt is a random arrangement of separated items like gemstones (large single crystals), coloured glass beads and metal pieces (silver, gold). Such arrangements concern the localisation, identification and characterisation of items buried in a difficult environment. Particularly interesting are the detection of single crystals (gemstone inlays) and the effects of silver and gold in the sample.

Nr. 10.

Fe or Al plate closed box (bent, soldered or glued). Inside: a solid wooden box with a cylindrical hole in the middle, which houses a bone/antler object (maybe wrapped in leather).

From the very beginning it was clear that PGAI is not well suited for the analysis of organic material because elemental compositions are difficult to determine and images of other than 'organic elements' are blurred. Neither suitable is NDT due to the amorphous nature of most of the sample, except remains of bio-mineralisation (bones, teeth etc). Nevertheless, since archaeologists have always questions about organic remains, the case should be tested.

Finally, it was also intended to have 2 or 3 boxes with guilt (silvered or tinned) walls in order to assess the effects of coating and the possibility of imaging thin layers.

Realisation

Based on the above box designs two series of boxes were manufactured, one with Al-walls by the Mineralogisch-Petrologisches Institut of the University of Bonn, the other with Fe-walls by the Hungarian National Museum in Budapest. The contents, exact structures and components of the closed and sealed boxes remained exclusively known to the producers until the research groups had declared their various experiments complete. Thus, investigating the cubes was under realistic circumstances, similar to those of non-destructively analysing a cultural heritage object of unknown composition and internal design.

Acknowledgement

Many thanks to Tamás Belgya and Zsolt Kasztovszky for their patient and clearly understandable explanation for archaeologists.

Reference

BELGYA, T. & KASZTOVSZKY, Zs. (2006): Half thickness for gamma radiation and for thermal neutrons in various materials. *Manuscript for Ancient Charm Kick-off meeting 20-21 January 2006, Abingdon.*

REALISATION OF THE PLANNED 'BLACK BOXES' IN THE HUNGARIAN NATIONAL MUSEUM

KRISZTINA DÚZS

Hungarian National Museum, Budapest, Hungary
Email: kriszta.duzs@ace.hu

Abstract

*In the framework of the Ancient Charm Project (*Analysis by Neutron resonant Capture Imaging and other Emerging Neutron Techniques: new Cultural Heritage and Archaeological Research Methods, http://ancient-charm.neutron-eu.net/ach), *imaging potentials of non-destructive neutron analytical methods are evaluated for archaeological applications. Prior to working on real archaeological specimens, so-called 'black boxes' were constructed (and characterised) for tests of the various methods. This paper is about the construction of these test boxes as realised by the team of the Hungarian National Museum.*

Kivonat

*Az Ancient Charm Program keretében (*Analysis by Neutron resonant Capture Imaging and other Emerging Neutron Techniques: new Cultural Heritage and Archaeological Research Methods, http://ancient-charm.neutron-eu.net/ach), *különféle neutron analitikai vizsgálatok képalkotási lehetőségeit vizsgáljuk a kulturális örökség körébe tartozó tárgyakon. Mielőtt a régészeti műtárgyakat vizsgálnánk, a különféle vizsgálatok lehetőségeinek felmérésére kísérleti tárgyakat, úgynevezett "fekete dobozokat" készítettünk, amelyeken a módszereket kipróbálhattuk. Az alábbi cikk a Magyar Nemzeti Múzeum restaurátor műhelyében készült próbatestek előállítását mutatja be.*

KEYWORDS: NEUTRON BASED IMAGING ANALYSIS, EXPERIMENTS

KULCSSZAVAK: NEUTRON ALAPÚ KÉPALKOTÁSI TECHNIKÁK, KÍSÉRLETEK

Introduction

In the framework of the Ancient Charm program, part of the responsibilities of the Hungarian National Museum was to prepare various test objects and copies (benchmark objects) before the specific methods covered by the project are to be applied on the archaeological specimens themselves. These test objects are important to learn about potentials of the various methods and find the 'best practice' solutions.

The 'black boxes'

Test objects of known geometry and contents were made after the plans of archaeologists (see Hajnal 2008, this volume). The task of constructing these 'black boxes' was shared between the Bonn University and the Hungarian National Museum (Kirfel 2008, volume). HNM produced boxes made of iron, 4 x 4 x 4 cm large. At BonnUni, 5 x 5 x 5 cm large aluminium boxes were made under the same principles and by the same basic ideas.

Planning the boxes was accomplished with an eye on existing archaeological situation foreseen, for example, in the case of composite objects like the round brooch from Kölked serving as an emblem for the Ancient Charm program (76.1.45, disc brooch with almandine inlays from Grave A 279) or belt-buckle from Környe (61.1.205, iron belt garniture with silver inlays, Grave 66), as well as other composite objects in the Archaeological Collections of the HNM. They may contain various metal components (iron, bronze, gold, silver, lead etc. …), ornamental stones, glass and a range of other materials as well.

In the conservator's workshops of the HNM, 9 different 'black boxes' were made, typically of raw materials generally used in our conservation practice. They were analysed, subsequently, by the Bonn University team: in the Appendix, the analytical results are presented directly after the data obtained from Armin Kirfel.

Box H-I.

In the first box, copper and brass rods of various diameter (d=2, 5 mm), copper wire (d=1, 2, 5 mm) as well as steel (1x36x10 mm) and zinc plates (0,75x36x5 mm) were placed (**Figs. 1**. and **2**). The individual items were fixed into a 2 mm thick cast layer of gypsum. The cover plate of the box was glued to the walls by two-component epoxy resin (Araldite).

Box H-II.

The second box was supplied with copper and brass spirals made of bent plate (**Fig. 3.**). They were also fixed to the bottom in a thin gypsum layer and closed by a cover plate glued to the walls, same as the previous box. (**Figs. 3.** and **4**).

HU ISSN 1786-271X; urn:nbn:hu-4106

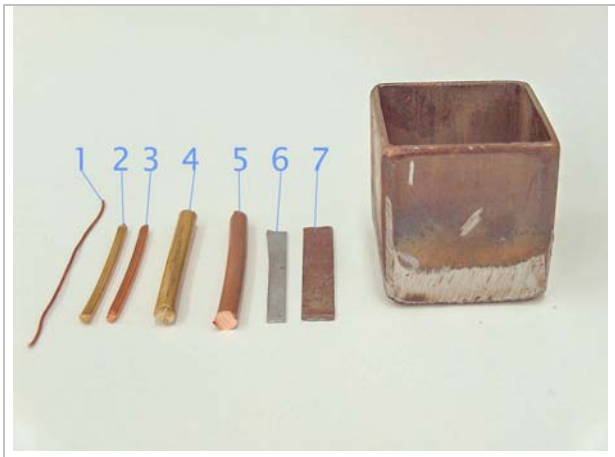

Fig. 1. Box H-I, contents

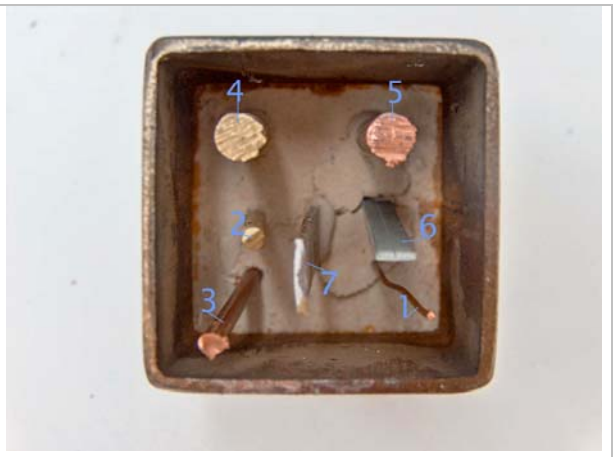

Fig. 2. Box H-I, mounted

Fig. 3. Box H-II, contents

Fig. 2. Box H-II, mounted

Fig. 5. Box H-III, contents

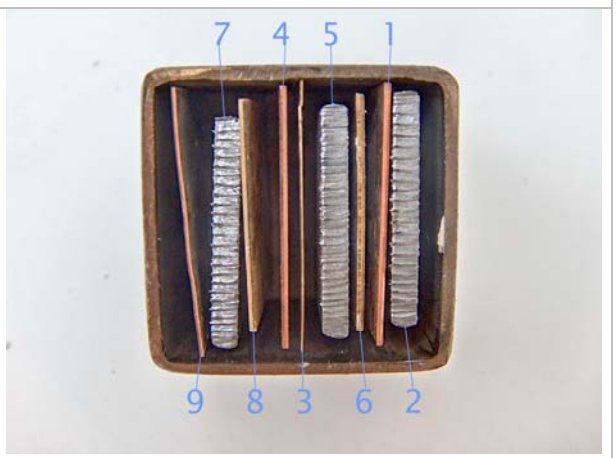

Fig. 6. Box H-III, mounted

Box H-III.

The third box was filled with metal plates of 3,8 x 3,8 cm size made of iron, steel, copper and brass. The thickness of the metal plates varies (see below). They were also fixed in a thin gypsum layer (~ 2 mm) and the cover plate glued on top (**Figs. 5.** and **6**).

1: copper plate width: 1 mm
2: iron plate width: 3 mm
3: brass plate width: 0,5 mm
4: copper plate width: 1 mm
5: iron plate width: 3 mm
6: brass plate width: 1 mm
7: iron plate width: 3 mm
8: brass plate width: 1 mm
9: copper plate width: 0,5 mm

HU ISSN 1786-271X; urn:nbn:hu-4106

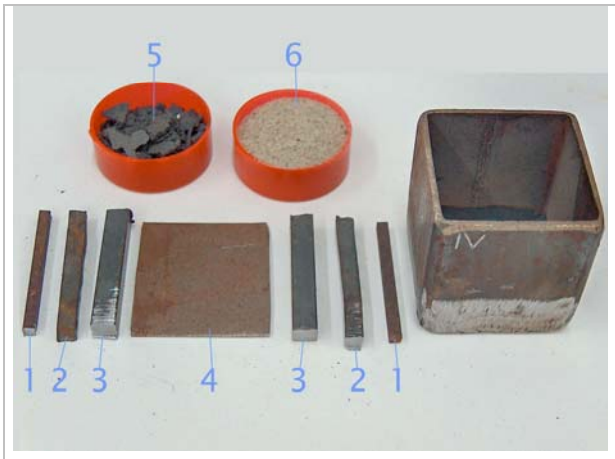

Fig. 7. Box H-IV, contents

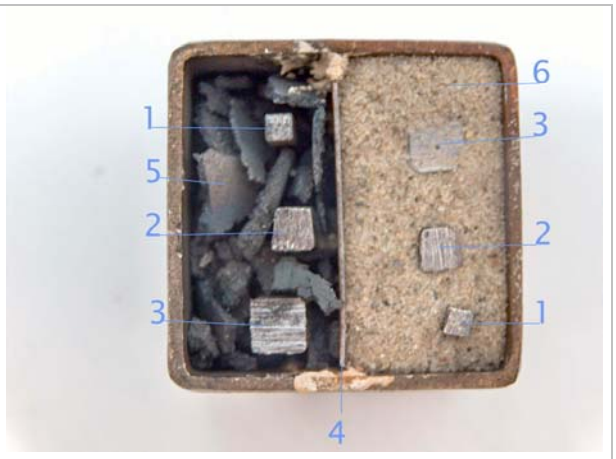

Fig. 8. Box H-IV, mounted

Fig. 9. Box H-V, contents

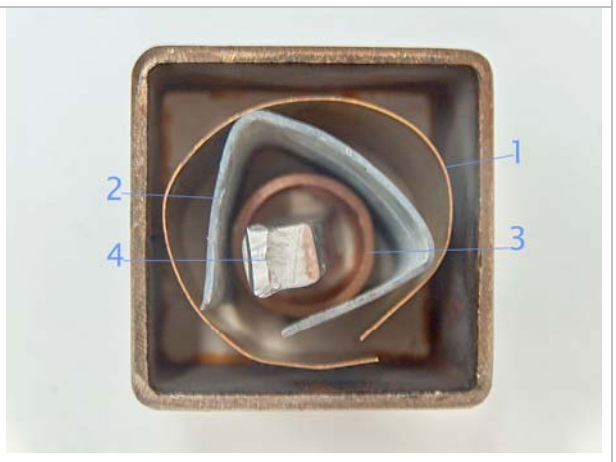

Fig. 10. Box H-V, mounted

Fig. 11. Box H-VI, contents

Fig. 12. Box H-VI, mounted

Box H-IV.

There were three steel rods of different cross-section (3, 4, 6 mm, respectively) placed inside the box. Two different filling materials were used to fill the whole volume separated by a thin steel plate. On one side we used discarded chips of hammered iron while on the other side fine-grained quartz sand was used. Before closing this box, an aluminium plate was glued under the cover to prevent the filling material from mixing and moving. (**Figs. 7.** and **8**).

Box H-V.

Use of various metals in one object is one of the aspects for neutron imaging. We tried to simulate this situation here. A cylinder shaped from brass

Fig. 13. Box H-VII, contents

plate, a triangle bent from lead sheet, a copper ring and a tin rod in the middle were placed into this box, fixed into a layer of gypsum. The box was sealed with an iron plate, glued to the side of the box. (**Figs. 9.** and **10**).

1: brass plate width: 0,5 mm
2: lead plate width: 1 mm
3: copper ring width: 2 mm
4: soldering tin width: 8 mm, h=8 mm, m=36 mm

Box H-VI.

Box VI contained materials that are frequently met on the surface of weathered objects. The internal parts were divided into four, roughly equal parts.

Fig. 14. Box H-VIII, contents

Fig. 15. Box H-VIII, mounted

Fig. 16. Box H-IX, contents

Fig. 17. Box H-IX, mounted

The first quarter contained fine-grained quartz sand, the second iron scraps, the third rock salt ($NaCl_2$) and the last one contained silver scraps hidden in ground talcum powder (**Figs. 11.** and **12**.).

Box H-VII

We were interested in testing the methodology, apart from metals, for objects made of ceramics as well. We have made two boxes using discarded

pieces of archaeological pottery with various temper and burnt on different temperatures. They were mixed in natural, unburned clay. (**Fig. 13.**).

Box H-VIII.

In Box Nr. H-VIII, archaeological pottery fragments were placed cast in gypsum (**Figs. 14.** and **15**).

Box H-IX.

Precious and ornamental stones frequently occur in composite archaeological objects. The last box, consequently, contained various minerals and ornamental stones, embedded into gypsum (**Figs. 16.** and **17**) .

1: agate
2: agate
3: amethyst
4: cornean
5: blue glass
6: cornean
7: agate ball
8: turquoise
9: pyrite crystal
10: gypsum crystal
11: silver

The different raw materials used for the production of the boxes were sent to Bonn University where our colleagues could perform the same analyses on them as reported by Kirfel on UniBonn boxes. They are presented here as an (appendix App.Figs 1-19.)

Acknowledgements

The author and the HNM team is grateful for analytical results provided on the black box construction materials for A. Kirfel and Bonn University.

References

HAJNAL Zs. (2008): Developing non-destructive 3D material analysis of cultural heritage objects: plans for 'black boxes' as test objects to be analysed in the Ancient Charm project. *Archeometriai Műhely / Archaeometry Workshop*, **2008/1** 3-6.

KIRFEL A. (2008): Construction and description of the UniBonn black boxes. *Archeometriai Műhely / Archaeometry Workshop* **2008/1** 21-34.

Ancient Charm object database, http://www.ace.hu/acharmdb/index.html

Appendix: X-ray Powder Diffraction Analyses of HNM 'Black Box' materials

Materials used for the production of the 'black boxes' at HNM. Analyses made at Bonn University by A. Kirfel and B. Barbier.

All measurements were carried out on a SIEMENS D5000 powder diffractometer using Cu-Kα radiation and secondary monochromator. Cleaning of surfaces with fine emery paper. Qualitative analyses, where necessary, by Rietveld fitting.

App.Fig. 1.

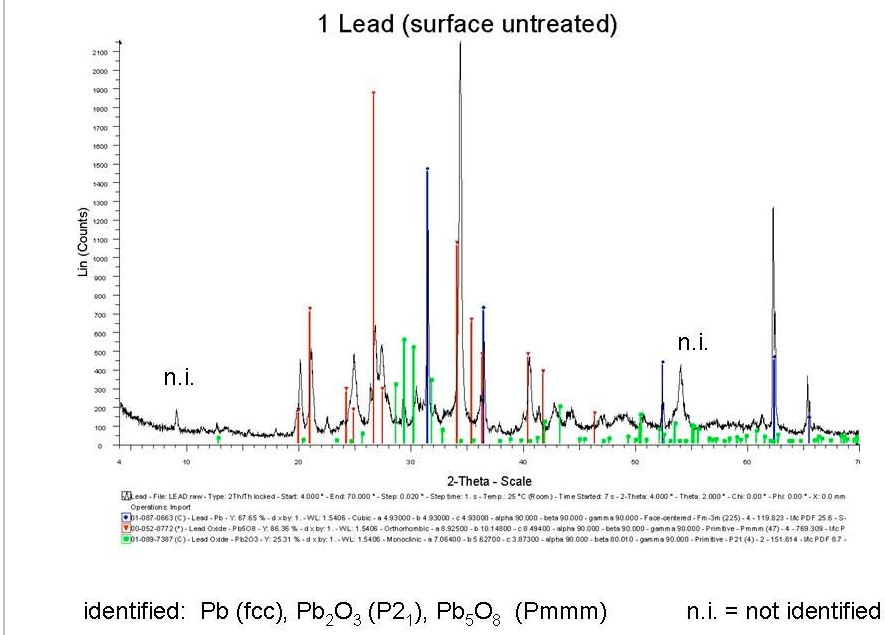

App.Fig. 2.	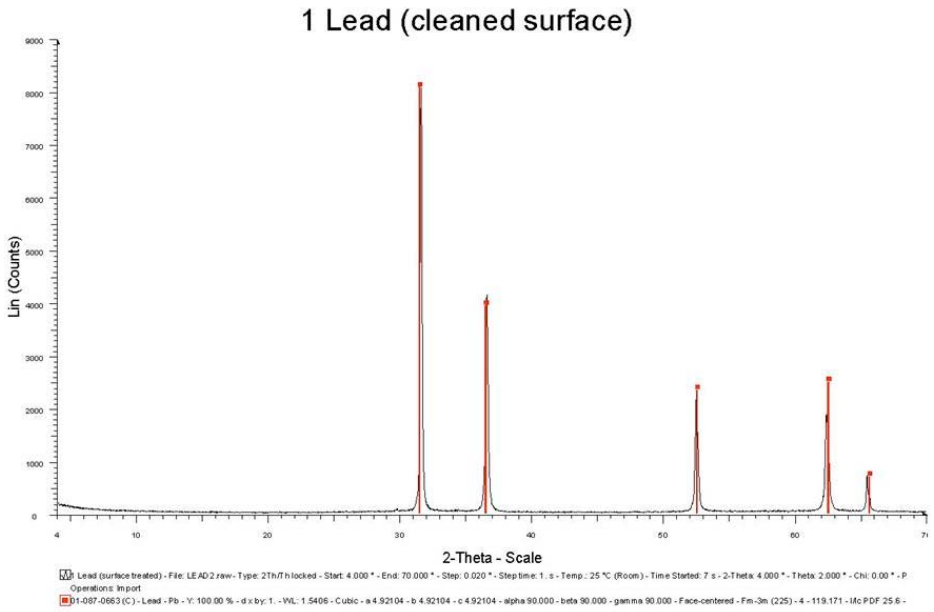 Identified: pure Pb (fcc)
App.Fig. 3.	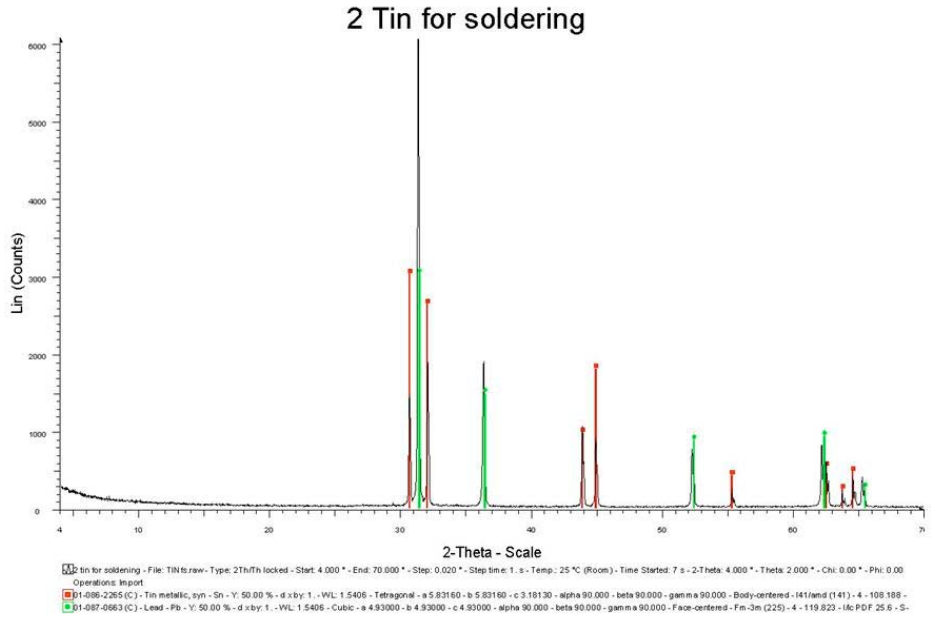 identified: Sn (red) ($I4_1/amd$), Pb (green) (fcc)

App.Fig. 4.

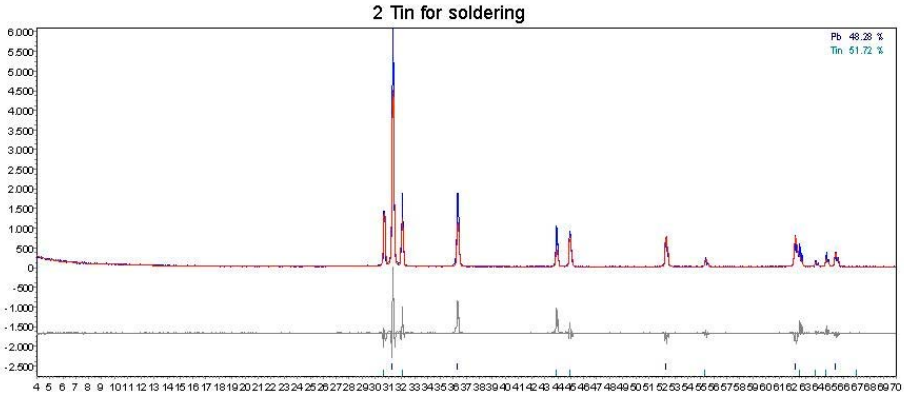

Rietveld refined: Sn (red) 52 %, Pb (green) 48 %

App.Fig. 5.

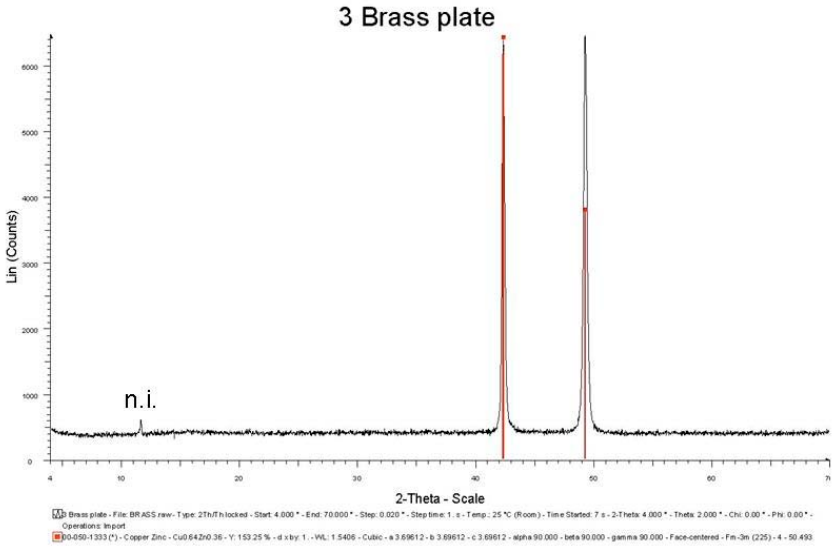

identified: Cu64Zn36 (fcc) n.i. = not identified

App.Fig. 6.

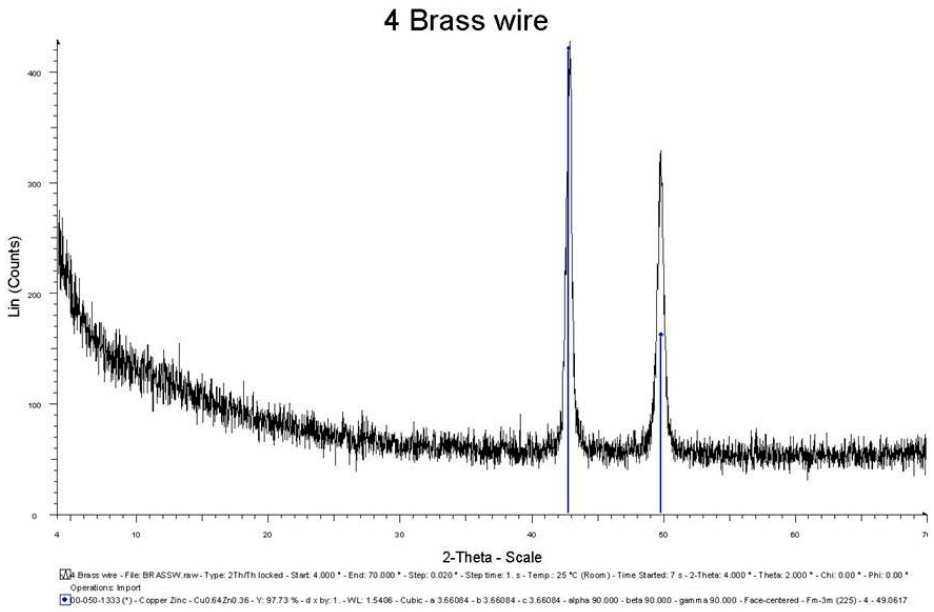

identified: Cu64Zn36 (fcc)

App.Fig. 7.

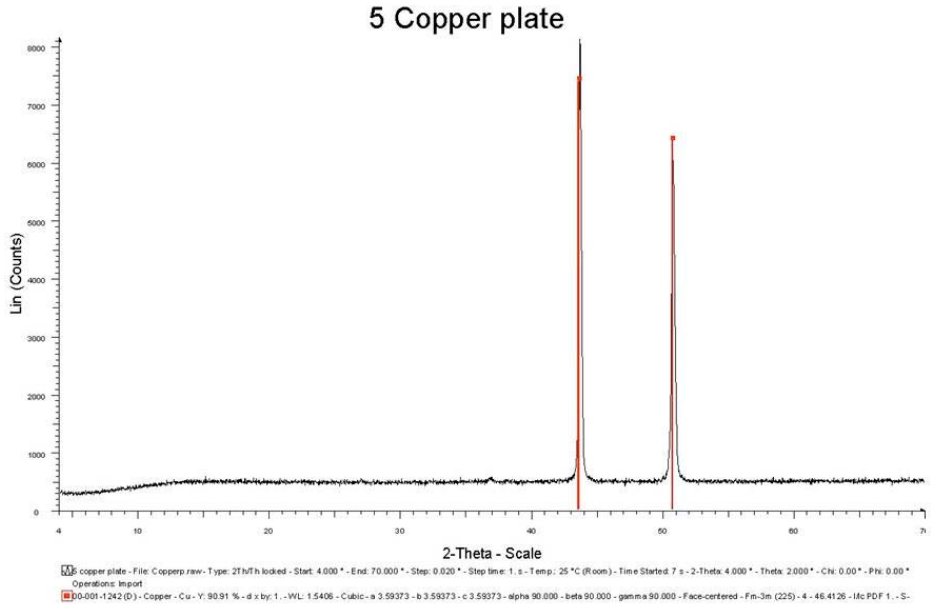

identified: pure Cu (fcc)

App.Fig. 8.

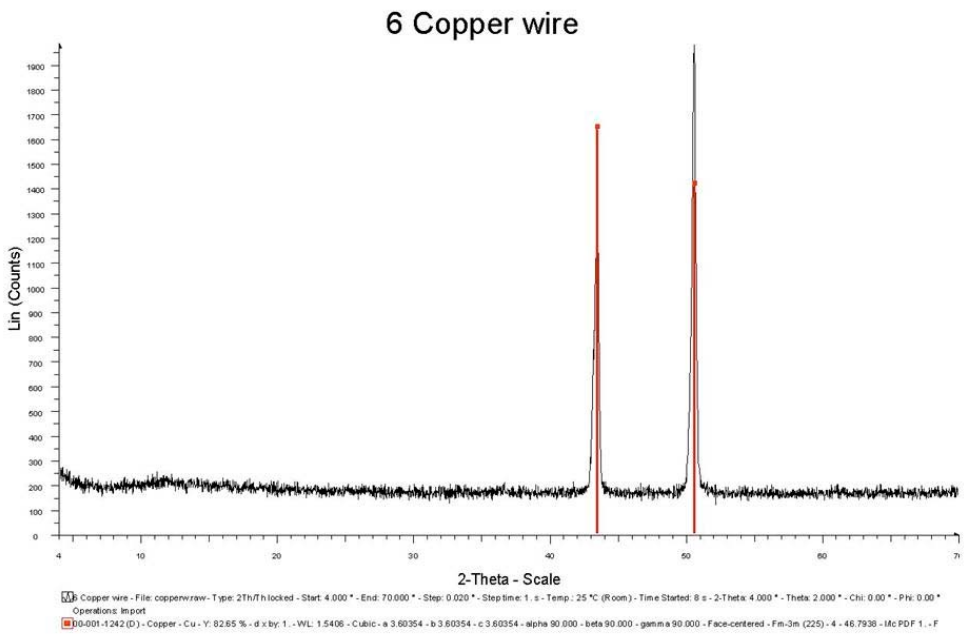

identified: pure Cu (fcc)

App.Fig. 9.

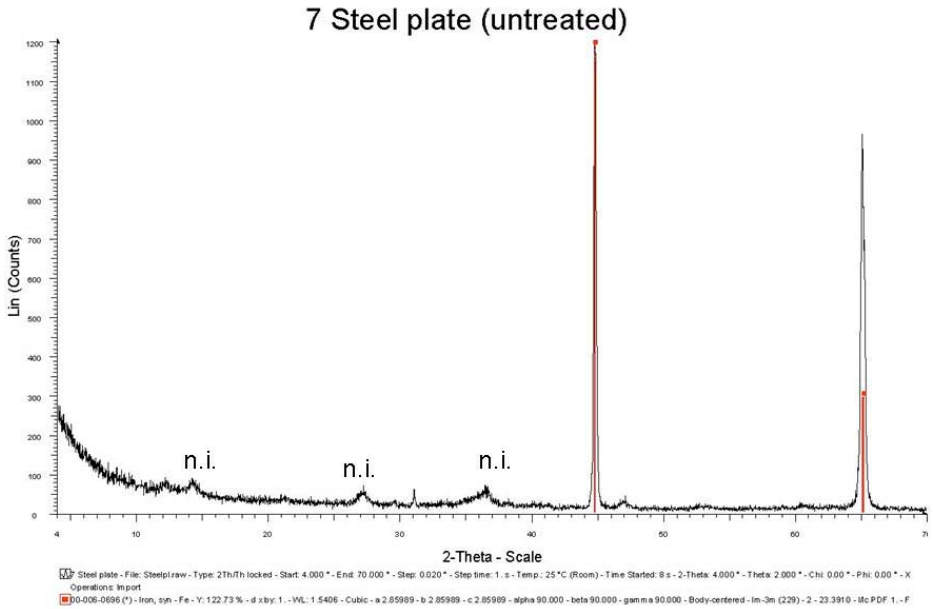

identified: Fe (bcc) n.i. = not identified

App.Fig. 10.

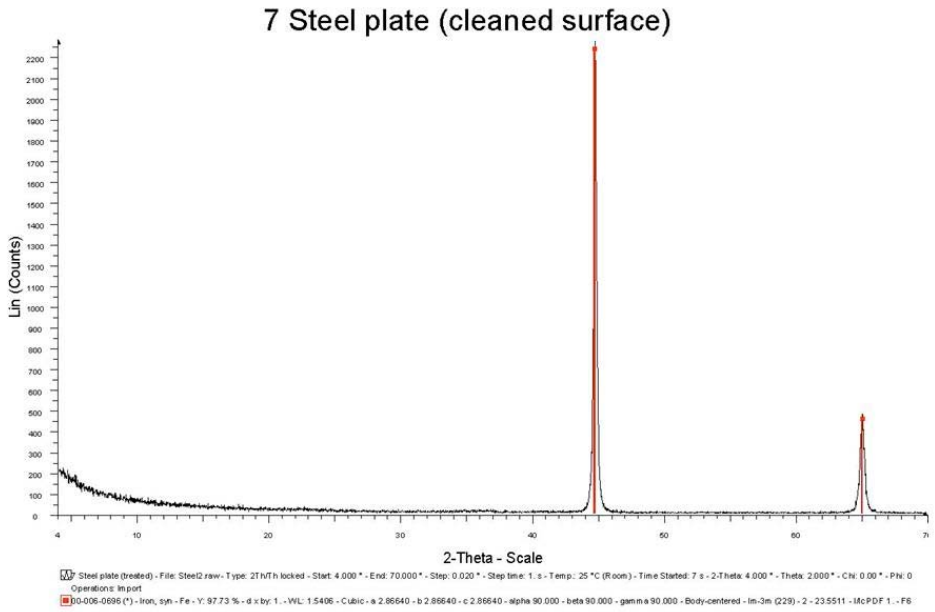

identified: Fe (bcc)

App.Fig. 11.

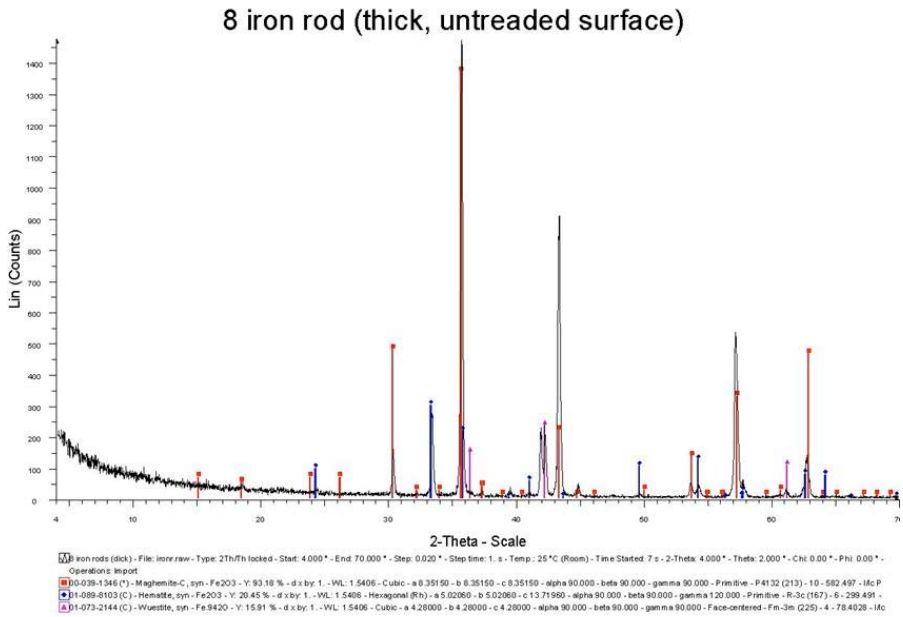

identified: maghemite, hematite, wüstite ?

App.Fig. 12.

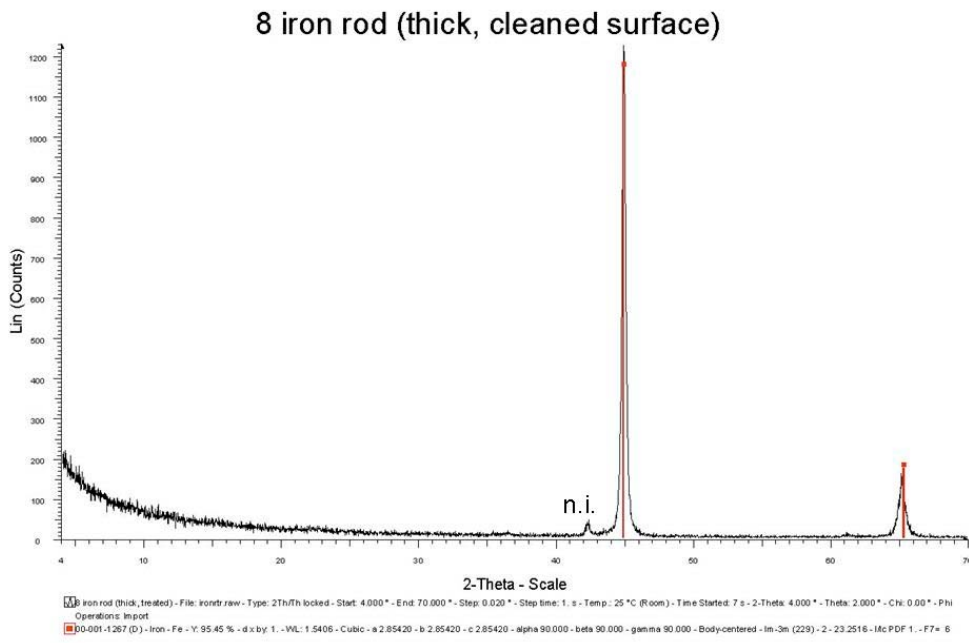

identified: Fe (bcc) n.i. = not identified

App.Fig. 13.

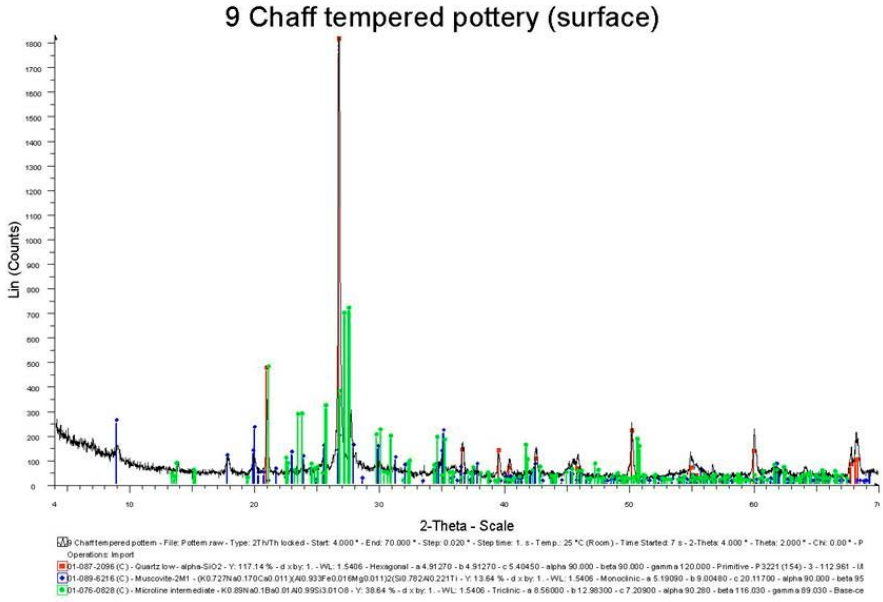

identified: quartz, muscovite-2M1, microcline ?

App.Fig. 14.

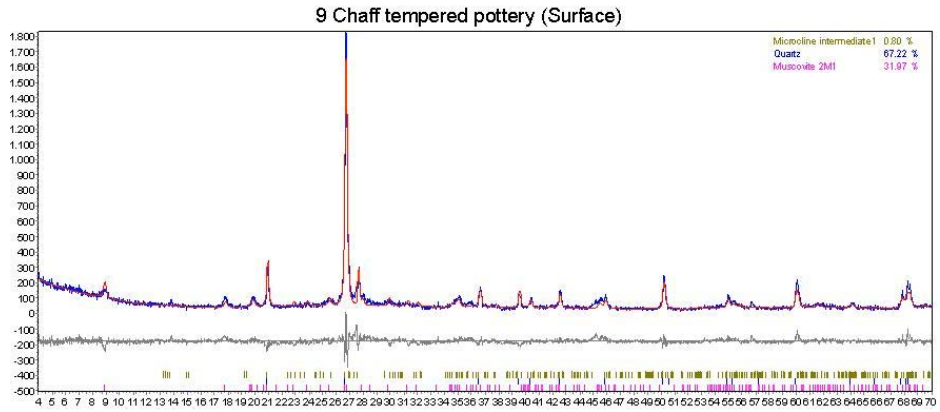

quartz 67 %, muscovite-2M1 32 %, microcline 1 % ?

muscovite-2M1: contains K, Na, Al, Si, O and traces of Ca, Mg, Ti, Fe,

App.Fig. 15.

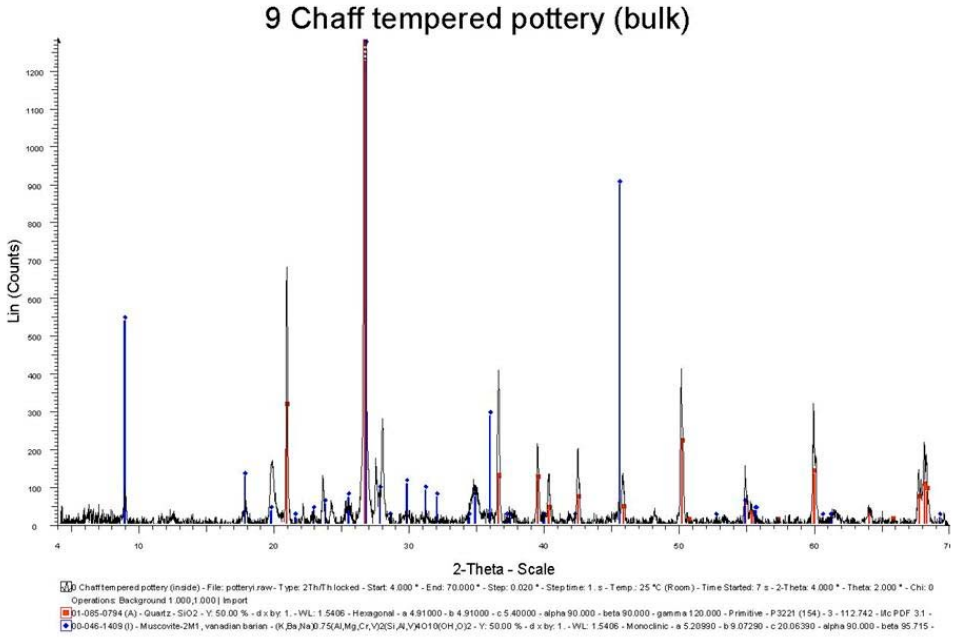

identified: quartz, muscovite-2M1, albite ?

App.Fig. 16.

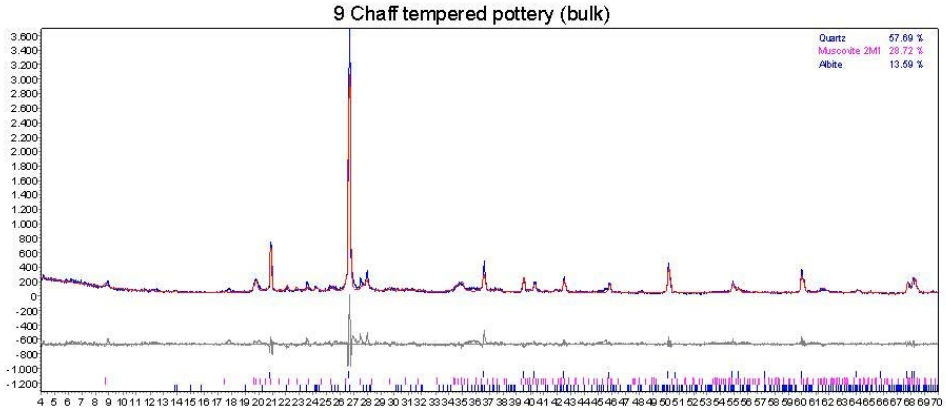

quartz 58 %, muscovite-2M1 29 %, albite 13 %

App.Fig. 17.

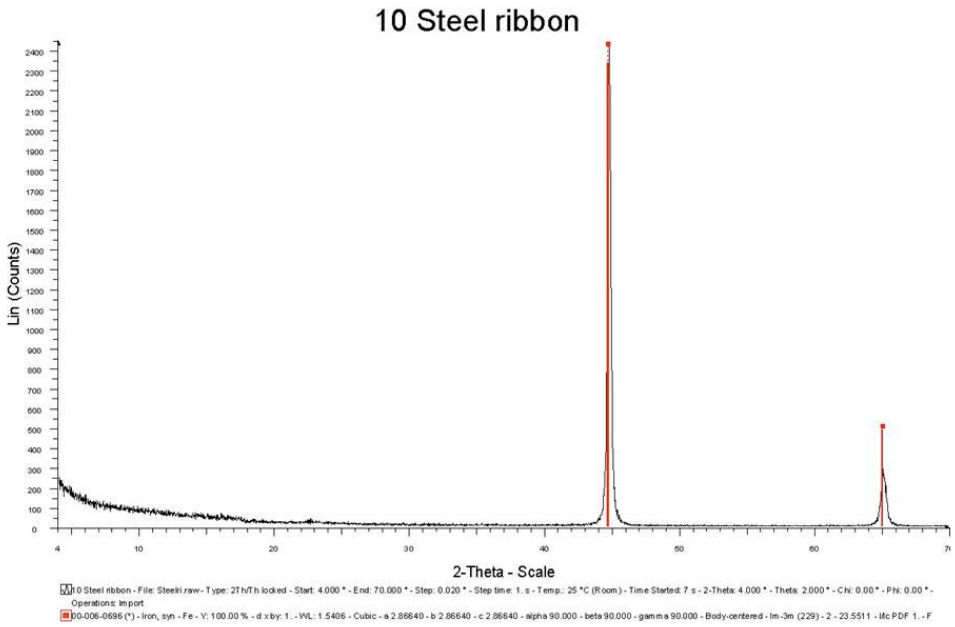

identified: Fe (bcc)

App.Fig. 18.

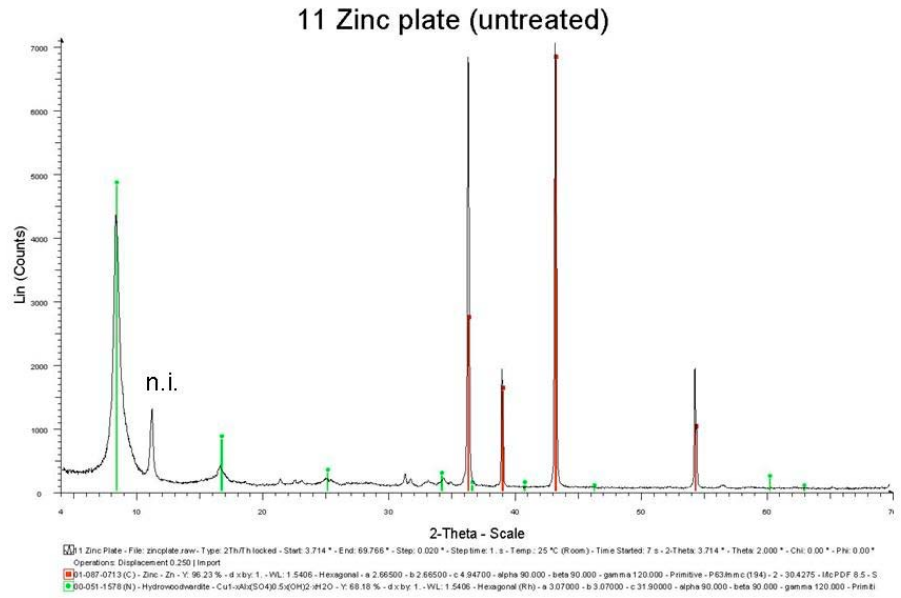

identified: Zn ($P6_3/mmc$) n.i. = not identified

hydrowoodwardite $Cu_{1-x}Al_x(SO4)_{0.5x}(OH)_{2x}H_2O$??

App.Fig. 19.

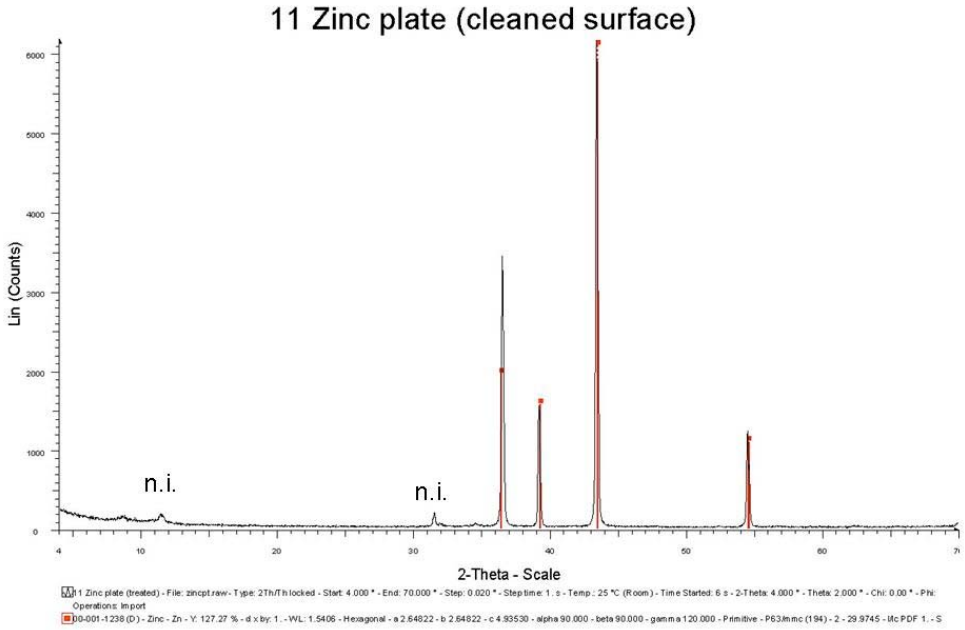

identified: Zn ($P6_3/mmc$) n.i. = not identified

CONSTRUCTION AND DESCRIPTION OF THE UNIBONN BLACK BOXES

ARMIN KIRFEL

Mineralogisch-Petrologisches Institut, Universität Bonn, Poppelsdorfer Schloss, D-53113 Bonn, Germany
Email: kirfel@uni-bonn.de

Abstract

*In the framework of the Ancient Charm Project (*Analysis by Neutron resonant Capture Imaging and other Emerging Neutron Techniques: new Cultural Heritage and Archaeological Research Methods, http://ancient-charm.neutron-eu.net/ach), *imaging potentials of non-destructive neutron analytical methods are evaluated for archaeological applications. Prior to working on real archaeological specimens, so-called 'black boxes' were constructed (and characterised) for tests of the various methods. This paper is about the construction of these test boxes as realised by the Bonn University team.*

Kivonat

*Az Ancient Charm Program keretében (*Analysis by Neutron resonant Capture Imaging and other Emerging Neutron Techniques: new Cultural Heritage and Archaeological Research Methods, http://ancient-charm.neutron-eu.net/ach), *különféle neutron analitikai vizsgálatok képalkotási lehetőségeit vizsgáljuk a kulturális örökség körébe tartozó tárgyakon. Mielőtt a régészeti műtárgyakat vizsgálnánk, a különféle vizsgálatok lehetőségeinek felmérésére kísérleti tárgyakat, úgynevezett "fekete dobozokat" készítettünk, amelyeken a módszereket kipróbálhattuk. Az alábbi cikk a Bonni Egyetemen készült próbatestek előállítását mutatja be.*

KEYWORDS: NEUTRON BASED IMAGING ANALYSIS, EXPERIMENTS

KULCSSZAVAK: NEUTRON ALAPÚ KÉPALKOTÁSI TECHNIKÁK, KÍSÉRLETEK

Introduction

According to the intense discussions in WP1, particularly with HNM, UNIBONN designed and manufactured 12 boxes, 11 of them filled with various items composed of materials of potentially archaeological relevance or else suited to assess the individual strengths of the different probe methods. The 11th box was empty in order to serve for calibration(s) and/or assessment of the wall materials contribution.

- all boxes were cubes of dimensions 50 x 50 x 50 mm^3 made of Al-sheets of 1 mm thickness.
- each box carries its own (engraved) coordinate system with axes directions x, y, z for unique and reproducible orientations with respect to local primary beams and experimental setups
- except for the open boxes I and III, all other boxes were sealed. Their contents were defined, analysed and documented by UNIBONN and only disclosed to HNM.

The envisaged hard X-ray tomography and neutron experiments to be carried out on selected (if not all) boxes were expected to reveal the strengths and potentials as well as the weaknesses or shortcomings of the different analytical methods and thus help to set up a sequence of analytical steps that is fit to yield maximum information with respect to the elemental and phase compositions as well as the geometrical arrangements of the sample materials within shortest possible time.

Box D-I

This box featured open (001) faces. It housed 3 rows of rods with different diameters (3, 6, 10 mm) made of 3 different materials : Cu, brass, Fe (steel). All rods were parallel x. The sequence of the materials was iron, brass, copper with respect to the y-direction (**Fig. 1**). The rods (as the sheets contained in the below following box D-III) were machined from the same pieces of bulk materials.

Fig. 1. - View of box D-I

HU ISSN 1786-271X; urn:nbn:hu-4106

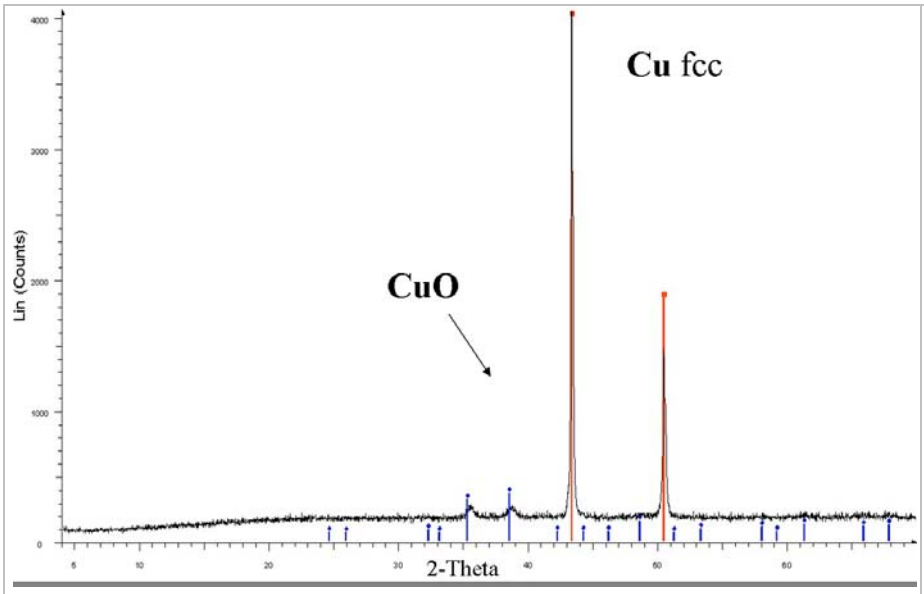

Fig. 2.

Diffraction pattern of Cu-rod

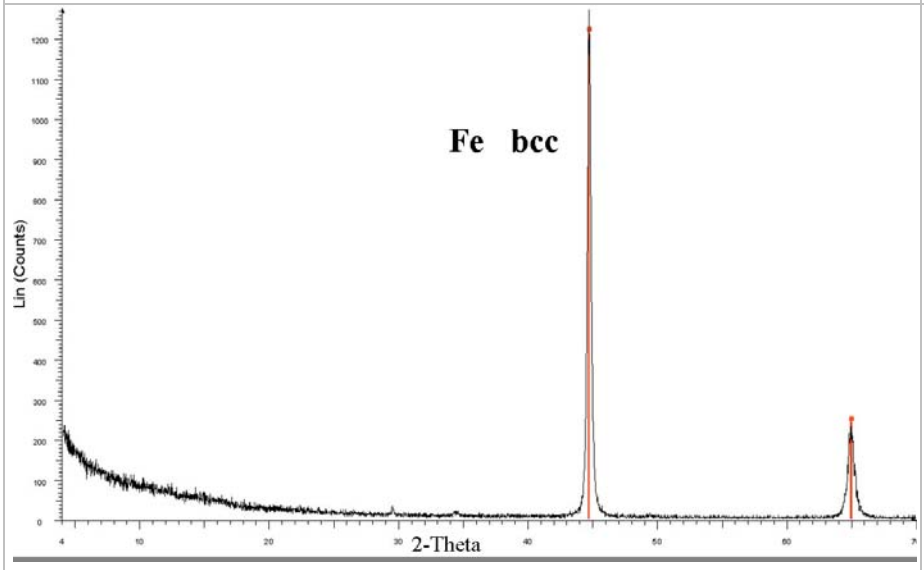

Fig. 3.

Diffraction pattern of steel rod

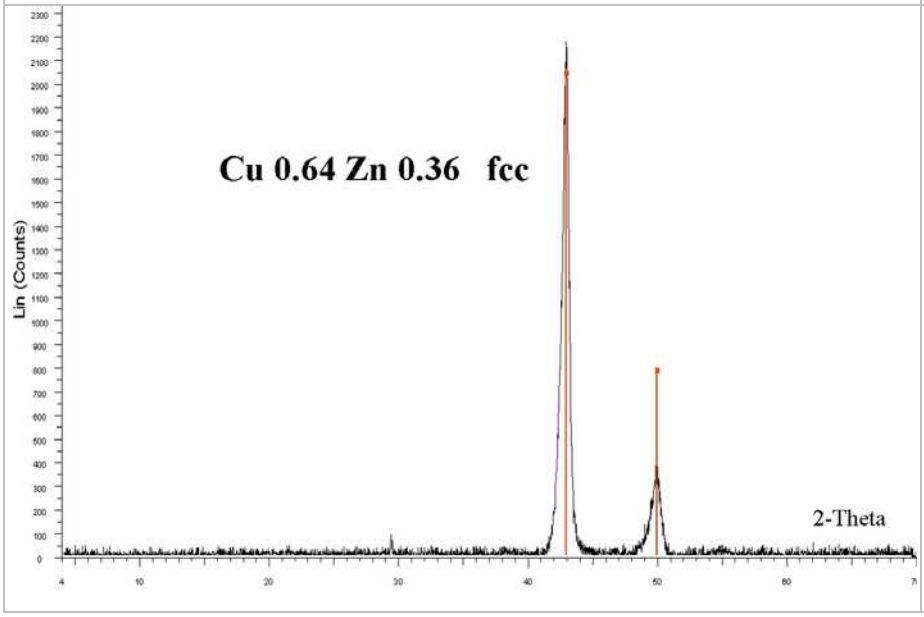

Fig. 4.

Diffraction pattern of brass rod

X-ray powder diffraction (Cu-Kα radiation) performed on these materials revealed:

1) pure Cu (fcc structure, a = 3.615 Å) along with an almost negligible amount of the oxidation product CuO (**Fig. 2**).

2) pure Fe with cubic bcc-structure (a = 2.866 Å, **Fig. 3**), and

3) brass (cubic fcc-structure) of composition Cu0.64Zn0.36 (a = 3.647 Å) along with a tiny contamination by hexagonal Pb (**Fig. 4**).

Comments :

This open box was designed mainly for calibration and exercising purposes so that X-ray or neutron tomography was neither needed nor (to my knowledge) done.

Box D-II

Contained two pairs of equally dimensioned and parallel oriented spirals made of 2 mm thick copper and brass wires, respectively. The helix axes of the spirals were along the x-direction. In z-direction, the sequence of the spiral pair materials was Cu, brass (**Fig. 5**). There was no filling material in the box.

According to X-ray powder diffraction experiments (Cu-Kα radiation) carried out on pieces of the two wire materials the copper wire turned out as pure Cu (**Fig. 6**) whereas the brass wire diffraction pattern indicated Cu0.64Zn0.36 crystallising in the cubic fcc-structure (a = 3.647 Å, **Fig. 7a**). Later, a part of the brass wire piece was ground in order to obtain a sample from the wire's interior. Its diffraction pattern (**Fig. 7b**) clearly showed a second phase of cubic symmetry, a = 2.85 Å in presence of Cu0.64Zn0.36.

This latter phase is most likely beta-brass (CuZn, Pn-3m, a = 2.95 Å) with Cu:Zn exceeding 1.

Comments:

It should be noted that in the laboratory diffraction analyses of the wire materials, due to absorption the Cu-radiation probed only the surfaces of the wire pieces. Differences between X-ray and neutron diffraction findings can therefore be caused by the much higher penetration of neutrons. Thus, the later reported neutron finding of a second brass phase in the brass spiral is not necessarily at variance with the X-ray result. It simply implies that the interior of the brass wire may differ from the surface region, as proved by the second diffraction analysis. This result presents a good example for the importance of bulk material analysis by neutrons because it non-destructively revealed the inhomogeneous nature of the brass wire.

For whatever reasons, the box coordinate system used in the tomographic X-ray experiment differs from that given on the box itself: $x_{tomo} = - z_{true}$; $y_{tomo} = - x_{true}$; $z_{tomo} = y_{true}$

Box D-III

As D-I box D-III featured open (001)- faces. **Fig. 8** shows the arrangement of parallel Cu- and iron-sheets of different thickness, all oriented perpendicular to x. The sheet sequence with respect to x was Cu 1 mm, Cu 3 mm, Fe 8 mm, Cu 4 mm, Fe 4 mm. All spacings between the sheets were 4.66 mm. This design was chosen in order to enable tests of the spatial resolution potentials of the different methods.

Comments:

The copper and iron material was the same as used for box D-I.

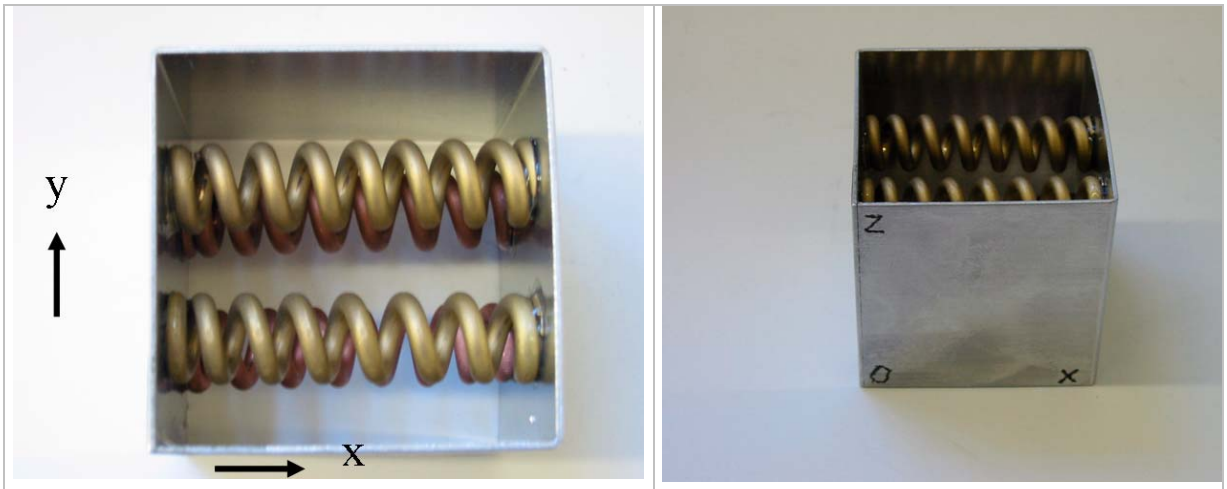

Fig. 5. - views of box D-II

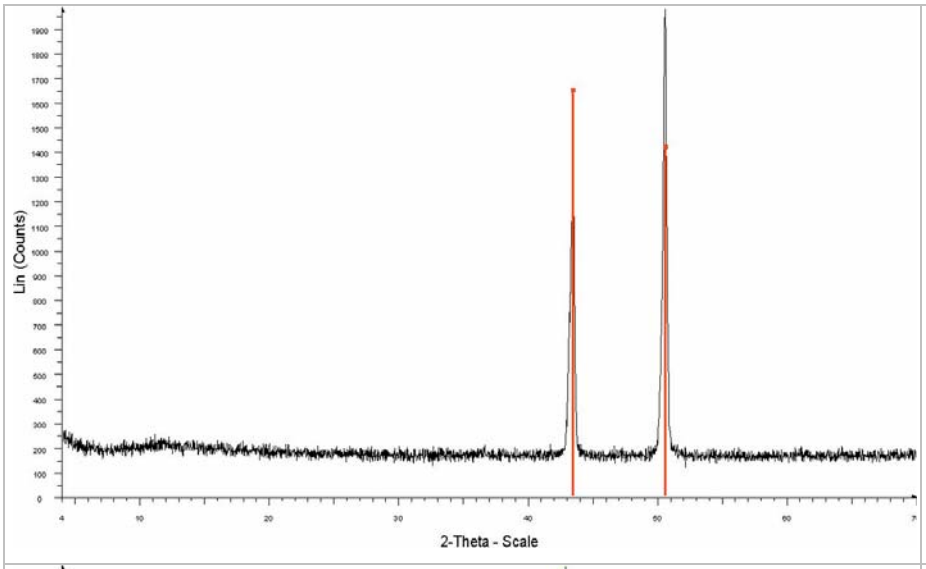

Fig. 6.

Diffraction pattern of Cu-wire

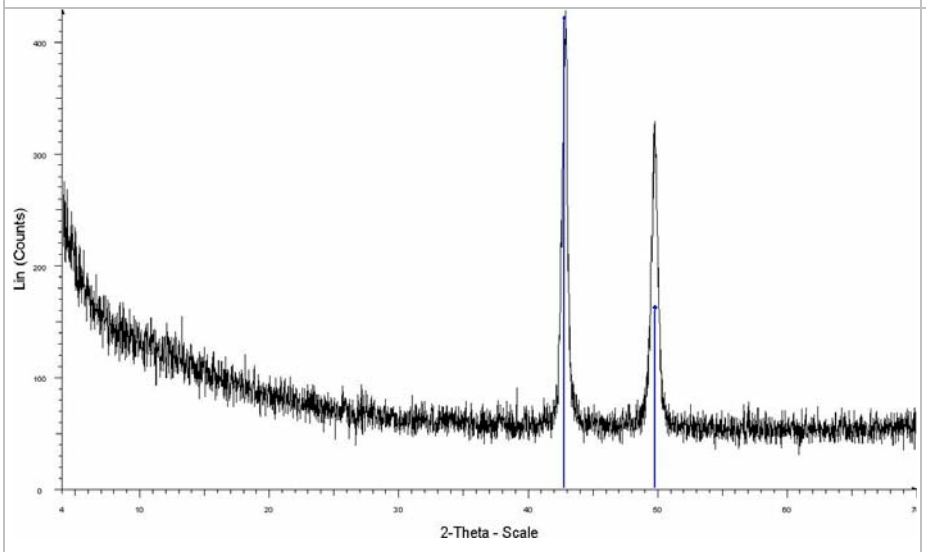

Fig. 7a.

Diffraction pattern of brass wire (surface region)

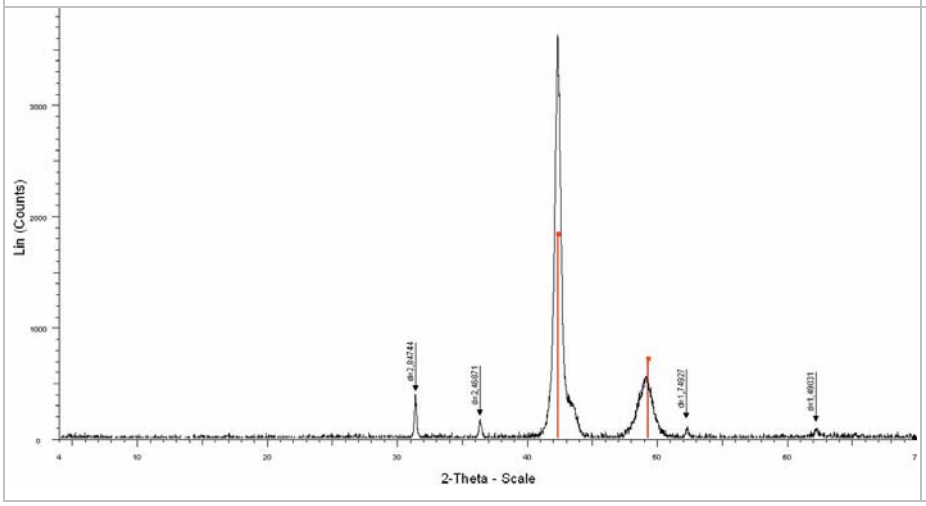

Fig. 7b.

Diffraction pattern of brass wire (bulk)

Box D-IV

Box D-IV (**Fig. 9**) contained a 1 mm thick Al-wall perpendicular to the x-direction creating two chambers of equal size. Each chamber housed two metal rods mounted parallel z and with diameters of 6 mm (low y) and 10 mm (high y), respectively. The rod material at low x was Cu, that at high x iron, both the same as used for D-I and D-III.

The Cu-rods were completely embedded in rocksalt (halite, NaCl), the steel rods in clay purchased in a hobby market. Both filling materials were analysed

HU ISSN 1786-271X; urn:nbn:hu-4106

by X-ray powder diffraction (Cu-Kα radiation): rocksalt was found as pure NaCl (**Fig. 10**). The clay pattern (**Fig. 11**) showed a mineral mixture which according to quantitative Rietveld analysis consisted of 51 % calcite, $CaCO_3$, 20 % quartz, SiO_2, 12 % muscovite 2M1, $KAl_2(AlSi_3O_{10})(OH)_2$ and 17 % kaolinite, $Al_4(OH)_8(Si_4O_{10})$.

Comments:

Due to the complicated mixture of low symmetry structures the clay material presents a challenge to ND considering phase identification and abundance determination. Also, the box presents a great variety of elements to PGAA: Cu, Fe, Na, Cl, Ca, Si, Al, Mg, O, C. Thus, it is particularly interesting to explore the degree to which elemental analysis can help with the characterisation of the clay material.

Box D-V

Box D-V contained no filling material. The hidden items (**Fig. 12**) were 3 concentric Cu-tubes of 48 mm length oriented along the z-direction. The first tube with circular cross section had a diameter of 40 mm and a wall thickness of 1.2 mm. This tube contained a second tube with a square cross section, edge lengths of 23 mm, a wall thickness of 1.4 mm and the faces parallel to x and y. The third tube inside the second possessed a regular triangular cross section with edge length of 15 mm and wall

Fig. 8. - Views of box D-III

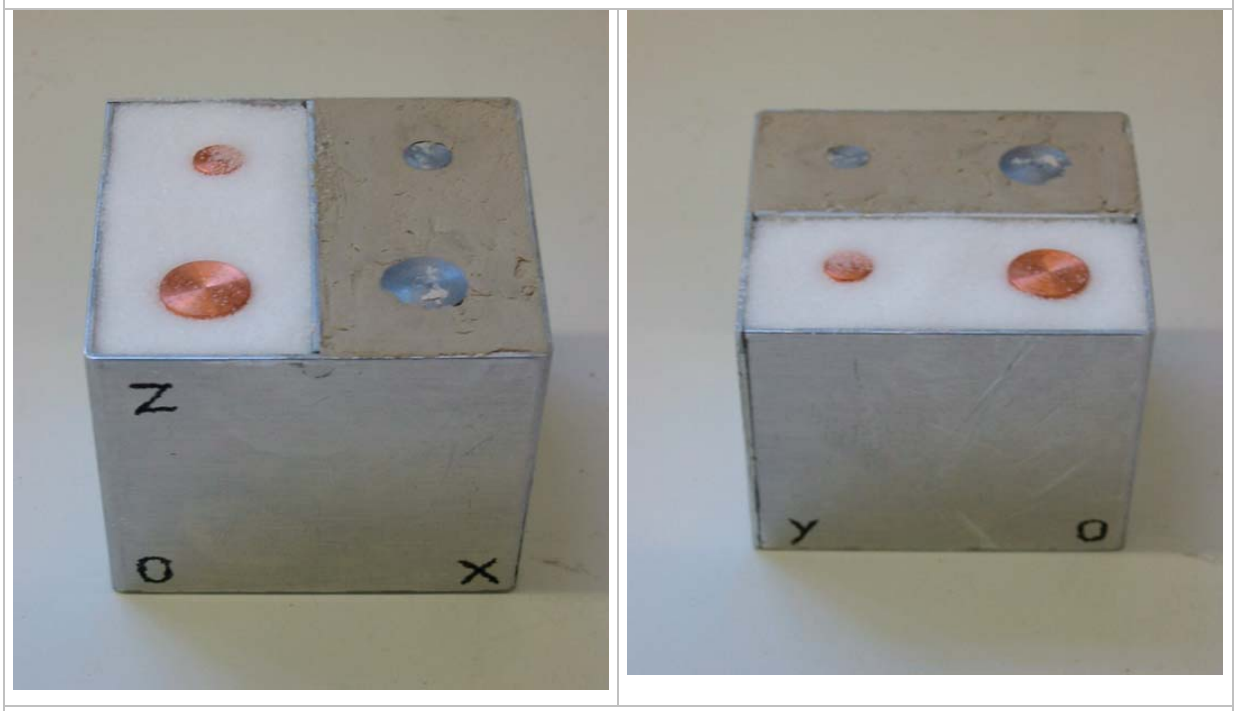

Fig. 9. - Views of box D-IV

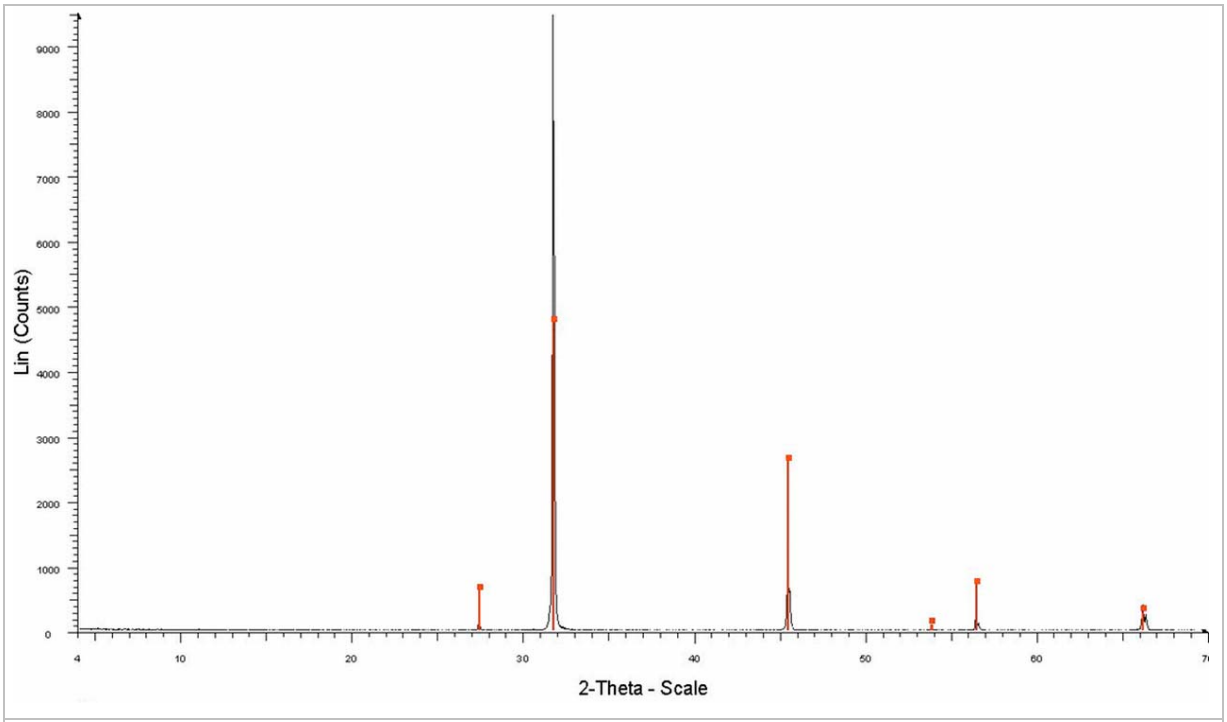

Fig. 10. - Diffraction pattern of cubic rocksalt

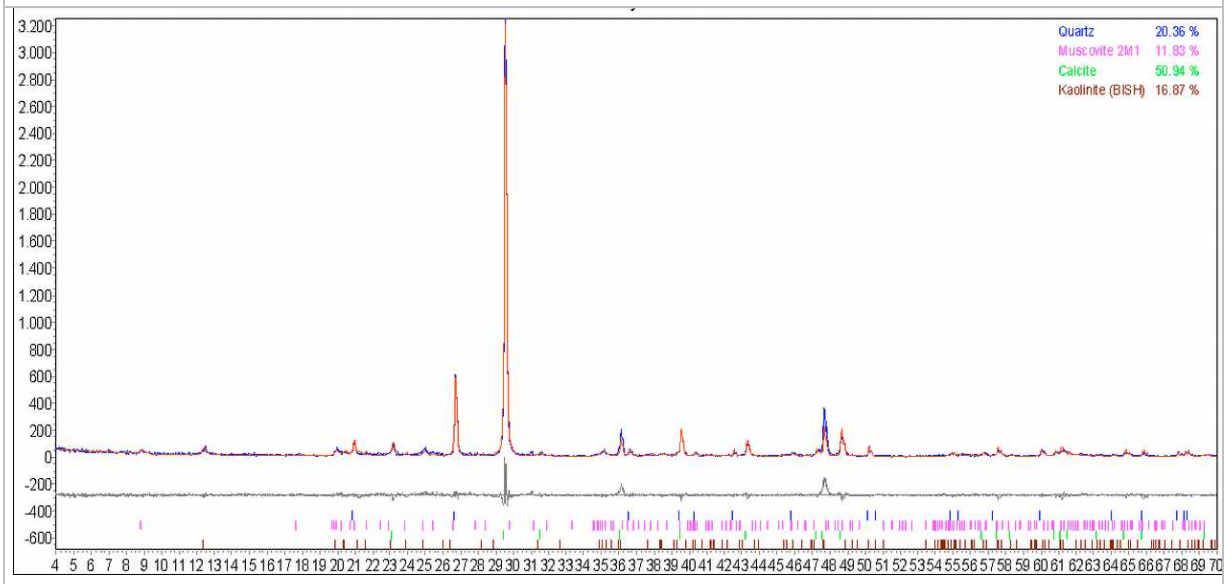

Fig. 11. - Diffraction pattern of clay

thickness of 1.4 mm, one tube face being perpendicular to the x-direction. With respect to ND the resulting concentric arrangement allowed for exploring the effects of transmission through and diffraction from up to 8 walls (Al included).

Comments:

Cu-material as before.

Box D-VI

The design of box D-VI is characterised by two iron plates of 6 mm thickness forming a 'Λ' in the x,y-plane, i.e. a wedge parallel z with mirror symmetry perpendicular to x (**Fig. 13**). The remaining space in the box was filled with synthetic hematite powder, Fe_2O_3, as possible oxidation product. The X-ray powder diagram is depicted in **Fig. 14**.

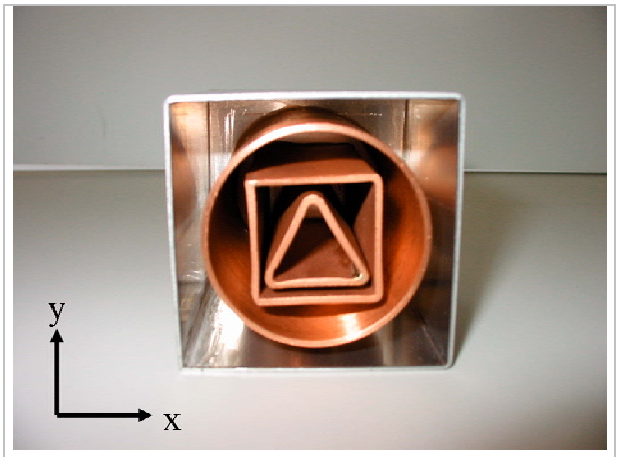

Fig. 12. - View of box D-V

This simple arrangement was expected to demonstrate that once exclusively Fe is identified by PGAA, ND is the method of choice to elucidate the nature of the Fe-bearing material(s).

Comments:

Fe-material as before. X-ray absorption tomography expected to exhibit only little phase contrast.

Box D-VII

Box D-VII was simply filled with three 16 mm thick layers of different materials oriented normal to z (**Fig. 15**). With respect to increasing z the layer sequence was: pre-sintered corundum), Al_2O_3, (with a central drill hole of 16 mm diameter), hot pressed graphite and commercial pyrophyllite, $Al_2Si_4O_{10}(OH)_2$.

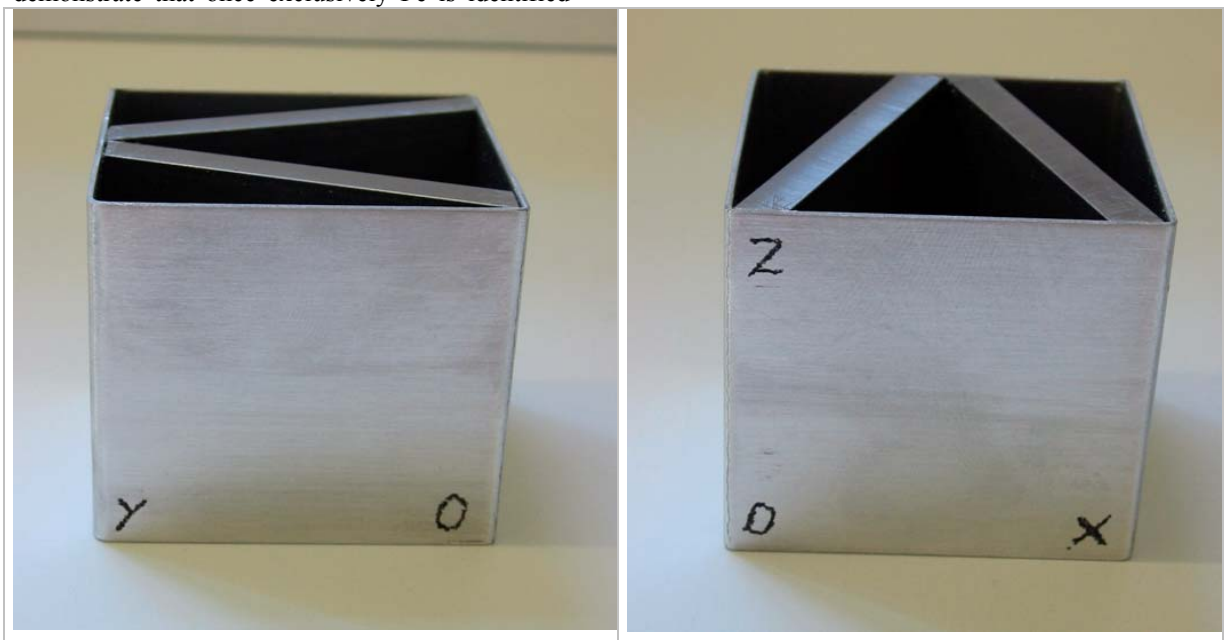

Fig. 13. - Views of box D-VI

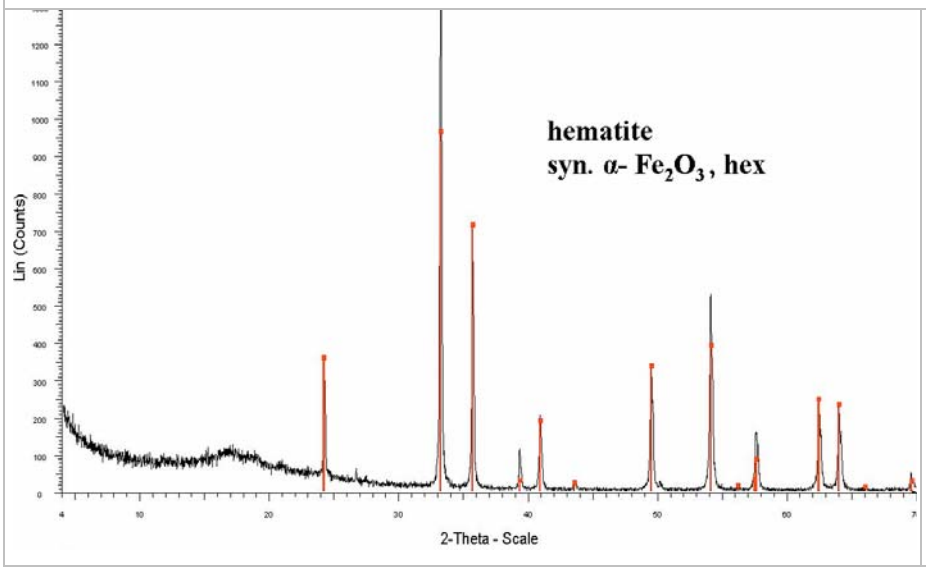

Fig. 14.

Diffraction pattern of trigonal hematite

Fig. 15 - Views of box D-VII

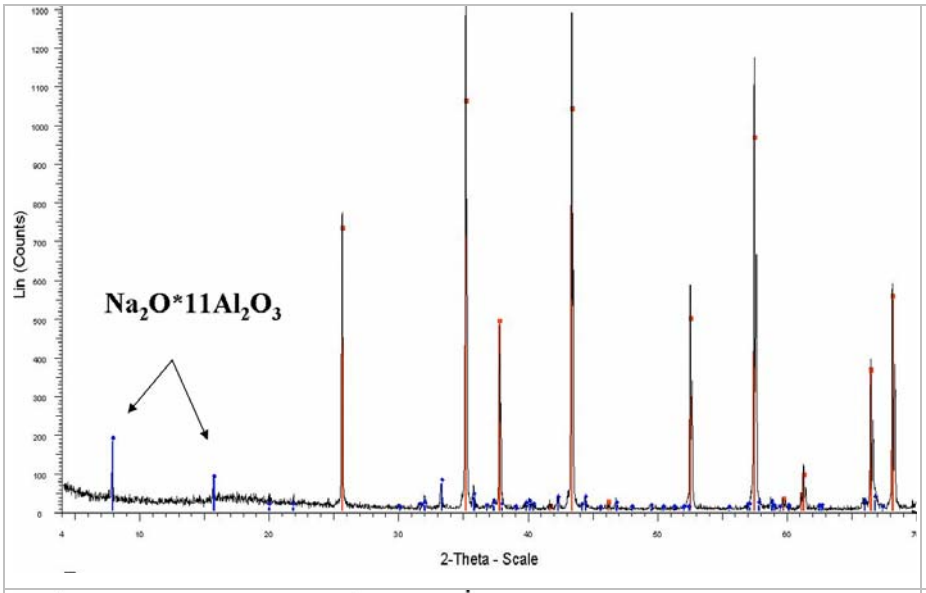

Fig. 16.

Diffraction pattern of trigonal corundum

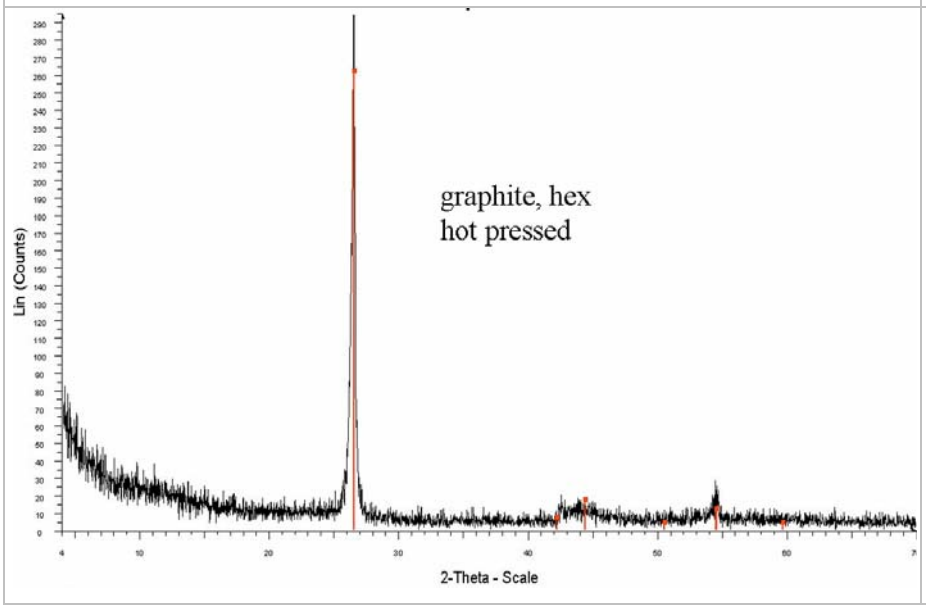

Fig. 17.

Diffraction pattern of commercial hot pressed graphite

HU ISSN 1786-271X; urn:nbn:hu-4106

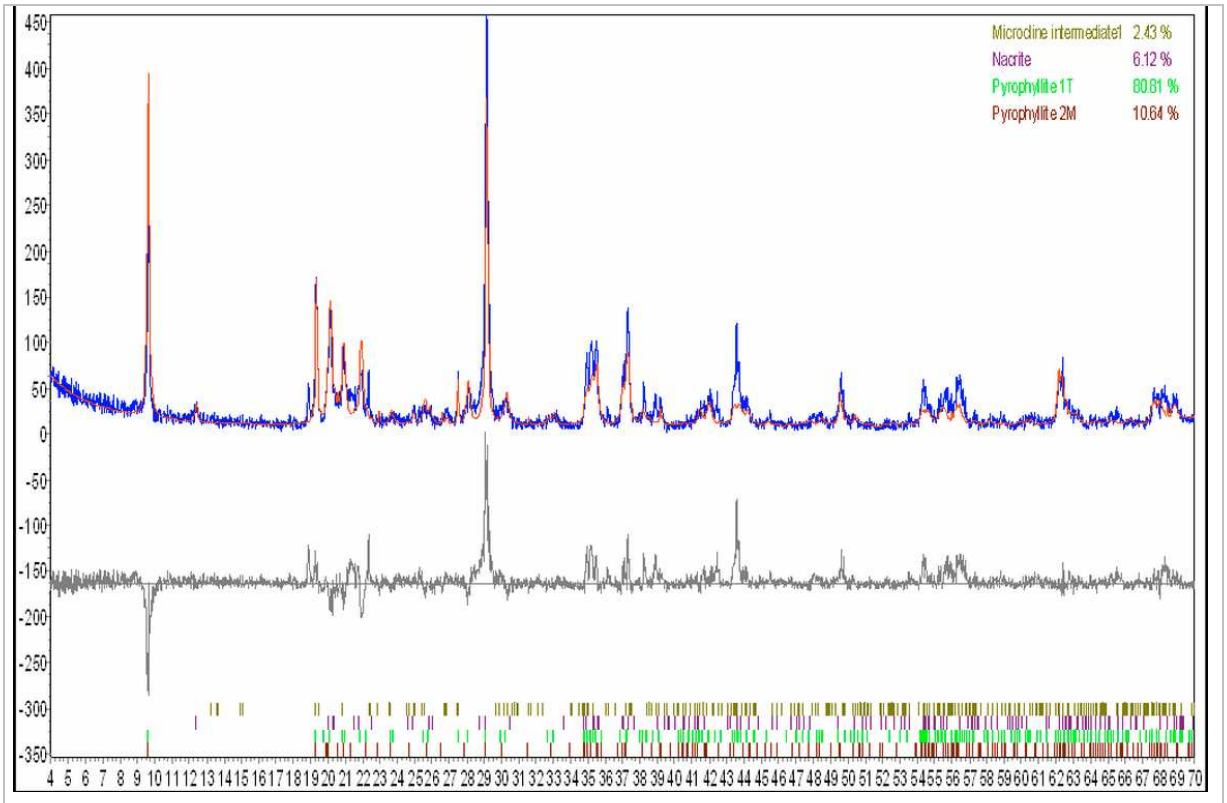

Fig. 18. - Rietveld refined diffraction pattern of commercial pyrophyllite

X-ray powder diffraction analyses (CuKα-radiation) revealed some contamination of corundum by diaoyudaoite, $Na_2O*11Al_2O_3$ (**Fig. 16**) , adding Na to the list of elements.

While the graphite plate showed the simple, typical pure carbon diagram (**Fig. 17**), the pyrophyllite diagram exhibited additional small amounts of the phyllosilicate mineral nacrite, $Al_2(Si_2O_5)(OH)_4$ and of the feldspar mineral microcline, $KAlSi_3O8$. Quantitative Rietveld analysis yielded 81 % pyrophyllite 1T, 11 % pyrophyllite 2M, 6 % nacrite, and 2 % microcline (**Fig. 18**). Due to the complex composition of the box content comprising K, Si, Al, Na, O, C and H, box D-VII challenged both PGAA and ND.

Fig. 19. - Views of box D-VIII

HU ISSN 1786-271X; urn:nbn:hu-4106 © by the author(s)

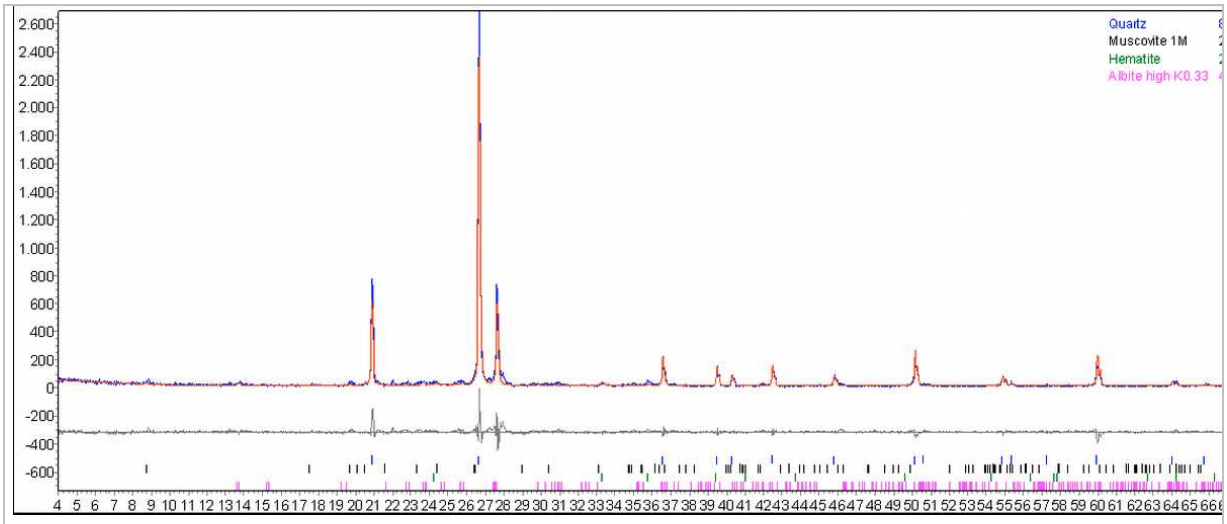

Fig. 20. - Rietveld refined diffraction pattern of fired clay (earthenware)

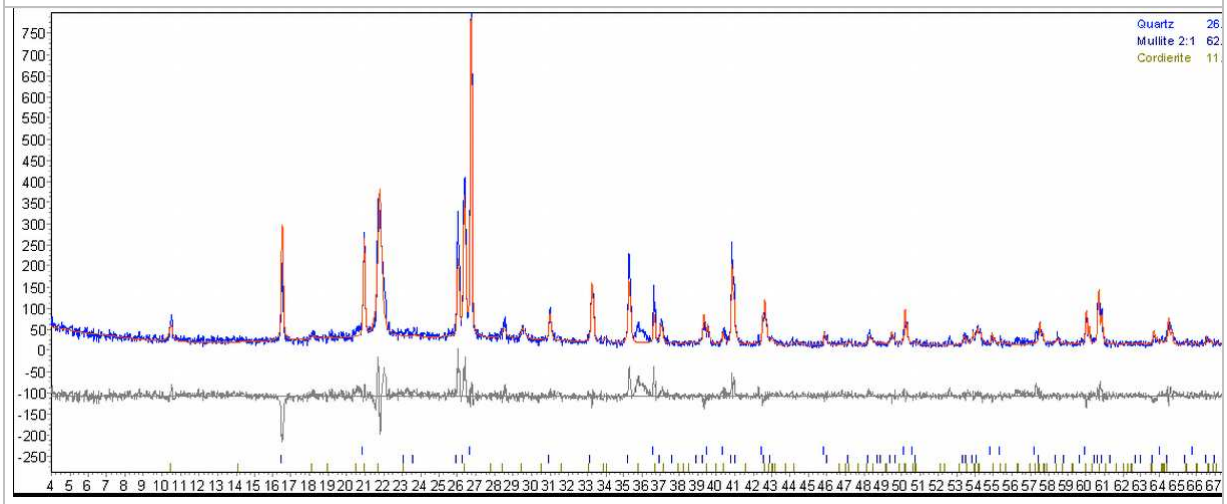

Fig. 21. - Rietveld refined diffraction pattern of fire brick (chamotte)

Comments:

Particularly for ND, it is of great interest to learn which information can be retrieved from an unknown diffraction diagram not only containing a large number of possibly overlapping reflection peaks but also peaks that can be offset from their true positions depending on the position of the scattering volume in the box. Can PGAA contribute to phase identification(s) ?

Box D-VIII

Apart from the drill hole in the bottom layer of D-VII, the design of box D-VIII repeated that of D-VII, however, with more difficult matter (**Fig. 19**). Again with respect to the z-direction, there was a sequence of three layers, here: clay, fired clay (earthenware) and fire brick (chamotte). Thus, different stages of pottery were simulated by earthenware as an intermediate firing product being sandwiched by a clay (educt) and a high firing product. Geometrically simple, D-VIII presented a very demanding case, because all three components consisted of mineral mixtures with low symmetry diffraction patterns. The X-ray diffraction patterns obtained on the earthenware and fire brick slabs are given in the **Figs. 20** and **21**, that of clay is shown in **Fig. 11.** According to Rietveld analyses the compositions of the materials were:

clay: 51 % calcite, , 20 % quartz, 12 % muscovite 2M1, 17 % kaolinite

earthenware: 90 % quartz, 5 % albite, 3 % muscovite 1M, 2% hematite

fire brick: 26 % quartz, 63 % mullite 2:1, 11 % cordierite

presenting the pottery typical list of elements: Fe, K, Ca, Si, Al, Mg, O, H

Fig. 22. - Views of box D-IX

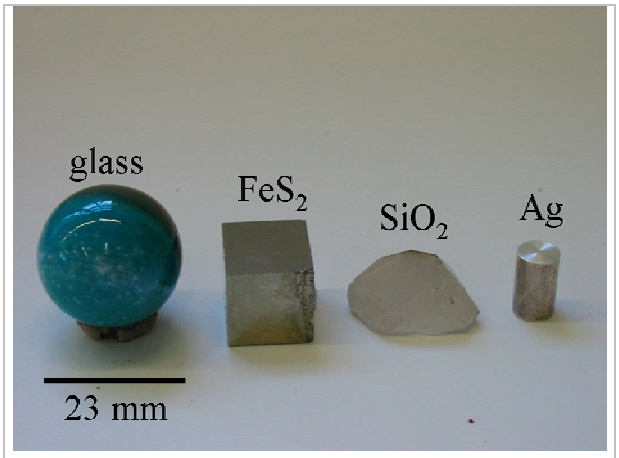

Fig. 23. - Items buried in gypsum

Comments:

The slabs were of different origins and not produced from the clay denoted as educt.

In view of the complexity of the whole sample one could expect that D-VIII presented more than a challenge, but as such a case that is well suited to shed light on the potential of combined absorption tomography, PGAA and ND.

Box D-IX

The question as to which degree relatively small single items (e.g. metal pieces, gem stones or glass) embedded in a difficult environment can be recognised, located and characterised in terms of element composition and eventually crystalline phase led to the design of box D-IX .

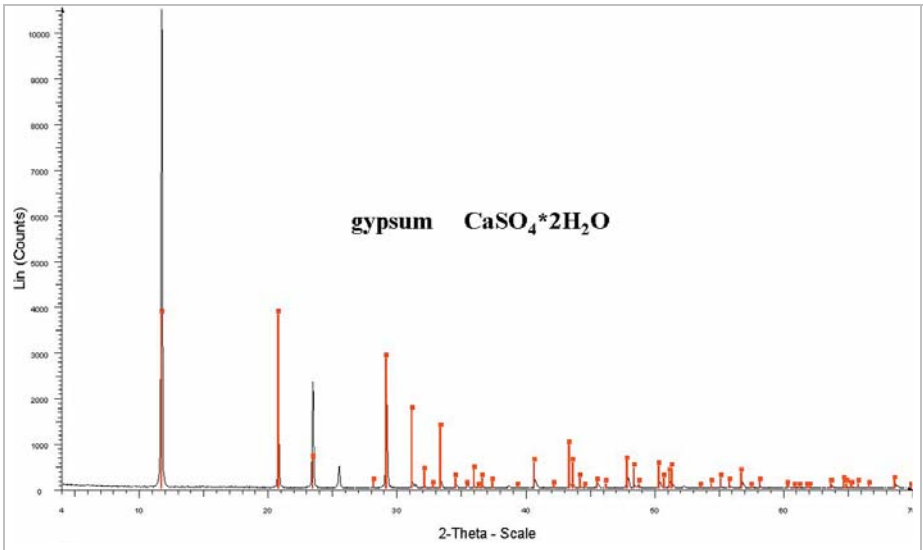

Fig. 24.

Diffraction pattern of gypsum

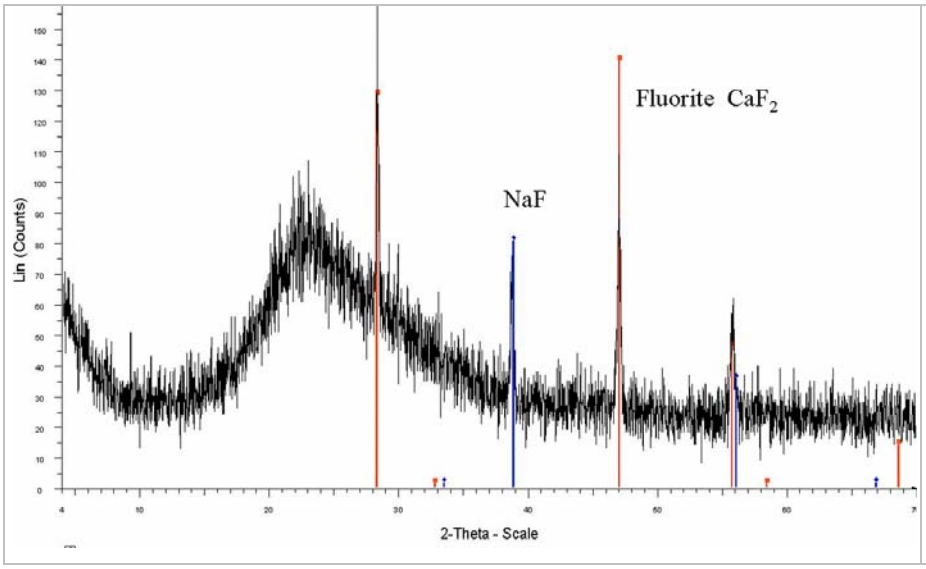

Fig. 25.

Diffraction pattern of blue coloured glass bead

As illustrated in **Fig. 22** and **23** the box contained separated from each other:

i) a quartz single crystal with pyramidal habitus, approximate dimensions 18 x 10 x 12 mm

ii) a coloured glass sphere of 23 mm diameter

iii) a pyrite (FeS_2) single crystal cube of edge lengths 14 x 14 x 16 mm^3

iv) an Ag rod of 7.5 mm diameter and 11 mm length

The remaining box volume was filled with gypsum, $CaSO_4$ *$2H_2O$, as difficult environment due to the presence of the large amount of hydrogen.

X-ray powder diffraction patterns showed pure synthetic gypsum (**Fig. 24**) and in particular (**Fig. 25**) for the glass sphere some inclusions of crystalline fluorite, CaF_2, and villaumite, NaF, causing the blue colour.

Comments:

Assumed absorption tomography could locate the 4 items, ND could be expected to identify the filling material and the Ag rod, and also to indicate the presence of the large single crystals by observation of single crystal reflections, which may even suffice to disclose the chemical composition by trial and error.

Box D-X

Contrary to the inorganic polycrystalline materials used so far the content of box D-X consisted to the greatest part of organic and thus 'amorphous' materials. The thigh bone of a badger was partly wrapped in leather and then deposited with orientation parallel to the z-direction in the centre of a closely fitting container made of beech wood. The assembly is shown in **Figs. 26** and **27**.

Fig. 26. - Views of box D-X

Fig. 27. - Items in box D-X

Clearly, apart from the 'bio-minerals' in the bone there was nothing in the box for which ND could produce structured diffraction patterns on top of a high background caused by hydrogen. On the other hand, due to the different absorption properties of the materials contrast rich tomography images could be expected.

Comments:

Most information would have to come from X-ray tomography and PGAA. However, a lack of results from ND would also present an important piece of information.

Box D-XI

Is an empty box for studying effects caused by the Al-walls.

Box D-XII

Box D-XII completes the series. It was built on special request by the PGAA group. This box housed a cubic tin box of 30 mm edge length and about 1 mm wall thickness positioned in the centre of the Al-cube. The tin box itself contained 2 discs made of copper and lead, respectively (both with 28 mm diameter and 9.3 mm height) and a third disc of Ag (10 mm diameter, 10.4 mm height). The material sequence along the z-direction was Cu, Pb, Ag. As shown in **Fig. 28** the remaining space in D-XII was filled with quartz sand.

Comments:

This box was directly dispatched to Gent and did not participate in the travelling program of the other boxes.

Fig. 26. - Views of box D-XII

HU ISSN 1786-271X; urn:nbn:hu-4106

NEUTRON AND X-RAY IMAGING OF THE 'BLACK BOXES' FOR THE ANCIENT CHARM PROJECT

PETRA KUDEJOVA for the Ancient Charm collaboration

Nuclear Physics Institute, University of Cologne, Zuelpicher Str. 77, D-50937 Cologne, Germany
Email: petra@ikp.uni-koeln.de

Abstract

The Ancient Charm project binds together archaeologists and neutron scientists. Their shared goal is a development of new neutron-based imaging techniques for non-destructive investigation of valuable archaeological objects, while the objects are treated with the highest precautions. One of the tasks of the Ancient Charm project was an analysis of test objects – so called 'Black Boxes' prepared by the archaeologist for the initial development phase of the new neutron-imaging techniques. Since such a development is a challenging task, we decided to use well established imaging methods first: With the help of the neutron resp. X-ray radiography and tomography, we were able to find out and define the shapes and forms of the unknown objects inside of the black boxes. Provided with these pieces of information, the new neutron imaging methods can be positioned to the spots of interest within the black boxes and make the measurements. The overview of the neutron and X-ray radiography and tomography of the black boxes is presented in this article.

Kivonat

Az Ancient Charm projekt összeköti a régészeket és a neutronokkal foglalkozó természettudományos szakembereket. Együtt törekszenek új, neutron alapú képalkotási technikák kifejlesztésére értékes régészeti tárgyak roncsolásmentes vizsgálata céljából. A kutatások során a tárgyakat a legnagyobb elővigyázatossággal kezeljük Vizsgálatukat megelőzően próbatesteket, úgynevezett fekete dobozokat ('Black Boxes') vizsgálunk, amelyeket a régészek tervei szerint készítettek a vizsgálati módszerek lehetőségeinek kipróbálására. Elsőként a jól ismert és már hagyományosnak tekinthető képalkotási technikákat használtunk a tárgyak belsejének felderítésére, mégpedig röntgen és neutron tomográfiát. Ezek segítségével észlelhető és meghatározható a fekete dobozok belsejében rejlő ismeretlen elemek körvonala és formái. Ezekre az ismeretekre alapozva eredményesen alkalmazhatók az új neutron analitikai módszerek, mert a fekete dobozon belül pontosan lehet pozícionálni a vizsgálandó területeket. A cikkben a röntgen- és neutron tomográfia rövid összefoglalását és a kísérletsorozatban elért eredményeinket mutatjuk be.

KEYWORDS: NEUTRON BASED IMAGING ANALYSIS, TOMOGRAPHY

KULCSSZAVAK: NEUTRON ALAPÚ KÉPALKOTÁSI TECHNIKÁK, TOMOGRÁFIA

Introduction

The aim of the ANCIENT CHARM project is a development and usage of the new neutron-based imaging techniques with a focus in the non-destructive analysis of valuable cultural heritage objects. The length of the EU6 projects is three years, starting January 2006 (Gorini et al., 2006). Very nice introduction to the Ancient Charm topic was written in this journal by Zs. Kasztovszky et al. (2006a). The new neutron techniques should provide a set of 3-D information (position sensitive information) on the elemental and phase composition of the selected archaeological objects of interest. As a result of the investigations with neutrons, archaeologists should obtain a complementary set of information, which can help them to solve typical questions about the production of the particular object: when, where and from which material it was made, manufacturing technique, and other potential questions of interest.

The new methods for the 3-D neutron analysis are being developed from well established methods and they are called: Prompt Gamma-Ray Activation Imaging combined with Neutron Tomography (PGAI/NT) (Zs. Kasztovszky et al., 2006b); Neutron Resonance Capture Imaging (NRCI) (Postma et al., 2006) and Neutron Diffraction Imaging (NDI) (Kockelmann et al., 2006).

Black Boxes

For testing purposes during the development phase of the new methods, the archaeologists prepared some testing objects: replicas of the real objects and the black boxes. These closed metal cubes were made of 1.2 mm thick iron plates (by Hungarian National Museum, Dúzs 2008) and of 1.0 mm aluminium plates (by University of Bonn, Kirfel 2008) and contained objects of various shapes, forms and elemental composition. Care was taken to choose characteristic materials and elements, which are representative to the composition of the real archaeological objects.

HU ISSN 1786-271X; urn:nbn:hu-4106

Figure 1. - Picture of one iron (left) and one aluminium (right) black box.

The task was to recognise the elemental composition and the rest-strain of the inner objects by the new methods. The well established methods of neutron resp. X-ray radiography and tomography were used to visualise the inner content of the black boxes and to help with targeting the coordinates of the interesting spots for the new 3-D neutron techniques.

The Hungarian iron black box dimensions are 4 cm × 4 cm × 4 cm and they are named H-I - H-IX. The Bonn aluminium black box dimensions are 5 cm × 5 cm × 5 cm and are named D-I – D-XI. The iron black boxes were closed by gluing the iron covers with an epoxy resin.

This material contains lots of hydrogen and is therefore not transparent for neutrons, which influences the quality of the neutron tomography and radiography result at those parts. An example photo of one iron and one aluminium black box is presented in **Figure 1.**

Neutron and X-ray radiography and tomography

The radiography with neutron beam or with X-ray beam (Röntgen ray) is based on transmission of the beam through the object. The transmitted image provides 2-D information about the content of the object according to how much of the beam is absorbed, scattered and transmitted through different parts and materials of the object. The gained 2-D image gives us some information about the shape and materials. Neutron and X-rays penetrate the materials by different physical ways, so the information given by those radiographs is complementary (neutrons and X-rays have different transmission coefficients for different elements). For example, X-rays penetrate easy through organic materials (like hydrogen, carbon) and are transmitted with more difficulty by heavy metals (e.g. gold, lead). By neutrons, their transmission coefficients vary randomly among elements: e.g. lead and aluminium are transparent for neutrons and hydrogen or cadmium are opaque for them. For both neutrons and X-rays the transmission of the beam intensity is exponentially decreasing with the given thickness of the material, which the beam has to pass through.

Table 1 - Parameters of the neutron radiography and tomography of the black boxes

Date	*13^{th} - 14^{th} of September 2006*
Neutron beam	thermal + cold neutron flux ~ $2.5 \cdot 10^7$ n/cm^2 s
L/D ratio	800
Radiography of black boxes	H-I - IX
	D-II, V, VII, VIII, IX and X
Tomography of black boxes	H-I, II, III, IV, V, VI, VII and IX
	D-II, V, VII, VIII, IX and X
Dimensions of 1 black box	~ 520 x 520 x 520 voxels (Al black box)
Resolution (voxel size)	~ 0.1 × 0.1 × 0.1 mm
Number of projections	400
Irradiation time / projection	7 s
CCD camera	16 bit, 2048 x 2048 pixels
Data reconstruction software	'All In One' Reconstruction tool, based on IDL software (IDL, 2007)

HU ISSN 1786-271X; urn:nbn:hu-4106

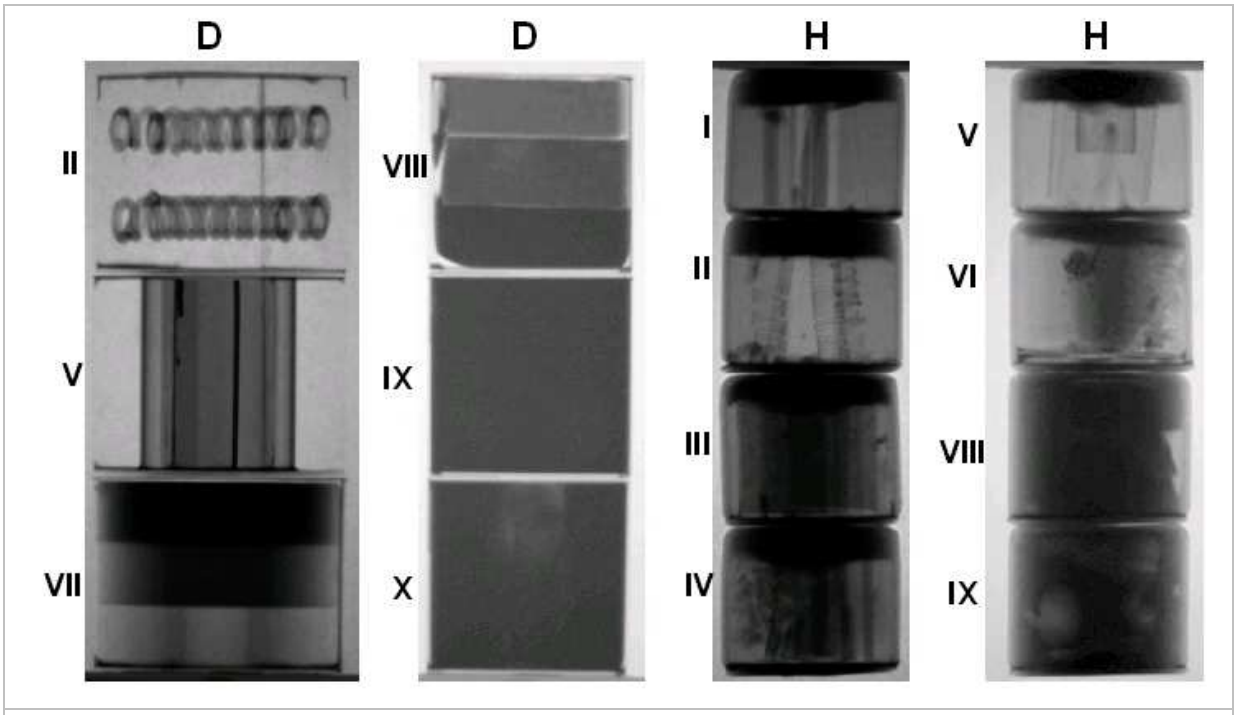

Figure 2 - Neutron radiographs of selected black boxes measured at ANTARES

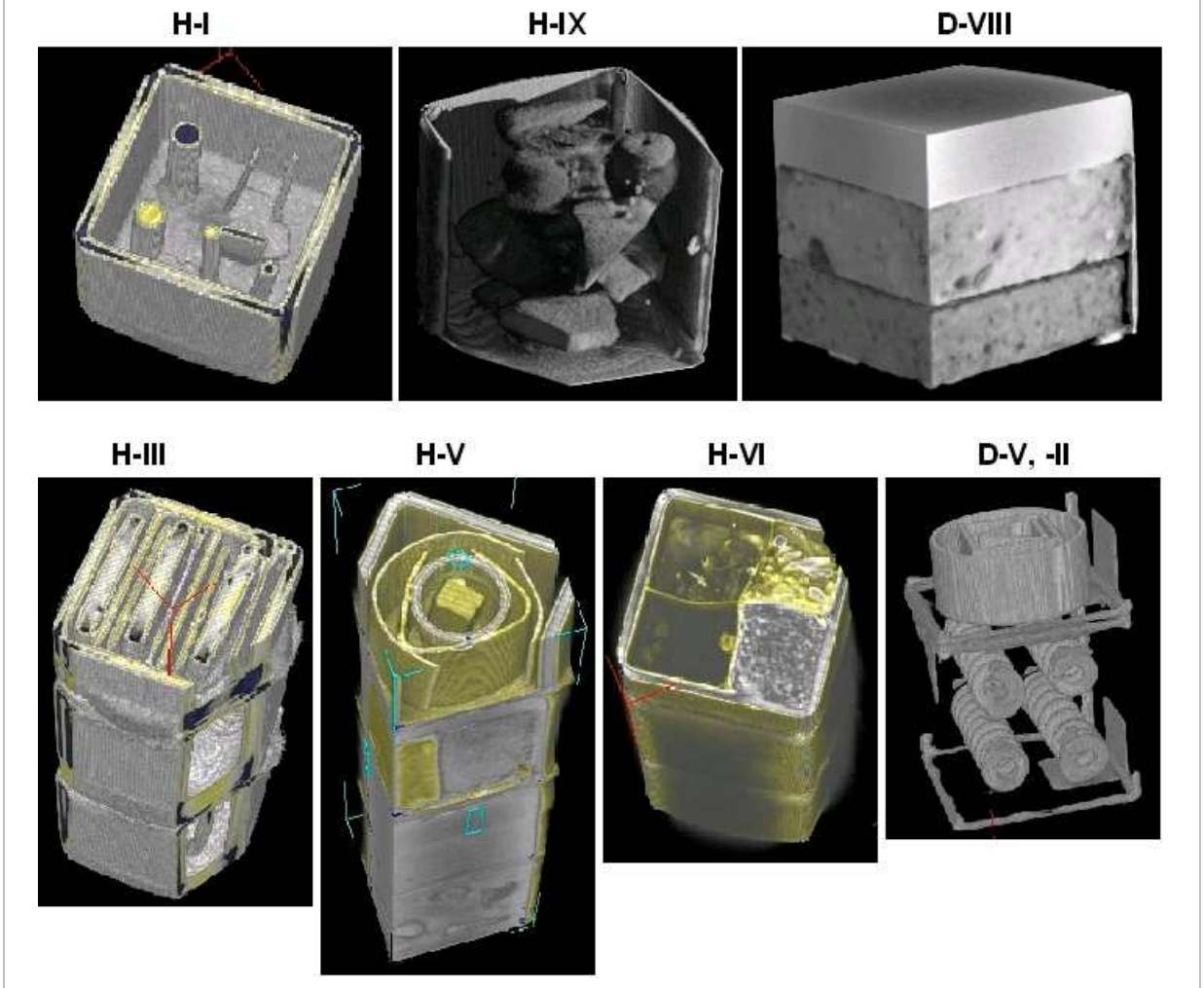

Figure 3. - Selected neutron tomographs of the black boxes measured at ANTARES

HU ISSN 1786-271X; urn:nbn:hu-4106

Table 2 - Parameters of the X-ray radiography and tomography of the black boxes

Date	*1st - 3rd of August 2006*
X-ray cone beam + 3 mm thick Cu filter	average energy ~ 80keV; maximum energy ~ 160keV
L/D Ratio	> 10000
Radiography of black boxes	H-I, II, III, IV, V, VI, VIII and IX D-II, IV, V, VI, VII, VIII, IX and X
Tomography of black boxes	H-VI, VIII and IX D-VIII and X
Dimensions of 1 black box	~ 600 x 600 x 600 voxels (Al black box)
Resolution (voxel size)	0.07 × 0.07 × 0.07 mm
Number of projections	500
Irradiation time / projection	10 s
CCD Camera/Image Intensifier	12 bit, 1024 x 1280 pixels
Data reconstruction software	OCTOPUS (Xraylab, 2007)

The tomography of the objects is actually based on producing a set of many radiographs of the object while rotating the sample around its vertical axis through about 400 equally spaced positions within 360°. Having these 2-D images (called projections) and making some corrections on them (like normalisation, correction for noise signal, white spot filter) filtered back-projection (or other reconstruction algorithms) is performed on them. The result is a 3-D image of the object, which can be sliced in different views by suitable visualisation software. Very nice introduction to the tomography with X-rays and neutron was published by Kardjilov & Moreno, (2006).

Experimental

Neutron Imaging

The neutron radiography and tomography of the black boxes were performed in cooperation with the ANTARES group (Antares, 2007) at the research reactor FRM II (FRM II, 2007). The analysis of the data was also done by the group itself. The parameters for the neutron radiography and tomography are presented in **Table 1**. Radiographs of some selected black boxes are shown in **Figure 2** and tomographs of other selected black boxes are shown in **Figure 3**. For the visualisation of the tomography images, VGStudio Max 1.2 (Volumegraphics, 2007) was used.

X-Ray Imaging

The X-ray radiography and tomography with selected black boxes were performed at the Centre for X-ray Tomography at the Ghent University (UGCT, 2007) in cooperation with the group of Prof. Dr. Luc Van Hoorebeke. Parameters presented in **Table 2** summarise the conditions of the measurements. Radiographs of some selected black boxes are shown in **Figure 4** and tomographs of other selected black boxes are shown in **Figure 5**.

Discussion and conclusion

The neutron and X-ray tomography brought some light into the black boxes. The tomography method gives information about the shape and form of objects. Although this information is not sufficient to determine the elemental composition of the objects inside of the black boxes, it is good enough to resolve some different materials (e.g. according to the colour pattern in Fig. 5, black box H-IX or Fig. 3, black box H-I). Neutron tomography is generally more convenient for any material mixtures (and metals) with close atomic numbers, where X-rays have very similar transmission coefficients (transmission coefficients of X-rays decrease with increasing atomic number). For objects containing organic materials and metals, X-rays may show better the inner structures and shapes. Having many scattering materials like Hydrogen, neutrons cannot penetrate such objects and those are not suitable for the neutron tomography. X-rays are useless for objects covered e.g. with lead walls. By using neutrons, the activation of the objects during the measurement must be taken into account and accordingly the cooling down time. This is mostly important for samples containing e.g. Silver, Cobalt, Zinc or Antimony.

HU ISSN 1786-271X; urn:nbn:hu-4106

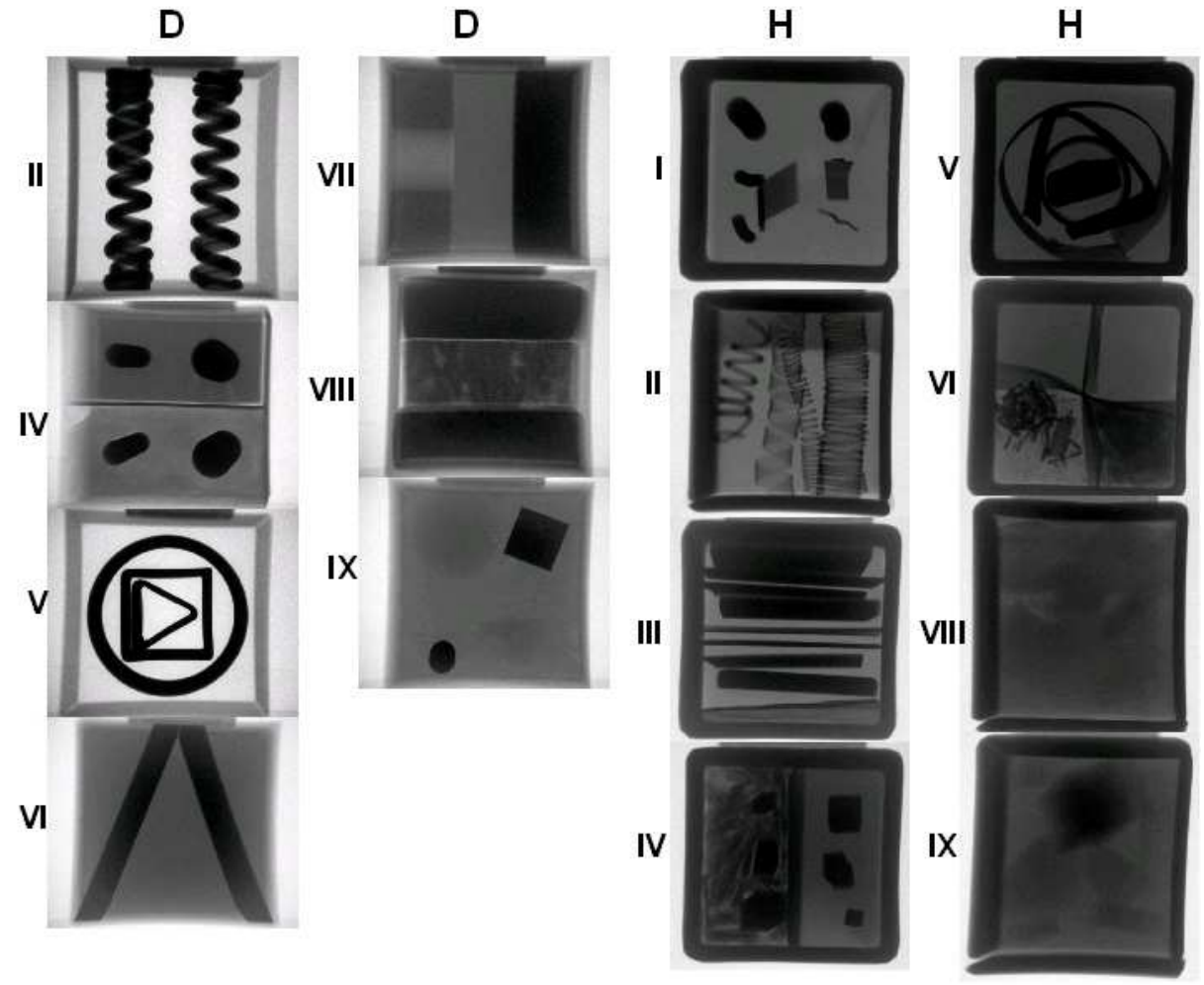

Figure 4 - X-ray radiographs of some selected black boxes measured in Gent

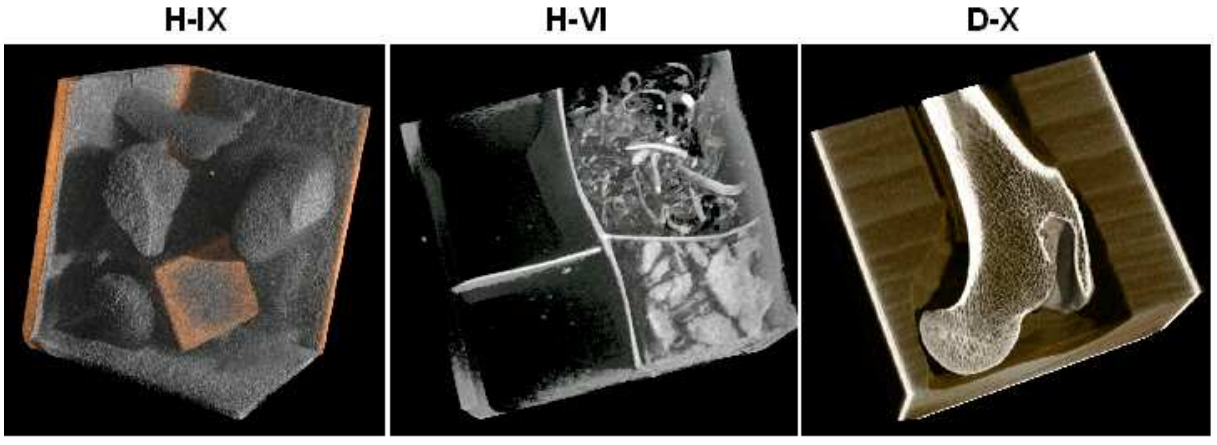

Figure 5 - Selected X-ray tomographs of some black boxes measured in Gent

More information to the black boxes and to the alignment of the neutron tomography to the X-ray tomography and so combining their results can be found in publication by Kudejova et al. (2007).

Using this 3D information about the shapes inside of the black boxes, the particular parts of them were measured at different experimental places to test the new methods like e.g. PGAI. The results of those measurements were presented at the 'Black box meeting' in Sárospatak, Hungary. The results of the measurement were afterwards compared to the real composition of the black boxes.

HU ISSN 1786-271X; urn:nbn:hu-4106 © by the author(s)

Acknowledgement:

Financial support of the Ancient Charm project by the European Community 'New and Emerging Science and Technology' Contract No 15311 is acknowledged. This work was supported by the University of Cologne and the research reactor FRM II in Garching near Munich. The work would not be possible without the help of B. Schillinger, M. Mühlbauer, and K. Lorenz from the ANTARES group as well as without the help of B. Masschaele, M. Dierick and J. Vlassenbroeck from Gent University.

References

ANTARES (2007): Neutron and X-ray tomography facility at the research reactor FRM II, Technische Universität München. http://www.physik.tu-muenchen.de/antares/

DÚZS, K. (2008): Realisation of the planned 'black boxes' in the Hungarian National Museum. *Archaeometriai Műhely / Archaeometry Workshop* **2008/1** 7-20.

FRM II (2007): Research reactor FRM II. Technische Universität München. http://www.frm2.tum.de/en/index.html

GORINI, G. for the Ancient Charm collaboration (2007): Ancient Charm: A research project for neutron-based investigation of cultural-heritage objects. *Il Nuovo Cimento*, **30/1**, 47-59.

IDL (2007): The Data Visualization & Analysis Platform. http://www.ittvis.com/idl/

KARDJILOV, N. & MORENO, F.G. (2006): Overview of imaging with X-rays and neutrons. *Notiziario Neutroni e Luce di Sincrotrone*, **11/1** 15-23.

KASZTOVSZKY, ZS., BELGYA, T. & the Ancient Charm collaboration (2006a): Non-destructive investigations of cultural heritage objects with guided neutron: The Ancient Charm collaboration. *Archaeometriai Műhely / Archaeometry Workshop* **3/1** 12-17.

KASZTOVSZKY, ZS., BELGYA, T. & the Ancient Charm collaboration (2006b): From PGAA to PGAI: from bulk analysis to elemental mapping. *Archaeometriai Műhely / Archaeometry Workshop* **3/2** 16-21.

KIRFEL, A. (2008): Construction and description of the UniBonn black boxes. *Archaeometriai Műhely / Archaeometry Workshop* **2008/1** 21-34.

KOCKELMANN, W., KIRFEL, A. and the Ancient Charm Collaboration (2006). Neutron Diffraction Imaging of Cultural Heritage Objects. *Archeometriai Mühely* **3/2** 1-15.

KUDEJOVA, P., CIZEK, J., SCHULZE, R., JOLIE, J., SCHILLINGER, B., LORENZ, K., MÜHLBAUER, M., MASSCHAELE, B., DIERICK, M. & VLASSENBROEK, J.,(2007) : A marker-free 3D image registration for the ANCIENT CHARM project. Case study with neutron and X-ray tomography dataset. Notiziario *Neutroni e Luce di Sincrotrone*, **12/2** 6-13.

POSTMA, H., CLARJIS, M., BOM, V. & VAN EIJK, C. (2006): Some aspects concerning neutron resonance caopture analysis and imaging. *Ancient Charm Report n. AC-06-IR02*.

SAROSPATAK (2007): Ancient Charm meeting in Sarospatak, Hungary, 23.-25.11.2007 http://www.ace.hu/acharm/minutes-sp.pdf

UGCT (2007): X-ray Radiography and Tomography Facility at the Ghent University (UGCT). http://www.ugct.ugent.be

VOLUMEGRAPHICS, (2007): VGStudio Max 1.2, Application Software. http://www.volumegraphics.com/products/vgstudiomax/index.html

XRAYLAB (2007): Octopus, client server tomography reconstruction software. http://www.xraylab.com

More tomography and radiography pictures can be found on this webpage: http://www.ikp.uni-koeln.de/~petra/AC/

PROMPT GAMMA ACTIVATION IMAGING ON 'BLACK BOXES' IN THE 'ANCIENT CHARM' PROJECT

Z. KIS[1], T. BELGYA[1], L. SZENTMIKLÓSI[1], ZS. KASZTOVSZKY[1], P. KUDEJOVA[2], R. SCHULZE[2]

[1]Institute of Isotopes HAS, POB 77, H-1525 Budapest, Hungary
[2]University of Cologne, D-50937 Cologne, Germany
Email: zkis@iki.kfki.hu

Abstract

The aim of the 'Ancient Charm' project is to combine Neutron Tomography (NT), Prompt Gamma Activation Analysis (PGAA), Time-of-flight Neutron Diffraction (TOF-ND), Neutron Resonance Capture Analysis (NRCA) and Neutron Resonance Transmission (NRT) in order to generate 3D images of the elemental and phase compositions of complex museum objects. For the development and benchmark of the combined methods, complex test samples, so called 'black boxes', were constructed and then analysed by the different techniques. These test objects are sealed iron or aluminium-walled cubes of 40 and 50 mm edge lengths, respectively, containing 2D or 3D arrangements of materials relevant to the compositions of archaeological samples. The Prompt Gamma Activation Imaging (PGAI) is a new terminology – introduced in the AC project – for determining the compositions of small volumes within the sample by scanning. The experimental results obtained from PGAI on boxes investigated at Budapest Neutron Centre (BNC, Hungary) are reported.

Kivonat

Az EU FP6 Ancient Charm projekt fő célkitűzése összetett, értékes műtárgyak elemeloszlásának, fázisszerkezetének háromdimenziós, roncsolásmentes feltérképezése neutronos analitikai módszerek kombinálásával: neutrontomográfia (NT), prompt-gamma aktivációs analízis (PGAA), repülésiidő neutrondiffrakció, neutron-rezonanciabefogás analízis (NRCA) és neutron-rezonanciatranszmisszió (NRT). A kombinált módszerek fejlesztéséhez és teszteléséhez ún. fekete dobozok készültek, amelyek vas ill. alumínium falú próbatestek, belsejükben régészeti szempontból fontosnak tartott anyagok komplex elrendezésével. A prompt-gamma aktivációs leképezés (PGAI) egy új terminológia; olyan 3D-s elemösszetétel vizsgálatot jelent, amelynek során keskeny neutronnyalábbal a minta kis térfogategységeit lépésenként elemezzük. Jelen cikk a Budapesti Neutron Centrumban a fekete dobozokon végzett PGAI vizsgálatok eredményeit mutatja be.

KEYWORDS: PROMPT GAMMA ACTIVATION IMAGING, NEUTRON, 3D ELEMENT MAPPING, ANCIENT CHARM

KULCSSZAVAK: PROMPT-GAMMA AKTIVÁCIÓS LEKÉPEZÉS, NEUTRON, 3D ELEMTÉRKÉP, ANCIENT CHARM

Introduction

The ultimate goal of the Ancient Charm (AC) project is to obtain 3D imaging of elemental and phase compositions of considerably complex museum objects by combining different neutron analytical methods (http://ancient-charm.neutron-eu.net/ach, Gorini 2007). In this paper the emphasis is on the extension of Prompt Gamma Activation Analysis (PGAA) towards the position-sensitive Prompt Gamma Activation Imaging (PGAI), and its comparison to Neutron Tomography (NT) and Time-of-flight Neutron Diffraction (TOF-ND).

PGAI is a new terminology - introduced by the project - for determining the compositions of small volumes within the sample by scanning (Kasztovszky & Belgya 2006). This volume is determined by the intersection of the collimated neutron beam and the viewing angle of a gamma detector. In medical imaging this kind of intersection is called isocenter, which is a fix-point in a space and which is the source of the information. In our case, it is a small volume rather than a point; therefore it is better called isovolume. If a sample is moved, with the isovolume fixed in space, we can collect spatially well-resolved analytical information by acquiring a gamma-spectrum at each sample position. This double-collimated arrangement substantially reduces the gamma counting rate thus increasing the time needed for the experiment. Usually such a measurement is not practical and economic. The solution comes at the price of reduced spatial resolution: the removal of the gamma collimation results in a wide viewing angle of the detector covering the whole object, thus photons emerging from a chord-shaped volume throughout the sample are detected. The schematic drawings of the two basic measurement setups are shown in **Figure 1**.

A complete 3D scan of the object - in either configuration - requires a lot of beam time. It is more efficient to identify first the regions of interest using the three-dimensional pattern obtained within few hours by X-ray and/or neutron tomography, and then to limit the (rather long lasting) PGAI experiment to the determination of the elemental compositions of these regions only.

HU ISSN 1786-271X; urn:nbn:hu-4106

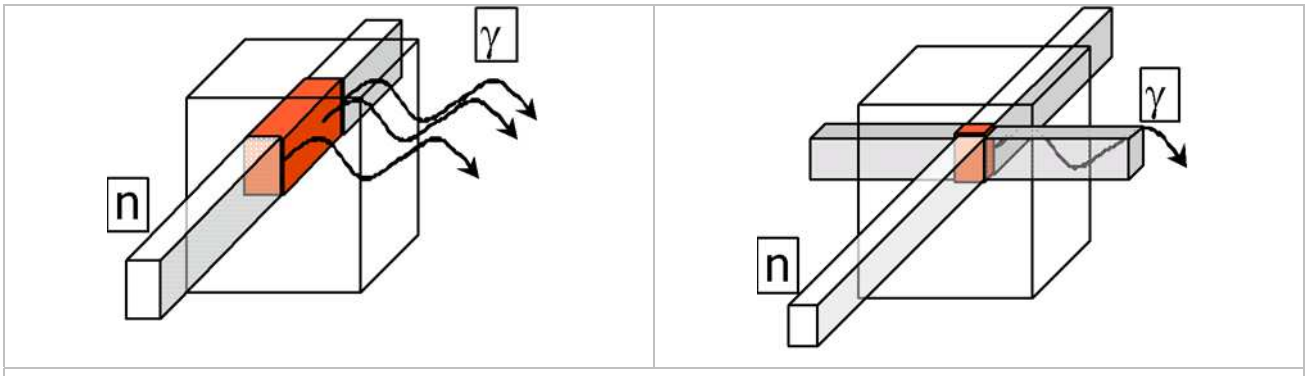

Fig. 1. - Schematics of the two basic measurement setups in PGAI. Left side: chord volume, Right side: isovolume

This approach considerably speeds up the investigation. As our first step towards the PGAI imaging method, the definition of such regions was based on 2D neutron radiography (NR) and X-ray radiography (XR) images provided by other members of the Ancient Charm consortium.

In order to establish a procedure to combine tomography, PGAI and diffraction data collected on the same archaeological object, test samples with varying degrees of complexity were analysed by the different methods. Two sets of sealed 'black boxes' were manufactured by the Hungarian National Museum (Dúzs 2008) and by the University of Bonn, Germany (Kirfel 2008). The contents of the boxes were constructed according to the design made by the archaeologists and conservators of the HNM, using typical materials occurring in archaeological contexts. The first set consists of ten iron cubes of 40 mm edge length (labelled as H-I through H-X, wall thickness 1 mm). The second set (labelled as D-I through D-X) comprises aluminium boxes with wall thickness of 1 mm and dimensions of 50 mm. The compositions of the internal parts, the filling materials, as well as the layout, were undisclosed to the experimentalists, however the constructors documented the production carefully.

The purpose of the experiments carried out at Institute of Isotopes (IKI), Budapest, was to reveal as much information as possible about the materials inside of the nine 'black boxes' selected for experiments applying PGAI-NR/NT. In several cases, complementary information from the other techniques was needed to find out the composition of the black boxes. There were cases, however, when PGAI-NR/NT yielded the same information about the boxes as was given by other method. It should be emphasised that all the boxes studied at IKI, Budapest, were investigated by TOF-ND at the ISIS Facility, Rutherford Appleton Laboratory (Chilton, UK) in the framework of the Ancient Charm project as well. In this paper, we focus on the implementation of the PGAI-NR/NT but highlighting the cases where the combination of PGAI with TOF-ND was very useful.

Experimental

The PGAI experiments were carried out on the standard PGAA station and/or on the newly installed PGAI-NR/NT setup on NIPS (Neutron Induced Prompt Gamma Spectroscopy) station of the Budapest Neutron Centre (Budapest, Hungary) that is operated by the Institute of Isotopes (IKI). The TOF-ND measurements were accomplished on diffractometers ROTAX and GEM at the ISIS Facility, Rutherford Appleton Laboratory (Chilton, UK).

The standard setup at the PGAA station of IKI

The PGAA experimental station (Révay et al. 2004), being in operation since 1996, is installed at the end of a horizontal cold neutron beam guide at the Budapest Research Reactor. The neutrons leaving the reactor core are cooled and are guided to the experimental stations with a neutron guide. The PGAA/NIPS system is situated 35 m away from the reactor wall. With a split beam, the PGAA station operates on the upper half of the beam, while the NIPS station uses the lower one.

At the PGAA station, the maximum available beam size is 20×20 mm^2, and the beam flux is 1.2×10^8 neutrons $cm^{-2}s^{-1}$. The neutron beam can be collimated to different cross sections down to 5 mm^2. Regularly, relatively small samples are positioned inside the sample chamber, while for larger objects the chamber can be removed. Prompt- and delayed gamma photons are detected with a 27% efficiency n-type HPGe detector, surrounded by a BGO annulus, operated in a background reduction mode called Compton-suppression.

HU ISSN 1786-271X; urn:nbn:hu-4106 © by the author(s)

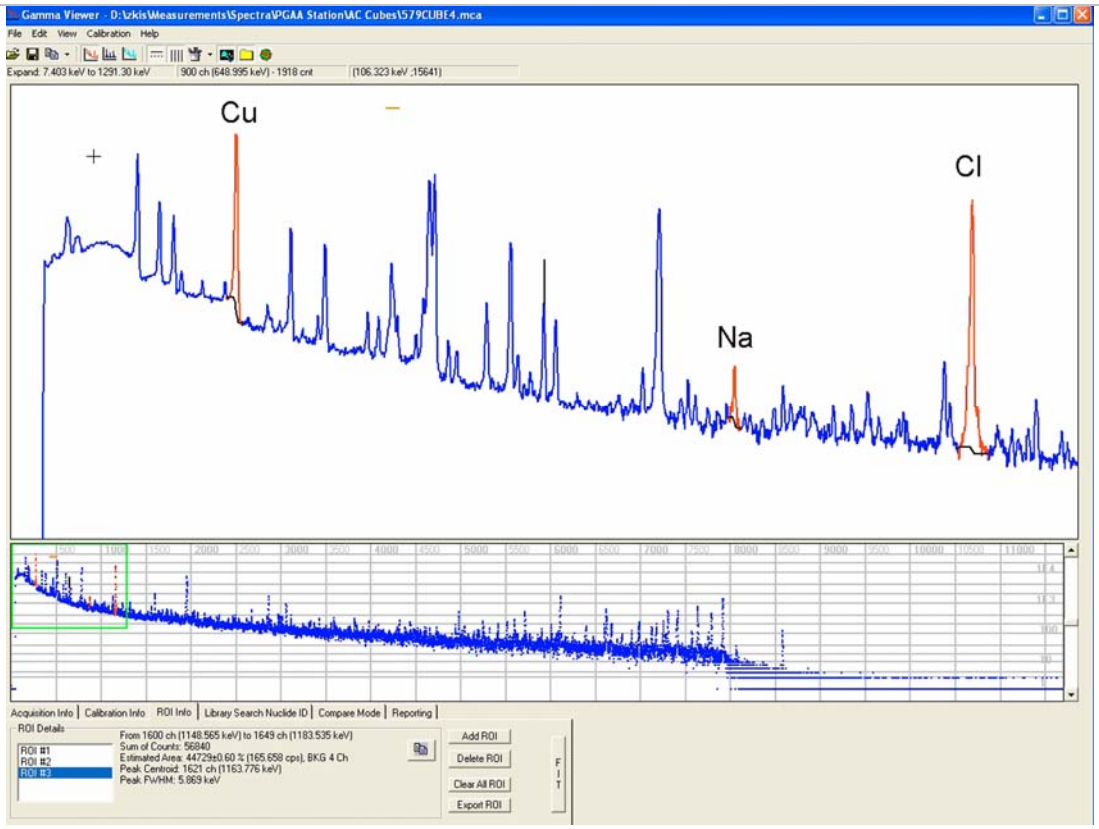

Fig. 2. - PGAA spectrum from the irradiation of black box D-IV (Al). The box was aligned so that the neutron beam could impinge on the top of one of the copper rods embedded in rocksalt.

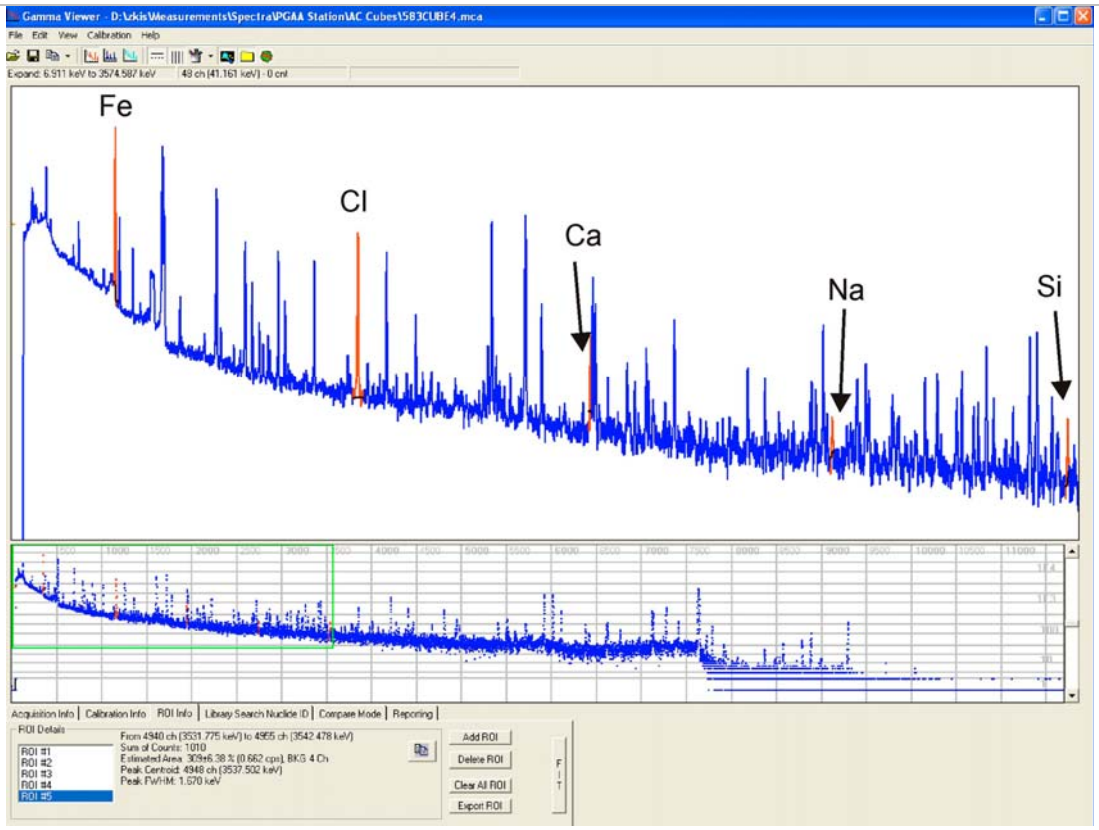

Fig. 3. - PGAA spectrum from the irradiation of black box D-IV (Al). The box was aligned so that the neutron beam could impinge on the top of one of the iron rods embedded in clay.

HU ISSN 1786-271X; urn:nbn:hu-4106

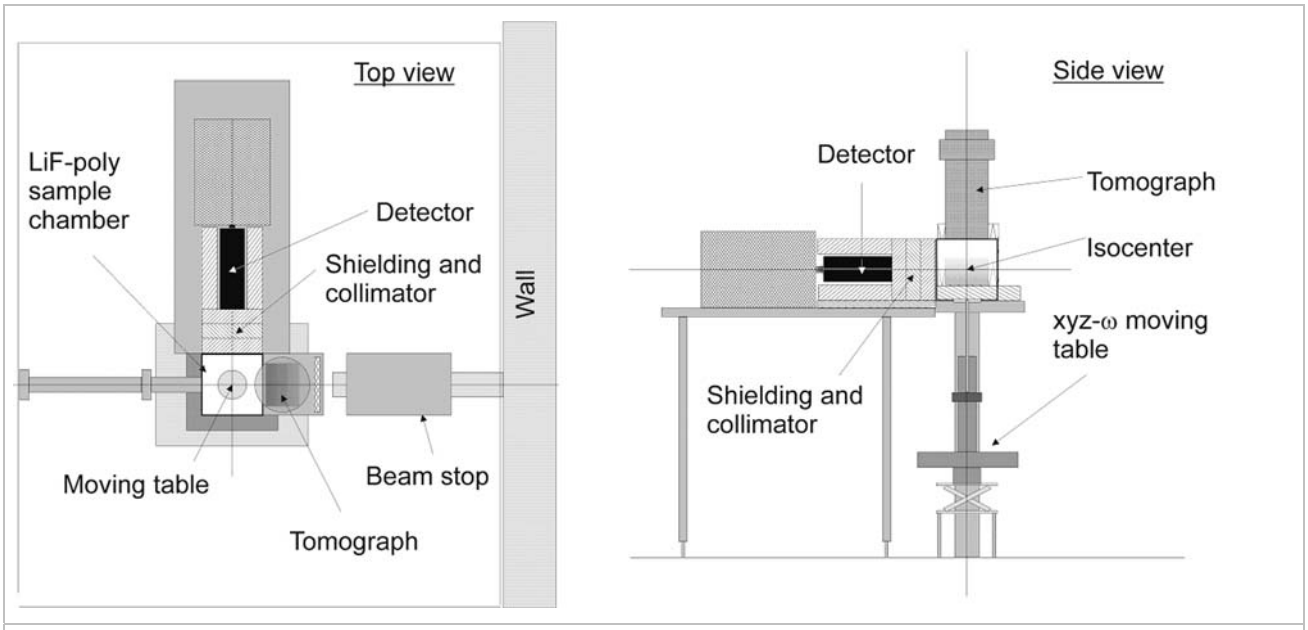

Fig. 4. - Sketch of the Budapest PGAI setup

The spectra are collected with a Canberra AIM 556 multichannel analyser and evaluated with Hypermet PC (Révay et al. 2005).

As examples, two PGAA spectra measured at the PGAA station are presented in **Fig. 2** and **Fig. 3**. The black box D-IV (Al) contains two iron and two copper rods parallel to z-axis, embedded in clay and rocksalt, respectively. During the irradiation it was aligned so that the neutron beam could impinge on the rods. One can find the several strong peaks of the composition materials. Some of the main peaks are labelled in the figures.

The new PGAI-NR/NT setup at the NIPS station of IKI

The setup is a result of the AC project and many consortium members contributed (design, hardware and/or software) to its realisation (Belgya et al. 2007). The schematic drawing of the PGAI-NR/NT setup is shown in **Figure 4.** This facility was designed to accommodate an object of maximum lateral size 10 cm by 10 cm, but the height of the object can be up to 20 cm. The available beam intensity is 7×10^7 neutrons $cm^{-2}s^{-1}$ and the L/D ratio is 150. The incident neutron beam has a maximum cross-section of ~23 mm by ~23 mm, when applied for neutron tomography. For PGAI, an adjustable neutron collimator was fabricated from a ^{6}Li-loaded polymer, with an aperture that shapes a 2-mm wide 'pencil beam' with a variable height of 2 to 20 mm. The sample is surrounded by a 20 cm × 20 cm × 20 cm sample chamber, made also of a ^{6}Li-enriched polymer, which has no bottom. The neutron tomograph is placed downstream from the sample position. The xyzω-moving table equipped with sample support is beneath the sample chamber. It holds the sample and reaches almost any point within the available space. A photograph of the setup is presented in **Figure 5**.

The gamma collimator is built up from lead bricks sitting on the top of an adjustable table. The collimator aperture can be adjusted from 2 mm × 2 mm to any meaningful rectangular size. A 13%-efficiency HPGe detector is placed behind the collimator to view the isovolume of the system. The detector signals are processed with an XIA PIXIE-4 digital signal processor (http://www.xia.com). An integrated data acquisition system can control the moving table and can take either gamma spectra, NT images, or both of them in a batch run. The measurements result in a large number of prompt spectra, which are analysed with the batch evaluation feature of the spectroscopy software HyperLab 2005b (Simonits et al. 2003; http://www.hlabsoft.com).

The neutron tomograph (NT) was provided by the University of Cologne, Germany. The neutron converter scintillator is made of ^{6}Li/ZnS, and the scintillation light is reflected to the optics by a silver-free mirror. The optics is attached to a high-resolution CCD camera (http://www.pco.de). The neutron beam stop placed after the tomograph is assembled from a ^{6}Li-enriched polymer, boron and lead. It is intended that for complex objects, to be investigated later in the project, the coordinates of regions of interest for PGAI will be taken from the NT reconstructions.

HU ISSN 1786-271X; urn:nbn:hu-4106 © by the author(s)

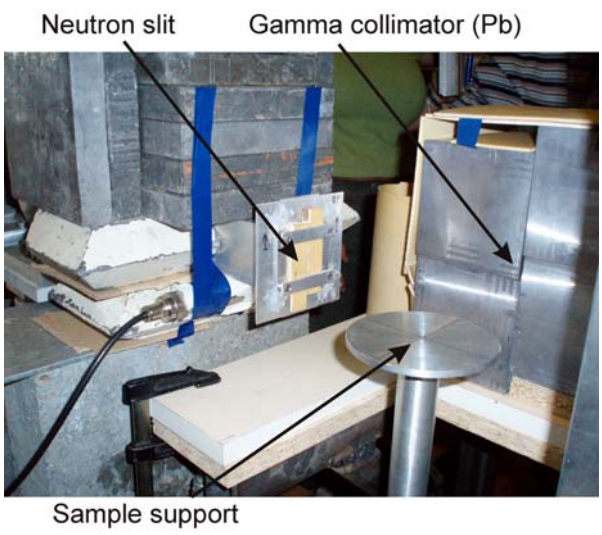

Fig. 5. - PGAI-NT setup

Prompt Gamma Activation Imaging

In total, nine black boxes were selected for the experiments at Institute of Isotopes, Budapest. They represented a wide range of material and structural variability and their measurements could be completed during the available beam time. Three aluminium and two iron boxes were investigated at the standard PGAA station, while three aluminium and four iron boxes were analysed at the newly installed PGAI-NT station of the Budapest Neutron Centre.

On the PGAA station of IKI, measurements were made in the sample chamber using standard neutron collimators available for normal PGAA. The appropriate sections of the objects were located using the radiography data collected earlier at the research reactor FRM-II in Garching, Germany, in cooperation with the ANTARES group (neutron radiography, hereafter referred as [NR-Gar]) and at the Center for X-ray tomography at the University of Ghent, Belgium (X-ray radiography [XR-Ghe]) (Kudejova et al. 2007).

Collimated neutron beams with 5 mm^2, 24 mm^2 and 44 mm^2 area cross-sections were available. The boxes were placed inside the chamber by hand, and positioned by eye as well as possible in the path of the neutron beam. All measurements were performed at ambient conditions, the acquisition times varied between 300 sec - 2700 sec depending on the analytical sensitivities of the elements present in the irradiated volumes. These measurements were made in PGAI chord type geometry for all five boxes investigated.

On the NIPS station of IKI, the positioning of the samples was carried out using the moving table and based on the radiography images taken with the neutron tomograph [NR-Bud]. The beam size was either 2mm × 20mm or 2mm × 10mm.

Table 1. - Comparison of the Budapest neutron facilities

PGAA station	NIPS station
☺ higher neutron flux	☺ more flexible geometry, larger sample chamber
☺ standardised geometry	☺ accurate positioning
☺ well-known efficiency	☺ radiography-driven PGAI
☺ background reduction with Compton-suppression	☺ better spatial resolution
	☺ use of multiple γ-detectors possible
☹ limited space in the sample chamber	☹ higher spectral background
☹ lower precision of sample positioning	☹ longer acquisition times in isovolume configuration
☹ no tomography/radiography possible	

HU ISSN 1786-271X; urn:nbn:hu-4106 © by the author(s)

Table 2. - Black boxes analysed by PGAI or PGAI-NR/NT at IKI, Budapest

Black box	Measurement setup	PGAI meas. type	Other measurement
D-IV (Al)	- PGAI on PGAA station - PGAI-NR on NIPS	- chord - isovolume	TOF-ND on ROTAX
D-V (Al)	PGAI-NR on NIPS	chord	TOF-ND on ROTAX
D-VI (Al)	PGAI on PGAA station	chord	TOF-ND on ROTAX
D-VII (Al)	- PGAI on PGAA station - PGAI-NR on NIPS	- chord - isovolume	TOF-ND on ROTAX
H-I (Fe)	PGAI-NR on NIPS	chord, isovolume	TOF-ND on GEM
H-III (Fe)	PGAI-NR on NIPS	chord	TOF-ND on GEM
H-IV (Fe)	PGAI-NR on NIPS	chord	TOF-ND on GEM
H-VI (Fe)	- PGAI on PGAA station - PGAI-NR on NIPS	- chord - chord, isovolume	TOF-ND on GEM
H-VIII (Fe)	PGAI on PGAA station	chord	TOF-ND on GEM

The height of the collimator aperture was chosen to fit the geometry of the selected section and to optimise the measurement time. The typical acquisition time varied between 200 sec and 3600 sec, depending on the investigated materials. All boxes measured on this station were studied in chord geometry, while four of them were also examined with the isovolume setup.

A comparison of the general features of the two experimental stations is shown in **Table 1.**

Time of Flight Neutron Diffraction

The complementary information content of time-of-flight neutron diffraction (TOF-ND) method was exploited in several cases in order to reveal the phase compositions of the sections investigated when the elemental compositions from PGAA did not provide the full information on the metal or mineral phases. Neutron diffraction experiments were performed on two different diffractometers at ISIS, on ROTAX (Kockelmann et al. 2000) and GEM (Day et al. 2004). The TOF-ND method (Kockelmann & Kirfel 2006) makes use of the polychromatic beam of neutrons possessing wavelengths over a broad wavelength range. For both diffractometers, the scattered neutrons are registered by detector banks at low and high scattering angles, i.e. each measurement on one of the instruments yields several diffraction patterns covering different crystallographic d-spacing ranges. For the data collections on the black boxes, the size of the incident beam was set to typically 10×10 mm^2. The boxes were measured at several analysis points where the neutron and X-ray tomographies [NR-Gar, XR-Ghe] indicated particular features. A more detailed description of the TOF-ND analysis on the black boxes is given by Festa et al. (2008).

List of experiments at IKI

The details of the experiments carried out on both stations of IKI can be found in **Table 2**. The particular details of the experimental conditions will be presented in the results section separately for each box. No gamma- and neutron self-absorption corrections were taken into account at this stage of the work, thus the results are only qualitative.

Results and discussion

After the experiments and following the data analysis, the layouts and the compositions of the boxes were revealed (Kirfel 2008, Dúzs 2008) and, hence can be compared to the measurement results. For the sake of clarity, we will compare the measured data and derived elemental compositions with the actual contents of the boxes.

Aluminium box D-IV.

For the layout, the description and the nominal composition of the box refer to Kirfel (2008).

Radiography images (**Fig. 6a, b**)

• the filling material greatly absorbs the cold neutrons, only the aluminium plates ‘shine’, as they are mostly transparent for neutrons [NR-Bud]

• for low-energy neutrons the depth of analytical information by PGAI is limited

• X-ray radiography [XR-Ghe] (left figure below) had to be used to move the parts of the box to the measuring position

HU ISSN 1786-271X; urn:nbn:hu-4106 © by the author(s)

Measurement points with PGAI (Fig. 6c)

• a chord type setup on the PGAA, beam size: 44 mm^2

• an isovolume setup on the NIPS, 2 mm × 10 mm pencil beam

• irradiations n1 - n6 carried out perpendicular to the rods: information about the filling material

• irradiations n7 - n10: neutrons hit the top of the rods touching the wall of the box, avoiding the attenuation in the filling materials.

PGAI conclusions

• for low-energy neutrons, this box is indeed a 'black' box

• 'A' and 'C' rods are made of iron, 'B' and 'D' are made of copper

• Na, Cl correctly identified; Si, Ca, Fe detected in the other section

• isovolume setup: hard to draw conclusions yet because of low count rate and too short acquisition time

TOF-ND conclusions (Festa et al. 2008)

• around 'A' and 'C' 75 wt% calcite ($CaCO_3$) and 25 wt% quartz (SiO_2)
• around 'B' and 'D' sodium chloride
• iron phase is ferrite (bcc iron), rather than steel

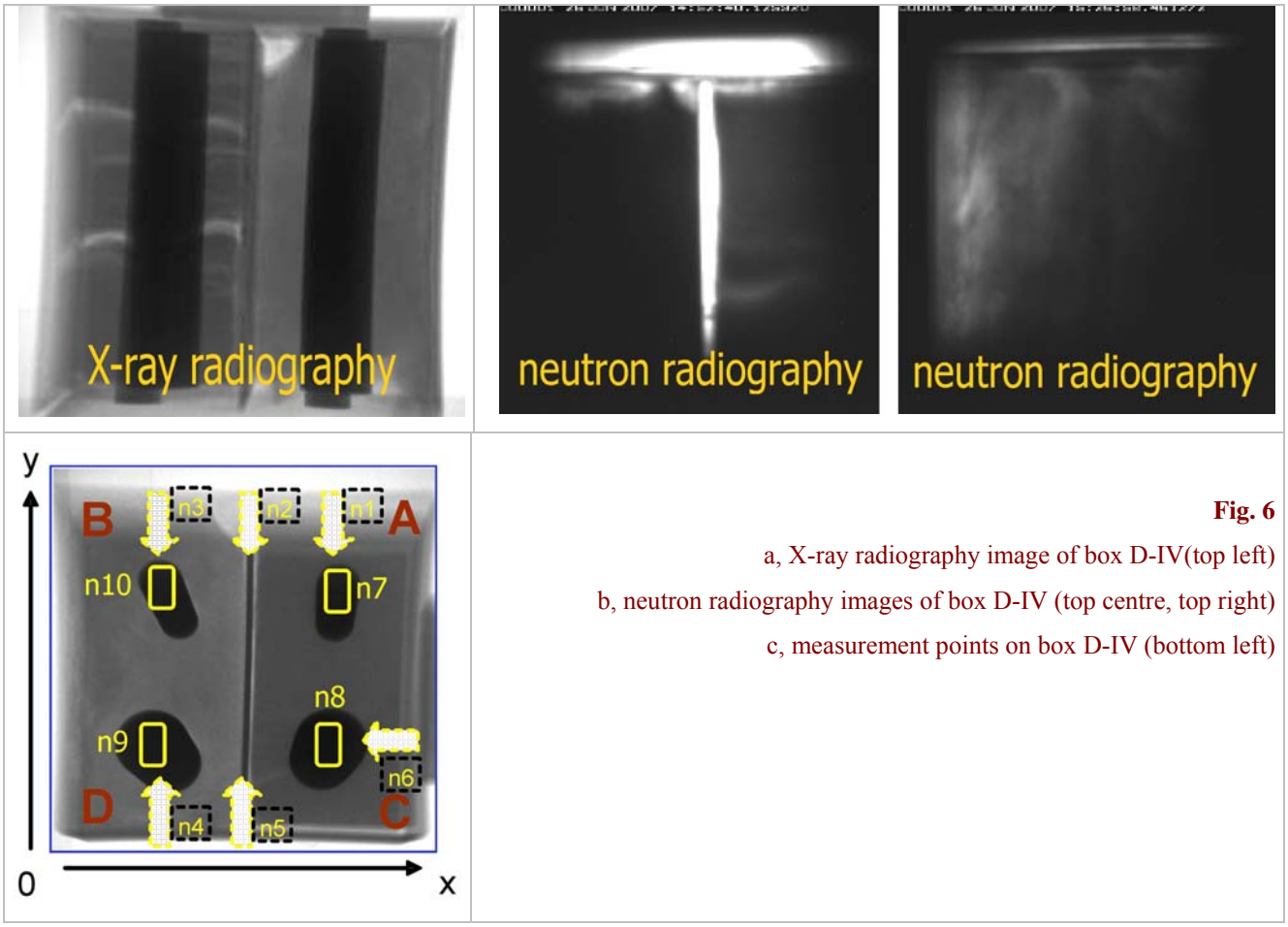

Fig. 6

a, X-ray radiography image of box D-IV(top left)

b, neutron radiography images of box D-IV (top centre, top right)

c, measurement points on box D-IV (bottom left)

Table 3. - Details of the composition of the box D-IV.

Nr.	**Nominal composition**	**Meas. type and Nr. of PGAI beam**	**PGAI results**	**TOF-ND results** (Festa et al. 2008)
1, 6, 7, 8	Fe in clay	chord: n1, n6, n7, n8	Na, Si, Cl, Ca, **Fe**	Fe-type = bcc: ferrite + cementite in calcite (75 wt%) + quartz(25 wt%)
2, 5	Al between clay and salt	chord: n2, n5	Na, **Al**, Si, Cl, Ca	No clear indications
3, 4, 9, 10	Cu in salt	chord: n3, n4, n9, n10	Na, Cl, **Cu**	Cu-type = fcc: steel (Fe) or copper (Cu), decision based on PGAA: Cu NaCl

Discussion

Based on PGAI measurements on the PGAA station, the 'A' and 'C' rods are made of iron, while the 'B' and 'D' are copper. PGAI can not distinguish between the phases of iron therefore a combination with neutron diffraction is fruitful. TOF-ND proves that the iron phase is ferrite (bcc iron), rather than steel. It is also important to note that TOF-ND has difficulties to distinguish between copper and steel (fcc-iron) which have the same structure and similar lattice parameters. In this case PGAI can help in the decision: rods 'B' and 'D' are made of copper.

According to PGAI, the filling material around rods 'A' and 'C' contains mainly Si and Ca apart from the Fe, while around 'B' and 'D' Na and Cl in equal atomic ratios were detected. TOF-ND confirms that the filling material surrounding 'B' and 'D' is sodium chloride, while that around 'A' and 'C' consists of 75 wt% calcite ($CaCO_3$) and 25 wt% quartz (SiO_2). There are no clear indications in the TOF-ND data about the compositions of the dividing sheet. The higher aluminium contribution observed in the n2 and n5 PGAI measurements may be originated from the irradiation of the dividing sheet. Detailed results are listed in **Table 3**.

Aluminium box D-V.

For the layout, the description and the nominal composition of the box refer to Kirfel (2008).

Radiography images (Fig. 7a, b)

• X-ray [XR-Ghe] and neutron radiography [NR-Bud] images: the embedded tubes aligned on an axis

• there is no sign of filling materials

Measurement points with PGAI (Fig. 7 c,d)

• chord type setup on the NIPS station, beam size: 2 mm × 20 mm.

• irradiations n1 - n3: parallel the common axis of the tubes.

PGAI conclusions

• all tubes are made of copper

• no filling material detected

TOF-ND conclusions (Festa et al. 2008)

• same results as in PGAI

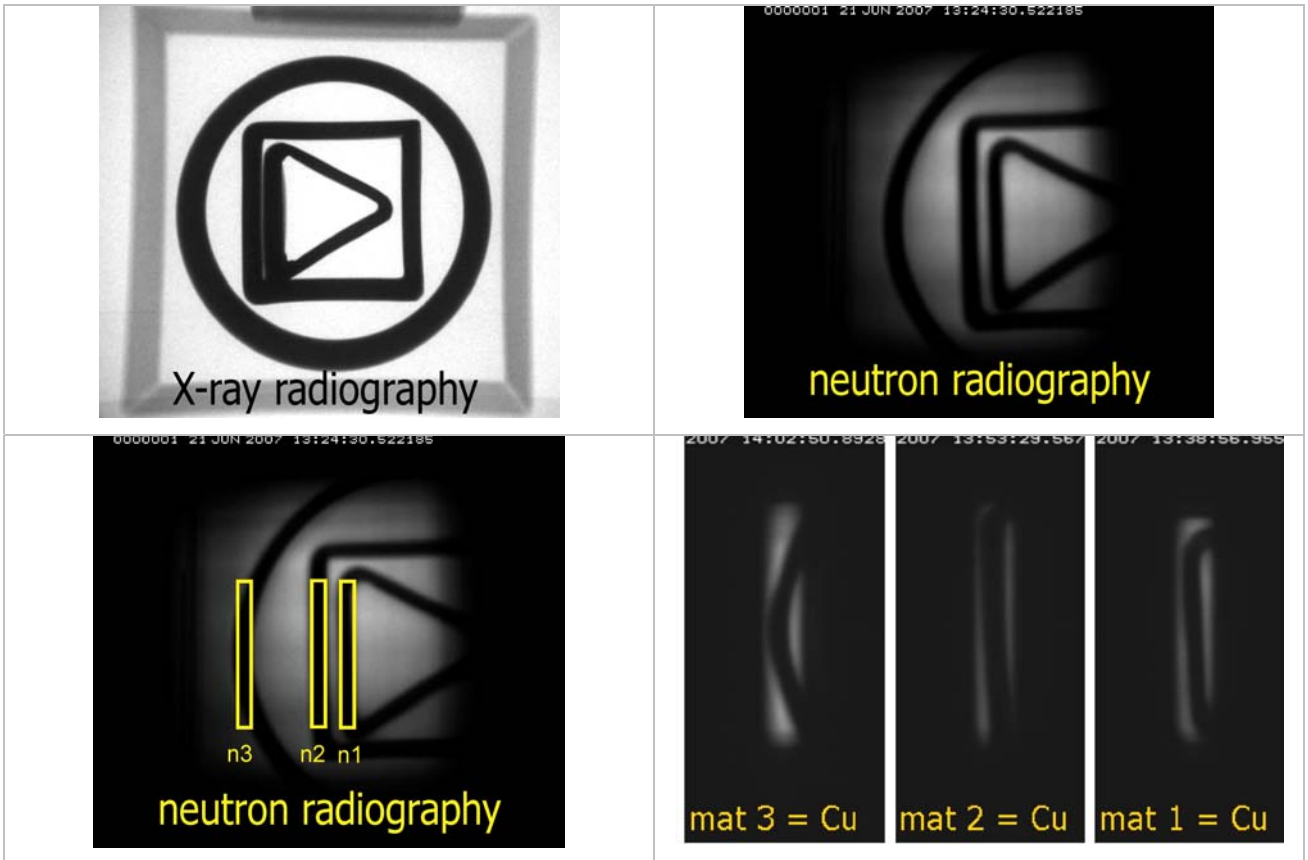

Fig. 7

a, X-ray radiography image of box D-V (top left); b, neutron radiography image of box D-V (top right)

c, measurement points on box D-V(bottom left); d, views through the collimator on box D-V (bottom right)

HU ISSN 1786-271X; urn:nbn:hu-4106 © by the author(s)

Table 4. - Details of the composition of the box D-V.

Nr.	**Nominal composition**	**Meas. type and Nr. of PGAI beam**	**PGAI results**	**TOF-ND results** (Festa et al. 2008)
1	Cu	chord: n1	**Cu**, **Al**	same result
2	Cu	chord: n2	**Cu**, **Al**	
3	Cu	chord: n3	**Cu**, **Al**	

Discussion

This box can be considered as an easy case for PGAI. Based on the results from the chord setup on NIPS it was concluded that all tubes are made of pure copper (see **Table 4**). In this case, TOF-ND and PGAI gave the same results.

Aluminium box D-VI.

For the layout, the description and the nominal composition of the box refer to Kirfel (2008).

Radiography image (Fig. 8a)

• the materials greatly attenuate the cold neutrons, neutron radiography images were not taken

• for low-energy neutrons, this box is again 'black'; the depth of analytical information by PGAI is limited.

• X-ray radiography [XR-Ghe] (figure below) was used to move the interesting parts of the box to the measuring positions.

Measurement points with PGAI (Fig. 8b)

• chord type setup on the PGAA station, beam size: 24 mm^2.

• irradiations n1 - n3: perpendicular to the V-arrangement.

• irradiations n1 and n3: information about the material of the sheets

• irradiation n2: characterises the filling material.

PGAI conclusions

• only Fe was identified both for sheet and filling materials

• significant difference between the count rates originating from sheets and filling material

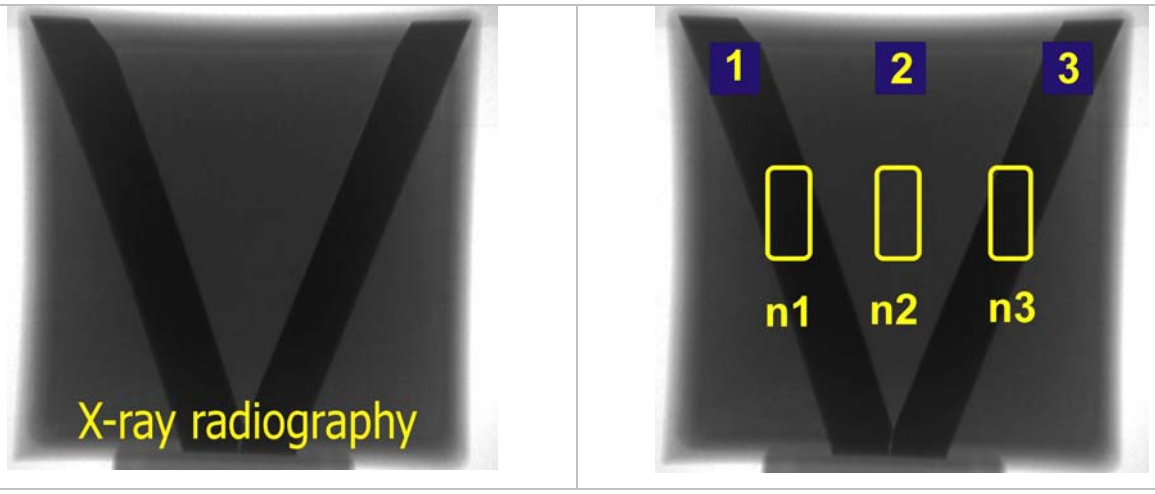

Fig. 8

a, X-ray radiography image of box D-VI (left), b, measurement points on box D-VI (right)

Table 5. - Details of the composition of the box D-VI.

Nr.	**Nominal composition**	**Meas. type and Nr. of PGAI beam**	**PGAI results**	**TOF-ND results** (Festa et al. 2008)
1	iron	chord: n1	**Fe**, Al	ferrite
2	hematite	chord: n2	**Fe**, Al	hematite (Fe_2O_3)
3	iron	chord: n3	**Fe**, Al	ferrite

HU ISSN 1786-271X; urn:nbn:hu-4106 © by the author(s)

TOF-ND conclusions (Festa et al. 2008)

• sheets (1 and 2) are ferrite (Fe)

• filling material (3) is hematite (Fe_2O_3)

Discussion

The results from the chord setup on the PGAA station seemed to indicate that the components and fillings inside the box were only made of iron. However, there was a significant difference between the count rates due to the different density of the sheets and filling material. PGAI can not distinguish between the phases or different chemical forms of iron therefore a combination with neutron diffraction is useful. TOF-ND shows that the iron phase in the sheets is ferrite (bcc iron), and the filling material is hematite (see **Table 5**).

Aluminium box D-VII.

For the layout, the description and the nominal composition of the box refer to Kirfel (2008).

Radiography images (Fig. 9)

• X-ray radiography images [XR-Ghe]: three parallel layers with different absorption coefficients

• layers composed of smaller blocks and geometrical shapes: in the middle of the lowest layer, there seems to be a hole or a different material.

Measurement points with PGAI (Fig.10)

• chord type setup on the PGAA, beam size: 24 mm^2: neutron beams are labelled as n1 and n2

• neutron radiography driven isovolume type measurements on the NIPS station, 2 mm × 10 mm beam: neutron beams labelled as n3, n4 and n5; gammas from isovolume labelled as g3, g4 and g5

PGAI conclusions

• very low count rate, hard to draw conclusions

• with PGAI on NIPS, mainly C and Al have been identified in the layers.

• PGAI identifies Na, which comes from diaoyudaoite.

• PGAI identifies Si and H, which comes from pyrophyllite

TOF-ND conclusions (Festa et al. 2008)

• TOF-ND indicates the presence of corundum (Al_2O_3), graphite (C) and other non-identified phases in layers z1, z2 and z3, respectively.

Discussion

Two of the irradiations (n1 - n2) were carried out in chord setup, three (n3 - n5) in isovolume setup. In the case of n1 the gamma radiation gives information about the material in layer z1. Unfortunately, the results from n2 characterise all the three layers together because the neutron beam goes through all of them; therefore it is difficult to separate the contributions of the different layers.

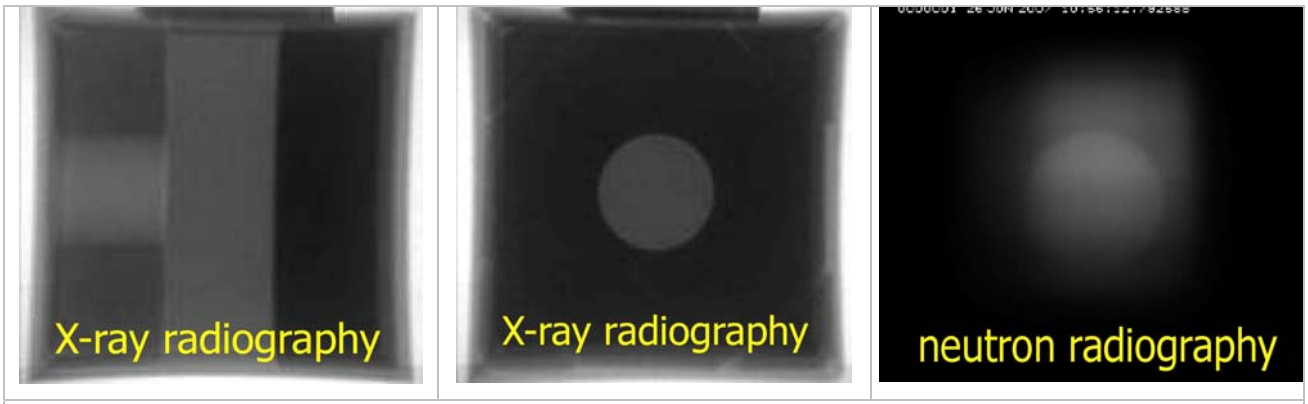

Fig. 9

a-b, X-ray radiography images of box D-VII (left, centre);

c, neutron radiography image of box D-VII (right)

Table 6 - Details of the composition of the box D-VII.

Nr.	**Nominal composition**	**Meas. type and Nr. of PGAI beam**	**PGAI results**	**TOF-ND results** (Festa et al. 2008)
z1	corundum	chord: n1, n2 isovolume: n3	H, Na, **Al**	corundum (Al_2O_3), graphite (C)
z2	graphite	chord: n2 isovolume: n4	H, **C**, Na, **Al**, Si	corundum (Al_2O_3), graphite (C)
z3	pyrophyllite	chord: n2 isovolume: n5	H, **Al**, Si	phase not-identified

HU ISSN 1786-271X; urn:nbn:hu-4106

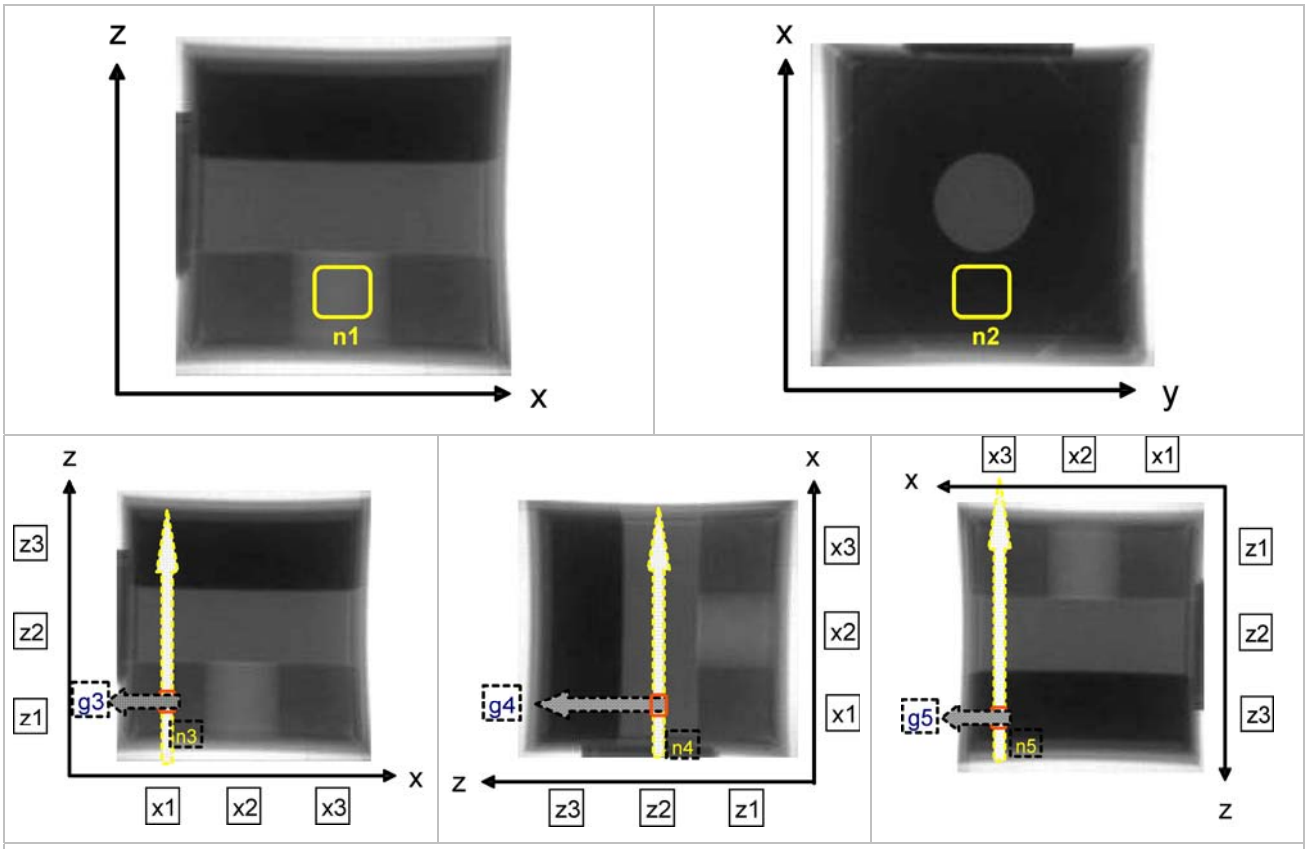

Fig. 10

a-e, measurement points on box D-VII from different orientation (a-b: chord, c-e isovolume)

In the isovolume arrangement one can better position the source of the analytical information (the isovolume) into the layer of interest, but in this case the count rate is very low. During the limited beam time, the counting statistics was not good enough to provide information about all components. A higher neutron flux could help to increase the low count rate.

With PGAI, mainly C and Al could be identified in the layers; however, other elements such as H, Na, and Si are also recognisable. TOF-ND indicates the presence of corundum (Al_2O_3), graphite (C) and some other non-identified phases in layers z1, z2 and z3 (see **Table 6**).

Iron box H-I.

For the layout, the description and the nominal composition of the box refer to Dúzs (2008).

Radiography images (Fig. 11)

• X-ray [XR-Ghe] and neutron radiography [NR-Bud]: the parallel rods have different absorption coefficients. The darker the colour the higher is the absorption.

• removable Gd dots were painted on the surface of the box to help with the positioning

Measurement points with PGAI (Fig. 12)

• studied in chord type, as well as in isovolume setup on the NIPS station

• beam size: 2 mm × 20 mm (chord setup), 2 mm × 10 mm (isovolume setup)

• neutron radiography driven chord type measurements, the beams (n1 - n3) hit more rods behind each other:

• Neutron radiography driven isovolume type measurements: Gd dots (see on the images)

HU ISSN 1786-271X; urn:nbn:hu-4106 © by the author(s)

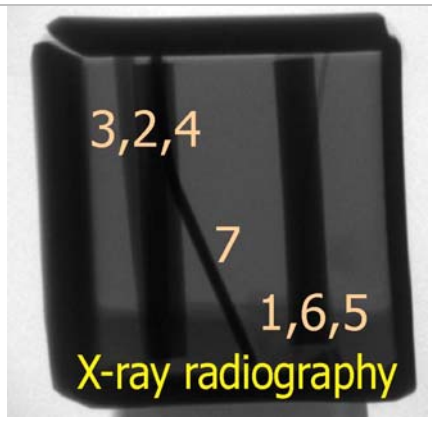

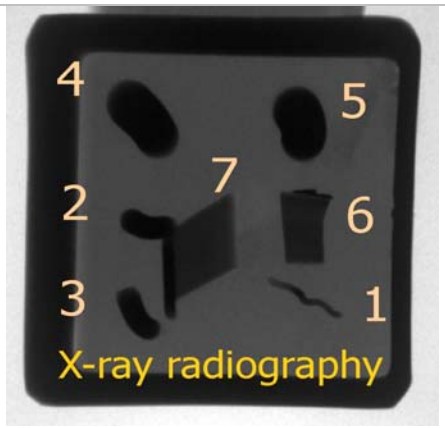

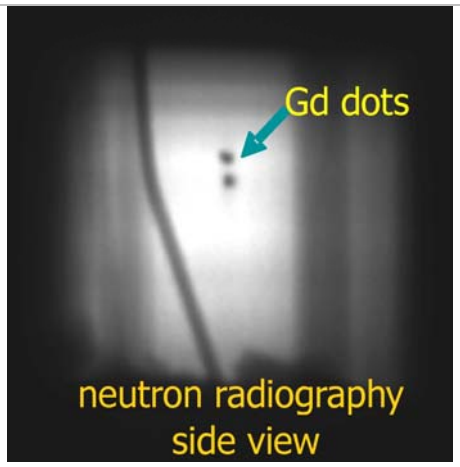

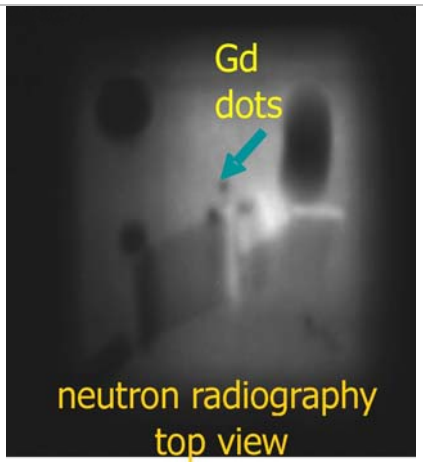

Fig. 11

a-b, X-ray radiography images of box H-I (top); c-d, neutron radiography images of box H-I (bottom)

Table 7. - Details of the composition of the box H-I.

Nr.	**Nominal composition**	**Meas. type and Nr. of PGAI beam**	**PGAI results**	**TOF-ND results** (Festa et al. 2008)
1	copper wire	chord: n2	**Cu**, Zn	copper or steel
2	brass wire	chord: n1 isovolume: n1	**Cu**, Zn	copper
3	copper wire	chord: n1 isovolume: n1	**Cu**, Zn	brass or bronze
4	brass rod	chord: n1	**Cu**, Zn	brass or bronze
5	copper rod	chord: n2	**Cu**, Zn	copper, indications of Zn
6	zinc plate	chord: n2	**Cu**, Zn	copper or steel, strong Al/Ag peaks
7	iron plate	chord: n3	**Fe**	indications of copper/steel

PGAI conclusions

- chord setup: rods in a line are measured together
- isovolume: low count rate
- need for removable Gd dots to orientate the box

TOF-ND conclusions (Festa et al. 2008)

- gypsum at each measurement point
- P1, P4, P5 were assigned correctly
- P2, P3 analyses are wrong: misalignment error
- P6: Zn is not identified
- P7: fcc-phase, in agreement with steel

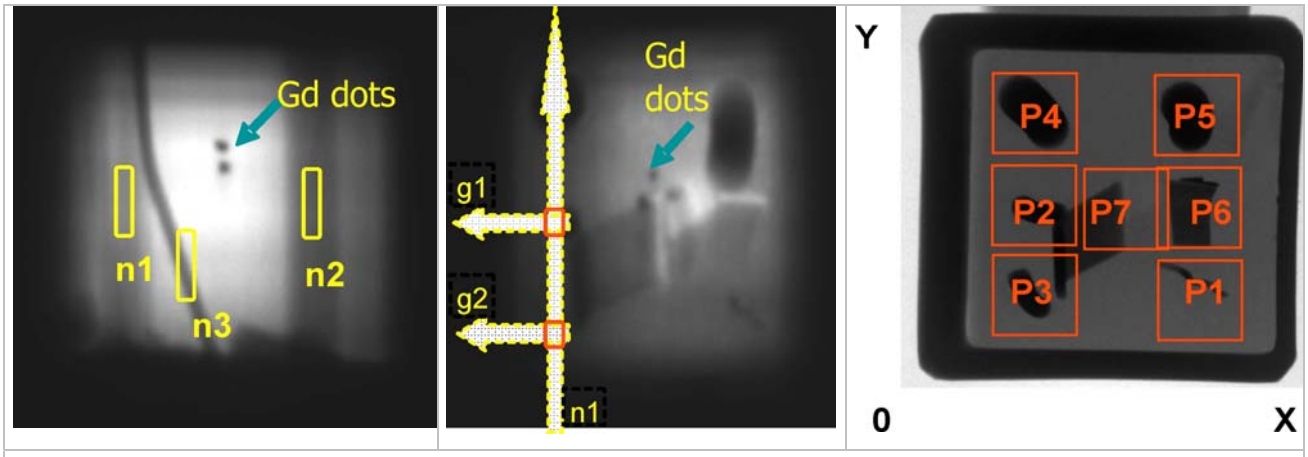

Fig. 12

a, measurement points on box H-I (chord); b, measurement points on box H-I (isovolume); c, TOF-ND measurement points on box H-I

Discussion

The X-ray radiography [XR-Ghe] and neutron radiography [NR-Bud] images present seven rods or wires arranged approximately parallel to each other. There are no clear differences in contrast visible in the radiographies. In the chord type experiments the gammas come from all the rods aligned with the neutron beam (n1 and n2). Therefore the rods in a line are indistinguishable. Based on the PGAI results the metal rods and wires contain copper and zinc; therefore some of them are brass or other zinc containing material. To find out the exact composition of two rods, the isovolume type arrangement was applied. The box was positioned using removable Gd dots painted on its surface. The neutron beam n3 impinged on a plate alone (it was bent for unknown reasons). PGAI yielded mainly iron and a negligible copper content. This latter may originate from the rods next to the path of the neutron beam. The detailed results can be seen in **Table 7**. The results from TOF-ND experiments which suffered from misalignment problems partially confirm the PGAI findings.

Iron box H-III.

For the layout, the description and the nominal composition of the box refer to Dúzs (2008).

Table 8. - Details of the composition of the box H-III.

Nr.	**Nominal composition**	**Meas. type and Nr. of PGAI beam**	**PGAI results**	**TOF-ND results** (Festa et al. 2008)
1	copper sheet	chord: n3	**Cu**	not used
2	iron sheet	chord: n2	**Fe**, Mn, Cu	
3	brass sheet	chord: n7	**Cu**, Zn	
4	copper sheet	chord: n8	**Cu**	
5	iron sheet	chord: n5	**Fe**, Mn, Cu	
6	brass sheet	chord: n4	**Cu**, Zn	
7	iron sheet	chord: n10	**Fe**, Mn, Cu	
8	brass sheet	chord: n9	**Cu**, Zn	
9	steel sheet	chord: n11	**Fe**, Mn, Cu	
-	void between Fe wall and 2	chord: n1	**Fe**, Mn	
-	void between 3 and 5	chord: n6	**Fe**, Mn, Cu	

HU ISSN 1786-271X; urn:nbn:hu-4106 © by the author(s)

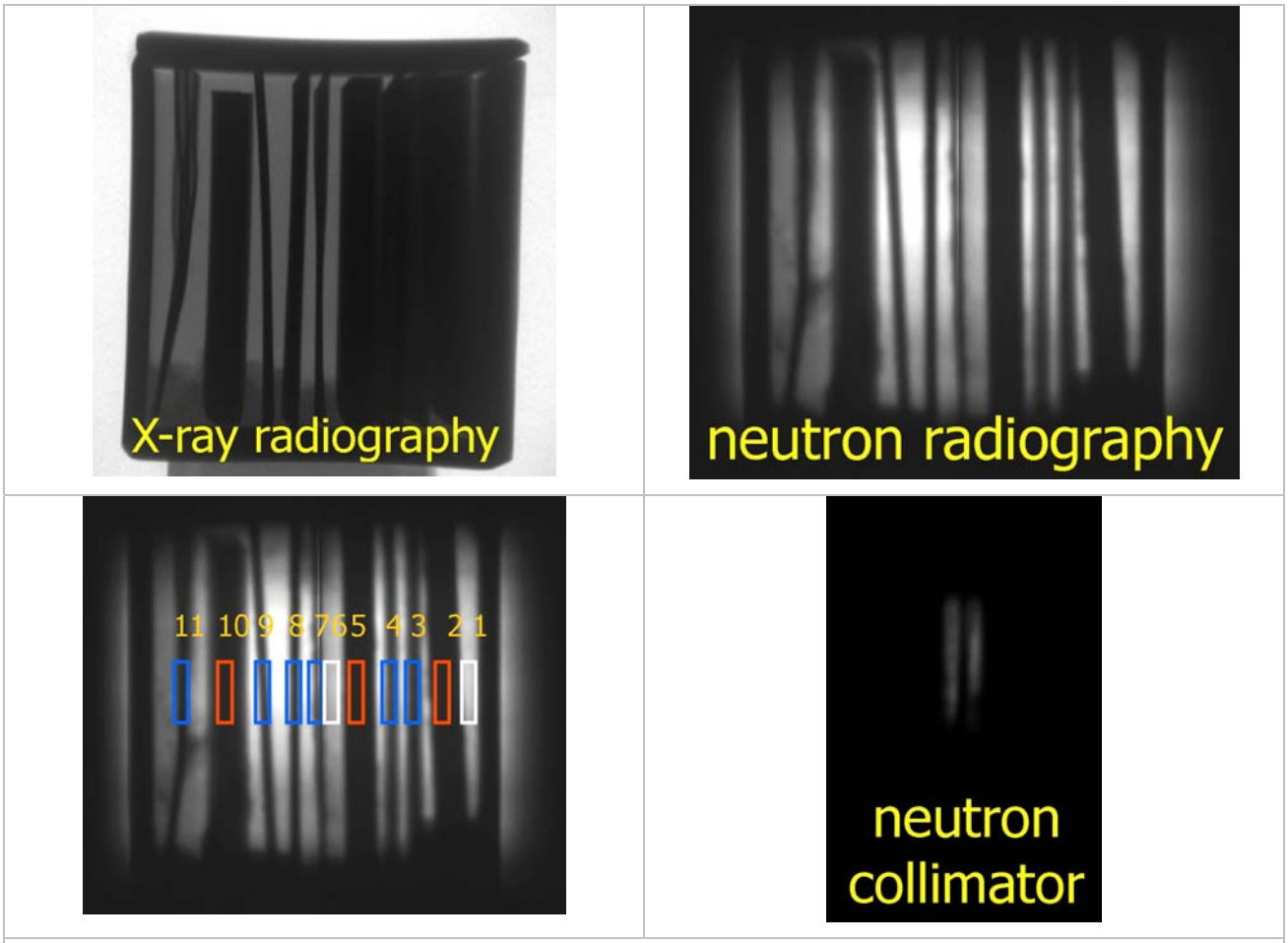

Fig. 13

a, X-ray radiography image of box H-III (top left); b, neutron radiography images of box H-III (top right); c, measurement points for box H-III (bottom left); d, view through the collimator on box H-III (bottom right)

Radiography images (Fig. 13a, b)

• X-ray [XR-Ghe] and neutron radiography [NR-Bud] images: parallel sheets with different mass absorption

• neutron radiography image: prepared by merging two separate shots because the neutron beam size was smaller than the dimension of the box

Measurement points with PGAI (Fig. 13c)

• neutron radiography driven chord type setup on the NIPS station: all nine sheets and two void volumes between them were analysed by PGAI

• beam size: 2 mm × 10 mm

• the collimated neutron beam is shown on **Fig. 13d**

• neutron beams are labelled as n1 - n11 (**Figs. 13c, 14**)

• distances on the neutron radiography image: determination of successive offsets of the moving table

PGAI conclusions

• 3 Fe sheets: n2, n5 and n10 (red rectangles) in accordance with the nominal ones, intensity indicates the self-absorption

• 2 Cu sheets: n3, n8 (blue rectangles) in accordance with the nominal ones

• 3 brass sheet: n4, n7, n9 (blue rectangles) in accordance with the nominal ones

• 1 Cu sheet: n11 (blue rectangle) in contradiction to the nominal one (Fe)

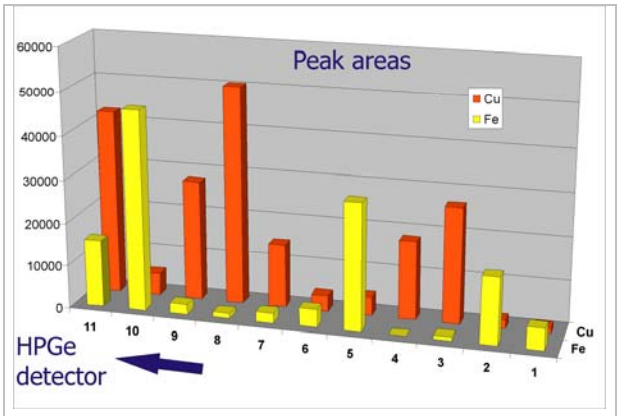

Fig. 14 – Peak areas of measurements for box H-III

TOF-ND conclusions (Festa et al. 2008)

• not used because of possible misalignment

Discussion

As seen in the X-ray radiography [XR-Ghe] and neutron radiography [NR-Bud] images, this box contains nine thicker and thinner metal sheets arranged parallel to each other. There is no visible filling material between the sheets. Based on the radiographs, eleven sections were measured by PGAI in a chord type setup. The successive offsets of the moving table are determined so that the sections to be measured are positioned in front of the neutron slit. In nine sections the neutron beam irradiated the metal plates and in two sections the void space between them.

The PGAI results indicated three iron, two copper and three brass sheets. The brass sheets were identified based on their copper and zinc contents (see **Table 8**). Sheet No. 9 showed different composition (copper) than to the nominal (steel). This issue will be verified by opening the box after all neutron measurements have been completed. The iron signal when measuring the voids is attributed to the box wall.

Significant gamma absorption can be observed by comparing the gamma intensities for spots n2, n5 and n10. The corresponding sheets are made of iron of similar thickness therefore the emission rate of their gammas should be equal. One can, however, note that the detected intensities from the sheets closer to the gamma detector are increasing. This is due to the decreasing amount of absorbing materials between the sheet of interest and the HPGe detector. The results from TOF-ND experiments were not involved into the assessment of the PGAI results, because all TOF-data show the same pattern. It has to be assumed that the scan was not, as planned, across the different plates. Maybe the incoming beam was impinging on the flat side of the sheets.

Iron box H-IV.

For the layout, the description and the nominal composition of the box refer to Dúzs (2008).

Radiography images (Fig. 15a-c)

• X-ray [XR-Ghe] and neutron radiography [NR-Bud] images: filling materials with different absorption coefficients.

Measurement points with PGAI (Fig. 15d)

• neutron radiography driven chord setup on the NIPS station, beam size: 2 mm × 10 mm.
• neutron beams: labelled as n1 - n5
• distances on the neutron radiography image: determination of successive offsets of the moving table
• beams n1 and n4 were let through the rods behind each other

PGAI conclusions

• very similar spectra from n1, n3, n4 and n5, except for the counting rates
• iron found
• some unexpected Cu and Al found
• spectrum from n2 is characteristic for sand

TOF-ND conclusions (Festa et al. 2008)

• at all points (P1-P9, *Fig. 15d*): quartz, gypsum and small amounts of copper alloys

• P1, P2, P4, P7 show iron oxides (FeO, Fe_3O_4)

• P1-3, P5, P6 indicate Al or Ag

Discussion

Based on the PGAI results the metal rods can be identified as iron with manganese content. The count rates of the spectra differ, which may be due to the different elemental (iron) contents in the path of the beam. Some copper and aluminium components were identified, which is in disagreement with the expected nominal composition of the box. This will be checked by opening the box after all neutron measurements are completed. The signals of silicon and aluminium in both of the compartments may indicate a leakage of the sand from one side into the other. The results of TOF-ND experiments show copper and aluminium as well, which is in disagreement to nominal composition.

The details of the results are shown in **Table 9** (please note that Nr. refer to the numbering of the neutron beam used in PGAI measurements only).

Table 9. - Details of the composition of the box H-IV.

Nr.	**Nominal composition**	**Meas. type and Nr. of PGAI beam**	**PGAI results**	**TOF-ND results** (Festa et al. 2008)
1, 2, 3 (right)	iron rod	chord: n1	**Fe**, **Mn**, C, Al, Si?, Cu	measurement points are different
1, 2, 3 (left)	iron rod	chord: n4	**Fe**, **Mn**, C, Cu, Al?	
4	thin steel sheet	chord: n3	**Fe**, **Mn**, C, Cu, B?, Al?	
5	fill grit	chord: n5	**Fe**, **Mn,** C, Cu, B?, Al?	
6	fill sand	chord: n2	**B**, **Al**, **Si**, K?, Ti?, Fe, Mn, C	

HU ISSN 1786-271X; urn:nbn:hu-4106

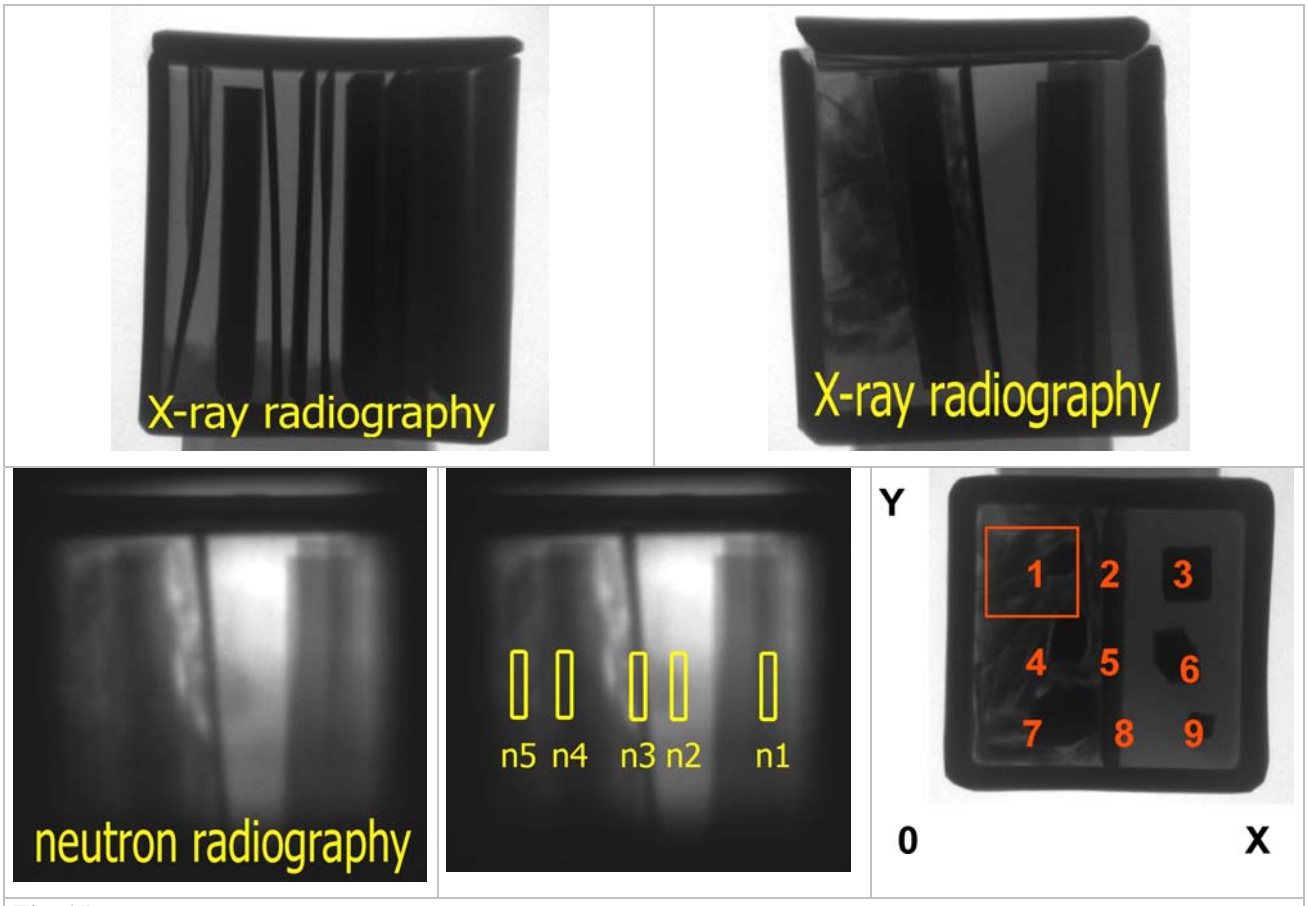

Fig. 15

a-b, X-ray radiography images of box H-IV (top); c, neutron radiography image of box H-IV (bottom left); d, PGAI measurement points on box H-IV (bottom centre); e, TOF-ND measurement points on box H-IV (bottom right)

Iron box H-VI.

For the layout, the description and the nominal composition of the box refer to Dúzs (2008).

Radiography images (Fig. 16a-b)

• X-ray radiography images [XR-Ghe]: four sections of equal sizes with different absorption coefficients. Darker colours indicate higher absorption.

• section (1+2): filled with some chipping material.

• sections 3 and 5: visible homogeneous filling material

• section 4: filled with granulated pieces

• The neutron radiography images [NR-Bud] are presented in the section 'Measurement points with PGAI' because they show the positions of the neutron irradiations as well.

Measurement points with PGAI (Fig. 16c-d)

• materials of all four sections were analysed by PGAI separately

• box was studied in a chord type setup both on the PGAA and on the NIPS stations; in isovolume setup only on the NIPS station.

• PGAI on PGAA station, chord-type measurements (beam size: 44 mm^2): the positions of the neutron beam in chord type setup are the same as on NIPS, only the irradiated areas are larger;

• PGAI-NT on NIPS, neutron radiography driven chord type and isovolume measurements (beam size 2 mm × 10 mm):

- neutron beams: labelled as n1 - n5
- beam used for isovolume experiment is labelled as n6, its gamma ray is g6.

PGAI conclusions

• section (1+2): fibre-like material (Ag chippings)

• section 3: predominantly Si

• section 4: predominantly Fe

• section 5: Na and Cl in a molar ratio 1:1

• Al in the sections (1+2) and 5

• Cu from the crossing point (7) of the sheets

HU ISSN 1786-271X; urn:nbn:hu-4106 © by the author(s)

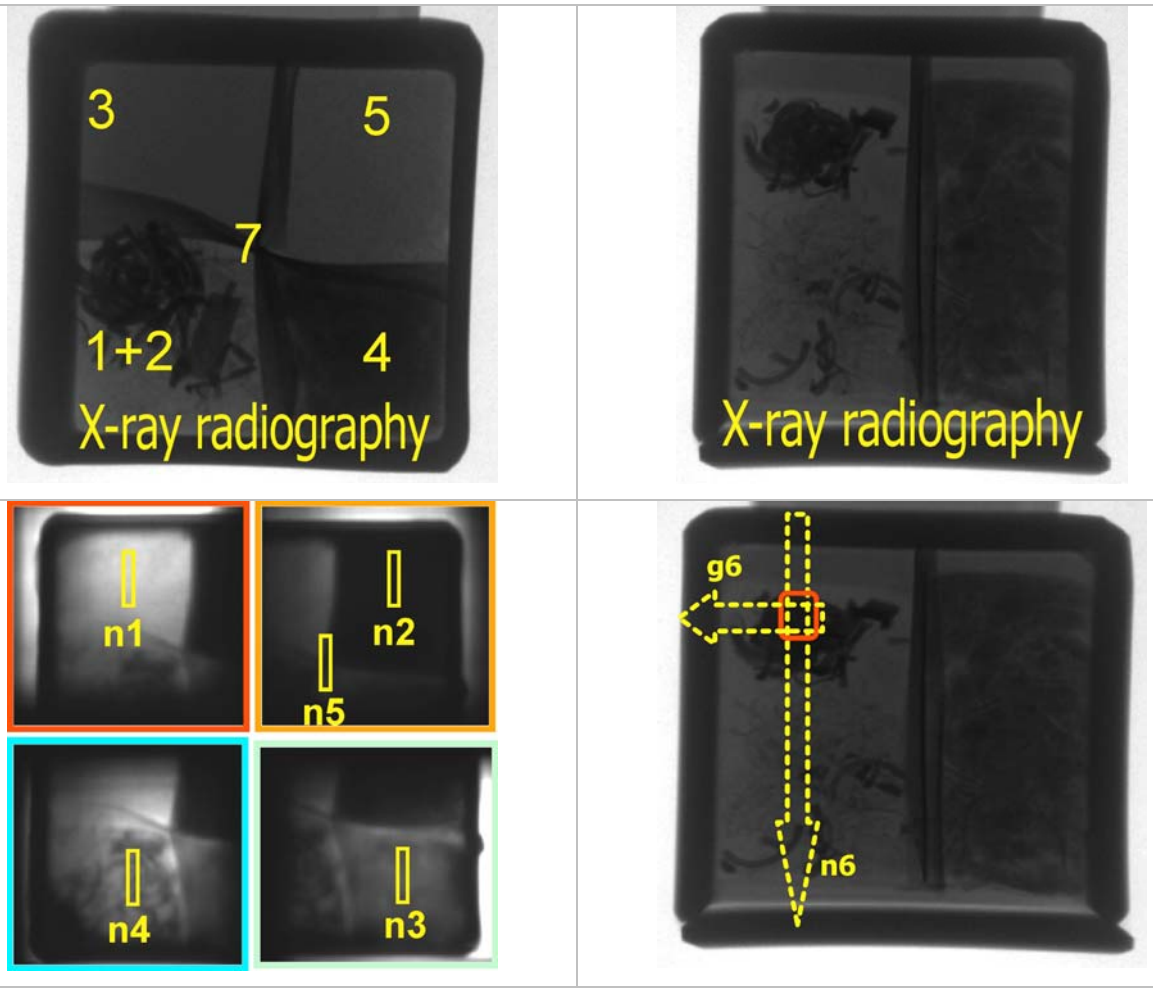

Fig. 16

a-b, X-ray radiography images of box H-VI (top); c, PGAI measurement points for box H-VI (bottom left, chord) d, PGAI measurement point for box H-VI (bottom right, isovolume)

Table 10. - Details of the composition of the box H-VI.

Nr.	**Nominal composition**	**Meas. type and Nr. of PGAI beam**	**PGAI results**	**TOF-ND results** (Festa et al. 2008)
1+2	Ag in talcum	chord: n4 isovolume: n6	H, Si, Cl, Mn, Fe, Cu, **Ag**	quartz (SiO_2), gypsum ($CaSO_4(H_2O)_2$), talc ($Mg_3(OH)_2$ (Si_4O_{10})), Al or Ag, based on PGAI: Ag
3	sand	chord: n1	H, B, Na, Al, **Si**, Cl, K, Ti, Mn, Fe, Cu	quartz, gypsum, talc, Al or Ag, Cu-type fcc (bronze, brass)
4	iron grit	chord: n3	H, B, Al, Cl, Mn, **Fe**	gypsum, talcum, Cu-type fcc (bronze, brass), wuestite (FeO), magnetite (Fe_3O_4)
5	salt	chord: n2	**Na**, Al, **Cl**, Cu	quartz, halite (NaCl), gypsum, talc, Cu-type fcc (bronze, brass)
6	Al plate	-	-	
7	Cu sheets	chord: n5	H, Na, Al, Si, Cl, Mn, Fe, **Cu**, Zn, Ag	halite (NaCl), gypsum, talc, Al or Ag, Cu-type fcc (bronze, brass), wuestite (FeO)

HU ISSN 1786-271X; urn:nbn:hu-4106 © by the author(s)

TOF-ND conclusions (Festa et al. 2008)

• gypsum and talc in all sections

• mainly Al or Ag in section (1+2) (cannot be distinguished)

• mainly quartz and sodium chloride in section 2

• mainly quartz in section 3

• mainly iron oxides in section 4

Discussion

According to the X-ray radiography [XR-Ghe] and neutron radiography [NR-Bud] images taken from different views, this box is divided into four sections of equal sizes with a crossing pair of separating sheets. Based on the different transmissions observed by radiography, the four sections apparently contain different materials. Moreover, a strong neutron absorber fibre-like material is placed in section (1+2). All four section materials were analysed by PGAI and TOF-ND. Details of the identified elemental and crystalline components are summarised in **Table 10**. With PGAI the fibre-like material in section (1+2) was identified as Ag. Predominantly Si was found in section 3 and Fe in section 4, whereas Na and Cl in section 5. Since the molar ratio of Na and Cl in section 5 is 1 to 1, it was asserted that this section contains simply sodium chloride. There were signals of Al in two measurements carried out in sections (1+2) and 5. It is due to the Al plate covering the sections. The measurement at the crossing points of the sheets confirmed the presence of Cu.

These results reasonably agree with the TOF-ND results. TOF-ND has identified gypsum and talc in all sections, probably as filling material. This result may indicate a misalignment or it may indicate that talc powder leaked from (1+2) into other compartments. TOF-ND identifies quartz in section (1+2) and 3, quartz and sodium chloride in section 5, iron oxides (wuestite, magnetite) in section 4, and Al or Ag in section (1+2) (see **Table 10**). TOF-ND cannot distinguish between Al and Ag, which have the same structure and almost the same lattice parameters. Based on PGAI results, the material proved to be Ag. The wuestite could probably be part of the iron box walls. TOF-ND shows an fcc-phase in some points with clearly larger lattice parameters than pure copper, indicating the presence of a copper alloy such as bronze or brass. The identification of Zn by PGAI decides for brass rather than bronze.

Iron box H-VIII.

For the layout, the description and the nominal composition of the box refer to Dúzs (2008).

Radiography image (Fig. 17a)

• investigated only on PGAA station, no neutron radiography images taken

• X-ray image [XR-Ghe]: the content of the box is almost homogeneous; some shadows of parts with higher absorption

Measurement points with PGAI (Fig. 17b-c)

• chord type setup on the PGAA station, beam size: 44 mm^2.

• spots are labelled as n1 - n8 in the figures below.

PGAI conclusions

• all spectra were very similar

• chord type measurements: not able to distinguish between different parts

TOF-ND conclusions (Festa et al. 2008)

• beam does not pass through the box

• moderate amorphous background at spot 1 and 2 but no distinct crystalline material *(Fig. 17d)*

Discussion

The pottery fragments and the gypsum filling material seem to have very similar elemental composition and neutron mass absorption coefficients, thus PGAI and NT were not capable of making a good distinction. The gamma spectra taken at different parts of the box were too similar to each other (**Table 11**) and the contrast in neutron images was hardly visible. Unfortunately, the TOF-ND results can not reveal the composition of the box, only Bragg peaks of ferrite (front wall) are observed and no crystalline material could be identified.

Conclusions

PGAA and TOF-ND are standard non-destructive techniques for bulk elemental or phase analysis. They both provide information averaged over the irradiated volume, which is primarily determined by the neutron beam dimension. PGAA with a wide beam spot is fast, but the spatial resolution is not sufficient to reveal fine details inside the objects. Narrowing the neutron beam makes the use of a chord or an isovolume setup feasible; this is the advent of PGAI. The actual composition and structural issues of the sample being under investigation will determine the usefulness and effectiveness of PGAI, either alone or in combination with TOF-ND. In some cases, applying radiography driven PGAI alone yields the information needed. However, in many cases it turned clearly out that the combination of results from TOF-ND and PGAI-NR/NT can sufficiently reveal the properties of the materials. An unlucky situation may happen when even the combination of the methods is unable to identify the exact compositions and structures of details inside the object.

HU ISSN 1786-271X; urn:nbn:hu-4106 © by the author(s)

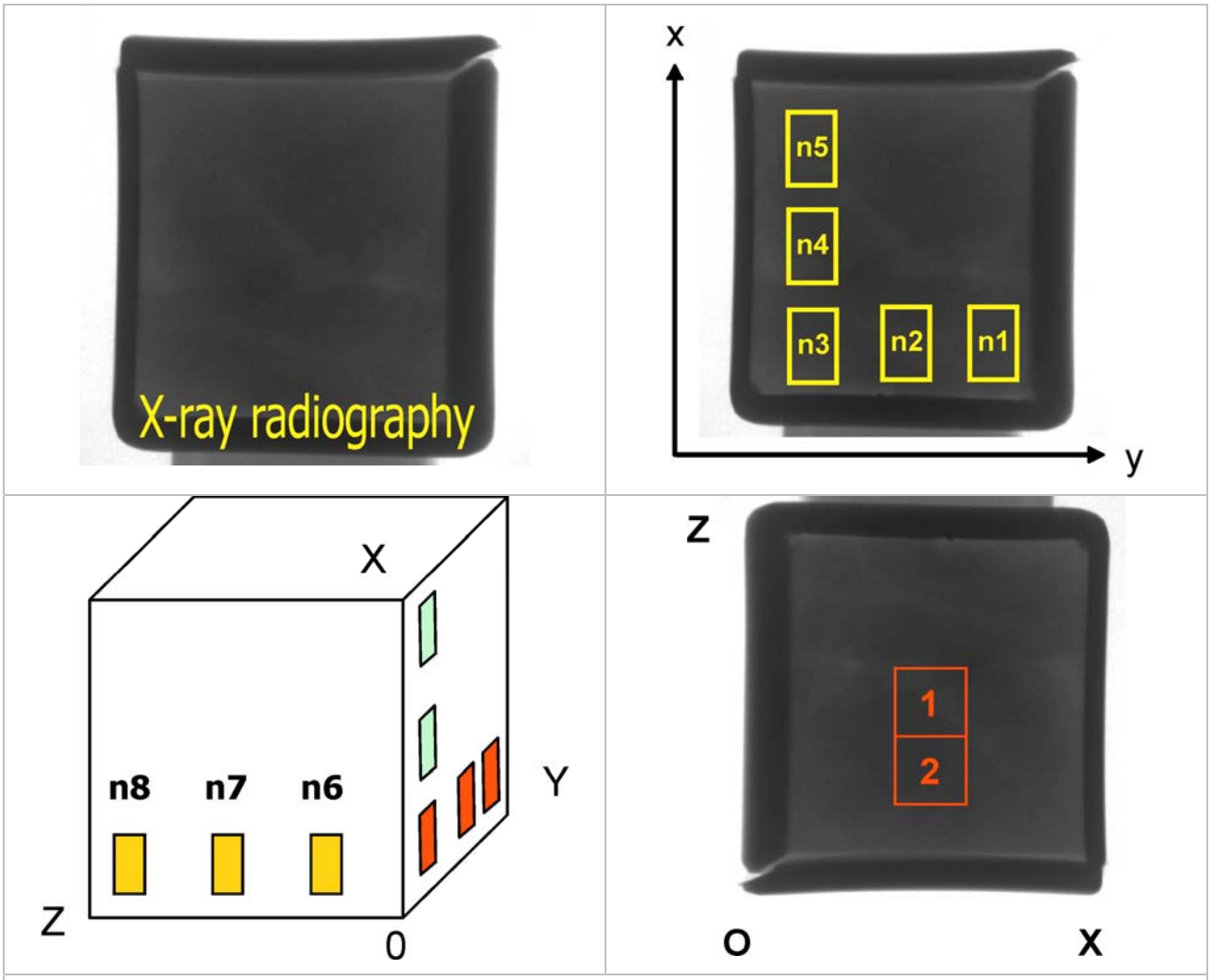

Fig. 17

a, X-ray radiography image of box H-VIII (top); b-c, PGAI measurement points for box H-VIII (top right, bottom left) d, TOF-ND measurement points for box H-VIII (bottom right)

Table 11. - Details of the composition of the box H-VIII.

Nr.	**Nominal composition**	**Meas. type and Nr. of PGAI beam**	**PGAI results**	**TOF-ND results** (Festa et al. 2008)
1	-	chord: n1	**H**, Si, **S**, K, **Ca**	moderate amorphous background; no distinct crystalline material identifiable
2	-	chord: n2	**H**, Al, **Si**, **S**, K, **Ca**, Ti	
3	-	chord: n3	**H**, Al, **Si**, **S**, K, **Ca**, Ti	
4	-	chord: n4	**H**, **Al**, **Si**, **S**, K, **Ca**, Ti	
5	-	chord: n5	**H**, **Si**, **S**, K, **Ca**	
6	-	chord: n6	**H**, **Si**, **S**, K, **Ca**	
7	-	chord: n7	**H**, **Si**, **S**, K, **Ca**	
8	-	chord: n8	**H**, **Si**, **S**, K, **Ca**	

According to the experiments on the black boxes, the methods (PGAI, TOF-ND and NR/NT) provide complementary information; usually none of them is being sufficient alone. NR/NT produces high-resolution 2D/3D images that are required to survey the object for geometrical structure and attenuation features. The contrast features observed in the NR/NT images is extended with a chemical and structural interpretation when information from PGAI and TOF-ND is added. PGAI can 'see' the elements in the chord and/or isovolume, which is an important analysis requirement in archaeological sciences. TOF-ND is phase sensitive and can identify structure and phases, for example distinguish between the different oxides of iron.

Furthermore, for a quantitative composition analysis, neutron self-shielding and gamma self-absorption correction should be introduced, using Monte Carlo calculations.

Acknowledgements

We acknowledge the support of ANCIENT CHARM EU FP6 NEST Contract No. 15311, the NAP VENEUS05 Contract No. OMFB 00184/2006 and the GVOP-3.2.1-2004-04-0268/3.0. The contributions of the ANTARES group at FRM-II, Garching, Germany and the Center for X-ray tomography at the University of Ghent on tomography experiments are also appreciated. This work was supported within the CNR-CCLRC Agreement No. 01/9001 concerning collaboration in scientific research at the spallation neutron source ISIS. The financial support of the Consiglio Nazionale delle Ricerche is hereby also acknowledged.

References

BELGYA, T., KIS, Z., SZENTMIKLÓSI, L., KASZTOVSZKY, ZS., FESTA, G., ANDREANI, C., DE PASCALE, M.P., PIETROPAOLO, A., KUDEJOVA, P., SCHULZE, R. & MATERNA, T. (2007): Working PGAI/NT system at the NIPS facility of the Budapest Research Reactor. *Deliverable D3 for Ancient Charm project:* http://ancient-charm.neutron-eu.net/FILES/DeliverableD3.pdf

DAY, P., ENDERBY, J.E., WILLIAMS, W.G., CHAPON, L.C., HANNON, A.C., RADAELLI, P.G. & SOPER, A.K. (2004): GEM: The general materials diffractometer at ISIS - multibank capabilities for studying crystalline and disordered materials. *Neutron News* **15(1)** 19-23.

DÚZS, K. (2008): Realisation of the planned 'black boxes' in the Hungarian National Museum. *Archaeometriai Műhely / Archaeometry Workshop* **2008/1** 7-20.

FESTA, G., KOCKELMANN, W., KIRFEL, A. (2008): Neutron diffraction analysis of black boxes. *Archaeometriai Műhely / Archaeometry Workshop* **2008/1** 61-72.

GORINI, G. (2007): Ancient Charm: A research project for neutron-based investigation of cultural-heritage objects. *Il Nuovo Cimento* **30C(1)** 47-58.

KASZTOVSZKY, ZS. & BELGYA, T. (2006): From PGAA to PGAI: from bulk analysis to elemental mapping. *Archaeometriai Műhely / Archaeometry Workshop* **2006/2** 16-21.

KIRFEL, A. (2008): Construction and description of the UniBonn black boxes. *Archaeometriai Műhely / Archaeometry Workshop* **2008/1** 21-34.

KOCKELMANN, W. & KIRFEL, A. (2006): Neutron diffraction imaging of cultural heritage objects. *Archaeometriai Műhely / Archaeometry Workshop* **2006/2** 1-15.

KOCKELMANN, W., WEISSER, M., HEINEN, H., KIRFEL, A. & SCHAFER, W. (2000): Application spectrum and data quality of the Time-to-Flight Neutron Diffractometer ROTAX at ISIS. *Materials Science Forum* **321-324 I** 332-337.

KUDEJOVA, P., CIZEK, J., SCHULZE, R., JOLIE, J., SCHILLINGER, B., LORENZ, K., MÜHLBAUER, M., MASSCHAELE, B., DIERICK, M. & VLASSENBROECK, J. (2007): A marker-free 3D image registration for the ANCIENT CHARM project. Case study with neutron and X-ray tomography datasets. *Notiziario Neutroni e Luce di Sincrotrone* **12(2)** 6-13.

RÉVAY, ZS., BELGYA, T. & MOLNÁR, G.L. (2005): Application of Hypermet-PC in PGAA. *Journal of Radioanalytical and Nuclear Chemistry*, **265(2)** 261.265.

RÉVAY, ZS., BELGYA, T., KASZTOVSZKY, ZS., WEIL, J.L. & MOLNÁR, G.L. (2004): Cold neutron PGAA facility at Budapest. *Nuclear Instruments and Methods in Physics Research B* **213** 385-388.

SIMONITS, A., ÖSTÖR, J., KÁLVIN, S. & FAZEKAS, B. (2003): HyperLab: A new concept in gamma-ray spectrum analysis. *Journal of Radioanalytical and Nuclear Chemistry*, **257(3)** 589-595.

NEUTRON DIFFRACTION ANALYSIS OF 'BLACK BOXES'

G. FESTA[1], W. KOCKELMANN[2], A. KIRFEL[3] and the Ancient Charm collaboration

[1]Università degli Studi di Roma Tor Vergata, Rome, Italy
[2]ISIS Facility, Rutherford Appleton Laboratory, Chilton, OX11 0Qx, UK
[3] Steinmann Institute, University of Bonn, D 53113 Bonn, Germany

Email: Giulia.Festa@roma2.infn.it

Abstract

The Ancient Charm *project addresses several aspects of neutron analyses of archaeological materials, with the specific aim to developing neutron activation and neutron diffraction into imaging methods. One of the central techniques is element determination by Neutron Resonant Capture Analysis (NRCA), besides the more established Prompt Gamma Activation Analysis (PGAA). Neutron diffraction is another technique employed in this project, for mapping the spatial distribution of crystallographic phases in a sample.* Ancient Charm *provides the prospect of combining several of these analytical neutron methods with neutron radiography in order to obtain a comprehensive characterisation of the interior of an artefact. This paper reports on neutron diffraction results on 17 of so-called 'Black Boxes', closed cubes containing geometrical arrangements of materials such as metals, minerals, ceramics, and organic matter. The measurements were carried out at the pulse neutron source ISIS at the Rutherford Appleton Laboratory in the United Kingdom. The aim of this 'Black Box' study was to identify strengths and weaknesses of neutron diffraction for analysing archaeological objects and to develop a best practice for a combined use of analysis methods for different combinations of materials*.

Kivonat

Az Ancient Charm *program keretében a régészeti leletanyag neutronfizikai alapokon történő vizsgálatának számos lehetőségét próbáljuk ki, a neutron analitikai vizsgálatok (aktivációs analízis, diffrakció) képalkotási lehetőségeinek gyakorlati kifejlesztésére. Az egyik legfontosabb technika a Neutron Rezonancia Befogási Vizsgálat (NRCA), a másik, már jobban kidolgozott eljárás a Prompt Gamma Aktivációs Vizsgálat (PGAA). A neutron diffrakció olyan eljárás, amelyet a projekt keretében arra alkalmazunk hogy feltérképezzük a minta belsejében kijelölt területek fázisösszetételét. Az* Ancient Charm *program lehetőséget ad többféle neutron alapú analitikai módszer együttes alkalmazására, neutron radiográfiával kiegészítve, hogy a műtárgy belsejének összetételéről részletes ismereteket szerezhessünk. Ebben a cikkben 17 kísérleti próbatest, ún. 'fekete doboz' neutron diffrakciós vizsgálatáról számolunk be. A zárt próbatestekben különféle fémeket, ásványokat, kerámiát és szerves anyagot helyeztek el, szimulálva geometriailag kontrollált körülmények között a tényleges régészeti leletekben előforduló vegyes összetételű tárgyakat. A vizsgálatokat a Rutherford Appleton Laboratory (Nagy-Britannia) ISIS nevű neutron forrásánál vizsgáltuk. A 'fekete dobozok' vizsgálatának célja az volt, hegy megismerjük a neutron diffrakciós vizsgálatok lehetőségeit, előnyeit és hátrányait, régészeti tárgyak vizsgálatára és kifejlesszünk egy eredményes módszertant a különböző vizsgálatok együttes alkalmazására*.

KEYWORDS: NEUTRON BASED IMAGING ANALYSIS, EXPERIMENTS, NEUTRON DIFFRACTION

KULCSSZAVAK: NEUTRON ALAPÚ KÉPALKOTÁSI TECHNIKÁK, KÍSÉRLETEK, NEUTRON DIFFRAKCIÓ

Introduction

Neutrons are a very suitable probe for the non-destructive examination of undisturbed objects and bulky samples made from materials as diverse as ceramics, pigments, glasses, pure metals and alloys. The most important property for material testing is that neutrons have a high penetration power due to the kind of probe-material interaction. In fact, neutrons easily pass through relatively thick samples and transport information about the interior in general and about internal parts in particular that are not visible from the outside. This is an essential characteristic of the neutron techniques, in the case that the analysis of the archaeological object has to be non-destructive.

Several neutron methods are available for the examination of objects, among them elemental analysis and structure analysis methods. An EU-sponsored research project, called ANCIENT CHARM, aims to develop neutron-based techniques into non-invasive methods for 3D imaging of the elemental concentrations and phase compositions of cultural heritage objects (Gorini 2007). The main emphasis of the project is on the development of a relatively new technique, Neutron Resonance Capture Analysis (NRCA) (Postma et al. 2004). This technique has already been frequently used at the neutron source GELINA in Geel, Belgium. One of the tasks in the project is the installation of NRCA on a high-intensity neutron source, the accelerator based pulsed neutron source ISIS in the United Kingdom. For NRCA, the sample is irradiated with 'epithermal' beam, i.e.

relatively fast neutrons, which activate the sample and prompt it to emit gamma radiation, which is particularly strong for certain element specific 'resonance' energies. The intensity of the emitted gamma radiation at a resonance informs about the concentration of the respective element in the irradiated part of the sample. Traditionally, NRCA is applied with wide neutron beams, several centimetres in diameters so that not much position-information of the elements is obtained. It is one of the goals of ANCIENT CHARM to further develop NRCA into a method with a much higher spatial resolution. In the same way and in parallel, other methods are being developed into imaging methods, Prompt Gamma Activation Analysis (PGAA) at the research centre in Budapest and at the research reactor in Munich, as well as Time-of-flight Neutron Diffraction (TOF-ND) at ISIS. The aim of the 'Ancient Charm' project is also to combine these methods with Neutron Tomography (NT) in order to generate a consistent set of 3D images of the internal elemental and phase compositions of complex museum objects.

The focus of the present paper is on neutron scattering, or more precisely, neutron diffraction analysis. In principle, diffracted neutrons can give information on the microscopic structure of a material in terms of crystalline phase abundance (e.g. minerals or metals), of the microstructure, of texture or porosity, and other structural properties. Structure parameters and phase composition(s) of a material are often related to the fabrication methods and treatments that a materials has seen, to the deformation history of the material, and to the corrosion behaviour and corrosion environment. For example, the phase composition of a ceramic object depends on the firing conditions; the microstructure of a metal object depends on the mechanical and thermal treatment during manufacture or usage. The application of neutron diffraction as a non-destructive archaeometric tool to study ceramic and metal artefacts was proposed a few years ago. The characterisation potentials were initially investigated on ceramics (Kockelmann et al. 2001) and archaeological bronze objects (Siano et al. 2002) using the powder diffractometer ROTAX at the pulsed neutron source ISIS. It is important to emphasise that neutron diffraction 'sees' mostly crystalline material, though also glassy materials leave traces in the diffraction data. As for NRCA, quantitative analysis by TOF-ND is typically performed using large neutron spot sizes of several square centimetres. This large beam illumination is sometimes considered an advantage of the neutron analysis because it can provide a representative overview of the sample material, averaged over a large illuminated volume. Neutron diffraction analyses are typically performed on one or several analysis points, either to check for homogeneity of the material or to survey a complex object composed of several parts of different materials. This non-destructive surveying of an object is limited by the available neutron flux, the available beamtime on the diffractometer, by the collection time, and last but not least, by the size of the diffracting volume, i.e. the size of the neutron sampling volume. This volume is defined by the beam cross section area multiplied by the sample extension along the given primary beam direction. It normally takes an one hour 'shot' to analyse one spot, i.e. the sample at a given position and orientation, so that the non-destructive inspection of an object rather than a few 'shots' needs several hours beam time.

For many archaeological objects, a systematic mapping of phases and structures rather than a few 'shot' is highly desirable, often even indispensable for obtaining useful information. Many cases require spatial resolution in the sub-millimetre range. It is obvious that the requirement for high-resolution diffraction imaging is difficult to meet, simply because neutrons are highly penetrating, which is just why they are used for non-destructive testing in the first place. There are essentially two approaches to achieve diffraction imaging, depending on the signal used for mapping. The signal can be extracted from the direct beam (transmission), or from the scattered beam (Bragg diffraction). The transmission techniques, being essentially modifications of conventional radiography/tomography, are fast, since the full object can be simultaneously illuminated. Scattering techniques are typically slow because of the low neutron fluxes compared to X-ray sources and because of the limited access to the diffracted neutrons due to the limited and expensive coverage of the space around a sample with detectors. A complete mapping of an object by neutron diffraction is therefore rather the exception than the rule, and it can only be done with comparatively low spatial resolution in the order of millimetres. In contrast, neutron tomography can produce images in the sub-millimetre resolution range. However, the attenuation images provide merely attenuation contrasts while they can not deliver direct information on the type and structure of materials. That is to say, radiography and tomographies often show high-contrast details of features inside objects but there is no clue to the elemental and structural consistency of the feature. This is why neutron diffraction methods are important; they can give the colours in the radiographies a physical and structural meaning. Consequently, it is generally desirable to use both tomographic and scattering methods aided by the elemental information that can be retrieved from activation methods such as PGAA and NRCA.

HU ISSN 1786-271X; urn:nbn:hu-4106

Table 1 - Analysed Black Boxes at ISIS. Instruments used by TOF-ND: time-of-flight neutron diffraction. PGAA: prompt gamma activation analysis. XR: x-ray radiography. NR: neutron radiography

Box	TOF ND	Complementary methods	Appendix Table
D-II (Al)	ROTAX	XR, NR	Table 1
D-IV (Al)	ROTAX	PGAA,XR	Table 2
D-V (Al)	ROTAX	PGAA, XR, NR	Table 3
D-VI (Al)	ROTAX	PGAA	Table 4
D-VII (Al)	ROTAX	PGAAXR, NR	Table 5
D-VIII (Al)	ROTAX	XR, NR	Table 6
D-IX (Al)	ROTAX	XR, NR, NRCA	Table 7
D-X (Al)	ROTAX	XR, NR	Table 8
D-XI (Al)	ROTAX		Table 9
H-I (Fe)	GEM, INES	PGAA, XR, NR	Table 10
H-II (Fe)	GEM, INES	XR, NR	Table 11
H-III (Fe)	GEM, INES	PGAA, XR, NR	Table 12
H-IV (Fe)	GEM, INES	PGAA, XR, NR	Table 13
H-V (Fe)	GEM	XR, NR	Table 14
H-VI (Fe)	GEM, INES	PGAA	Table 15
H-VIII (Fe)	GEM	PGAA, XR, NR	Table 16
H-IX (Fe)	GEM, INES	XR, NR	Table 17

An overview of aspects and techniques of neutron diffraction imaging is given in Kockelmann & Kirfel 2006.

In the present paper, we report on the neutron analyses of test samples, the so called 'Black Boxes', which were analysed by the different techniques, including neutron diffraction. These test objects are sealed iron or aluminium-walled cubes of 40 and 50 mm edge lengths, respectively, containing 2D or 3D arrangements of materials relevant to the compositions of archaeological samples. One and the same samples were measured with different probes (fast neutrons and slow neutrons, X-rays), different techniques (PGAA, TOF-ND, NT), on different instrument stations, and at different neutron sources in Europe, the Institute of Isotopes in Budapest (Hungary), ISIS (UK), FRM-II Munich (Germany), and GELINA Geel and Ghent (Belgium). The goals of the Black Boxes analyses were to:

- obtain more insights into the potentials and weaknesses of the different methods
- develop a ‘best practice’ procedure of combined efforts,

both with respect to different combinations of materials.

Here, we report on the results of the diffraction analyses on altogether 17 Black Boxes, in comparison with results from other methods, i.e. from neutron radiography and X-ray radiography (Kudejova et al 2007; Kudejova 2008) and PGAA (Kis et al. 2008). In most cases, and at different stages (experimental, data treatment) of the analyses, complementary information from the other techniques was definitely needed to efficiently determine the correct structural composition of a Black Box by diffraction. The paper is organised as follows: **section 2** contains a short description of the samples. In **section 3**, we describe the experimental aspects of the TOF-ND analysis at the ISIS Facility at the Rutherford Appleton Laboratory (Chilton, UK). **Section 4** deals with some of the crystallographic information and peculiarities of the diffraction experiment, as far as important for understanding the diffraction results on the boxes. In **section 5** we discuss the experimental results, mainly referring to the tables in the appendix.

HU ISSN 1786-271X; urn:nbn:hu-4106

In **section 6** the diffraction results are discussed in comparison to results from the other methods as well as to the true compositions of the boxes (reality check) (Kirfel (2008), Dúzs (2008)) revealed after completion of the analyses. Finally, **Section 7** summarises the learned lessons, and draws conclusions of the Black Box analyses. In the appendix, the bulk of the analysis results for each box is summarised in tabulated form. The first part of each table reports on the own diffraction results. These are compared in the second part with information obtained from other methods and also with the now disclosed composition of a box.

Black Boxes

Two sets of sealed Black Boxes were manufactured by the Hungarian National Museum (HNM), Budapest and by the University of Bonn, Germany, respectively. The contents of the boxes were according to the plans and designs proposed by the archaeologists and conservators of the HNM, using typical materials often found in an archaeological context (Hajnal 2008). The first set consists of ten iron cubes of 40 mm edge length (labelled as H-I through H-IX, wall thickness 1 mm; Dúzs 2008). The second set (labelled as D-I through D-XII; Kirfel 2008) comprises twelve aluminium boxes with wall thickness of 1 mm and dimensions of 50 mm. The compositions of the internal parts, the filling materials, as well as the individual layouts were unknown to the experimentalists. The boxes represent increasing levels of complexity, with geometrical 2D or 3D arrangements of different materials.

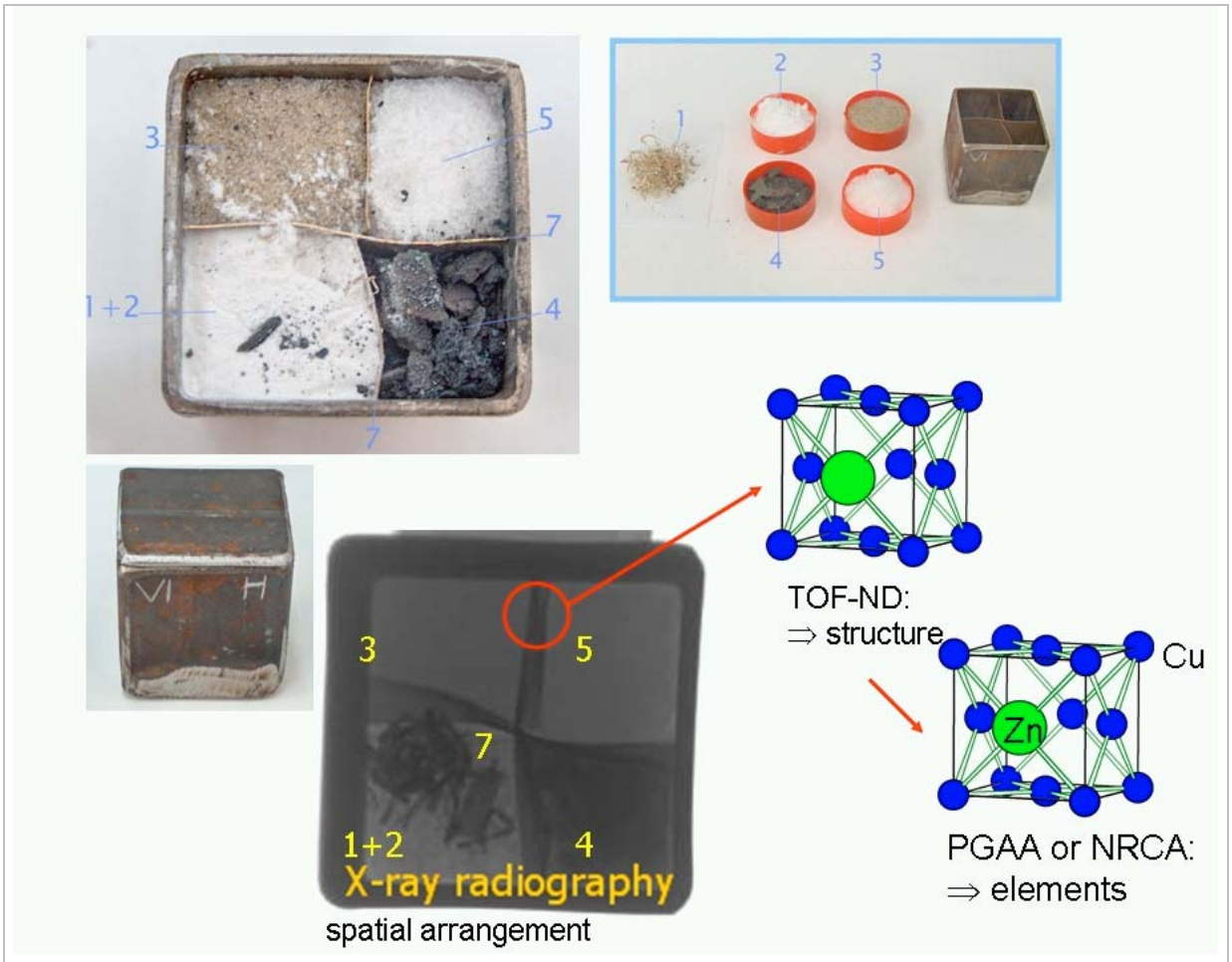

Figure 1.

Construction of Black Box H-VI and X-ray radiograph. Dimension: 4 x 4 x 4 cm3. The radiograph was used to guide the TOF-ND analyses and PGAA analysis. In the highlighted case, neutron diffraction identifies a copper alloy fcc phase as the material of a dividing wall, whilst PGAA is necessary to detect the presence of zinc as alloying element.

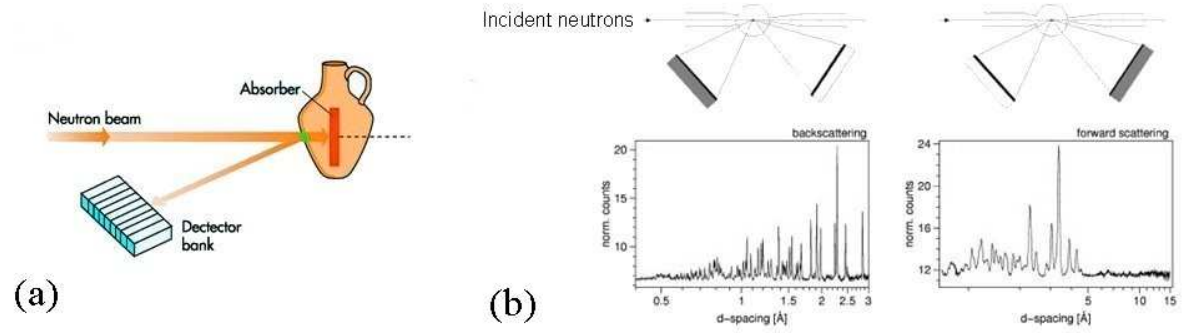

Figure 2.

(a) TOF-ND schematic; (b) patterns collected with detectors at different angles provide different d-spacing ranges with different d-resolutions

The combination of different materials in a particular box was not always following realistic compositions in an archaeological context, but rather chosen to test the capabilities and limitations of the utilised neutron methods, by realising varying degrees of complexity. In this sense, the Black Boxes served as samples in a round-robin for testing the different neutron methods and examining the degree to which the results from the different methods can be combined and made consistent.

Figure 1 shows one of the H-boxes and schematically highlights the complementarity of radiography, structure analysis by TOF-ND and element analysis by PGAA and NRCA. Details of all Black Boxes and their constructions can be found in the same issue of AM (Kirfel, 2008; Hajnal, 2008; Dúzs, 2008).

Experimental

Figure 2a illustrates the basic set-up of a time-of-flight neutron diffraction (TOF-ND) experiment. A neutron beam hits a stationary sample. The 'thermal', relatively slow, neutrons interact with the atoms in the material. Most of the neutrons pass through the material or are absorbed, some of the neutrons are scattered by the nuclei of the atoms and collected with one or more neutron detectors. Elastically scattered neutrons, i.e. those that have not changed their energy during the scattering process, carry the information on the structure of crystalline material. The TOF-ND measurements were carried out on the diffractometers ROTAX (Kockelmann et al. 2000), GEM (Day et al. 2004), and INES (Imberti et al; 2008) at the ISIS Facility, at the Rutherford Appleton Laboratory (Chilton, UK). ISIS is a pulsed neutron source, and as such, capable of providing a sequence of sharp neutron pulses (50 pulses per second), which are required for the TOF technique. Neutrons, after interaction with the sample, are recorded by detectors arranged in banks that measure both the 2Θ scattering angle and the flight time. The data for each bank are converted into a diffraction pattern, neutrons versus crystallographic d-spacing (Å), which are comparable to conventional X-ray powder diffraction patterns (**Figure 2b**). Each detector bank produces a separate histogram; but all histograms for one 'shot' can be entered into the data analysis procedure. The 'backscattering' pattern (see left pattern in **Figure 2b**) has a special relevance for the Black Box analysis because neutrons are scattered (reflected) back into the detector and provide information even if the box contains highly absorbing material. For the forward scattering bank (right pattern in **Figure 2b**) the primary neutron beam, as well as the scattered neutrons, have to cross the full length of the sample so that forward scattering data are much more prone to absorption effects.

Figure 3 shows schematics of the three ISIS instruments used for the Black Box analysis. Although these instruments use the same type of technique they have different characteristics, performances and setups as given in the figure.

Figure 3.

ISIS TOF-diffractometers ROTAX, GEM and INES, with some instrument characteristics.

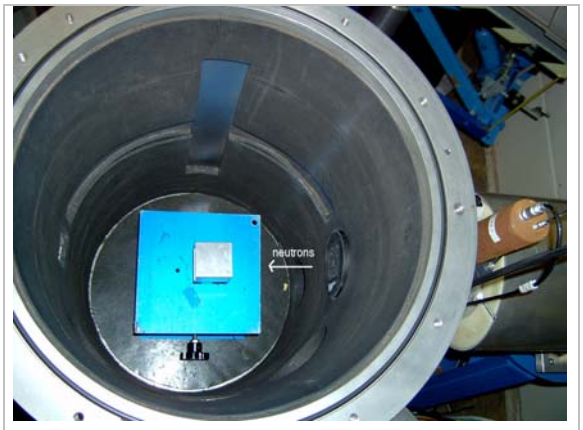

Figure 4.

(a) Black Box in the ROTAX sample chamber. The neutron beam is coming from the right;

(b) schematic experimental set-up (for details, see text). Li is the flight path of the incident neutrons, in meters.

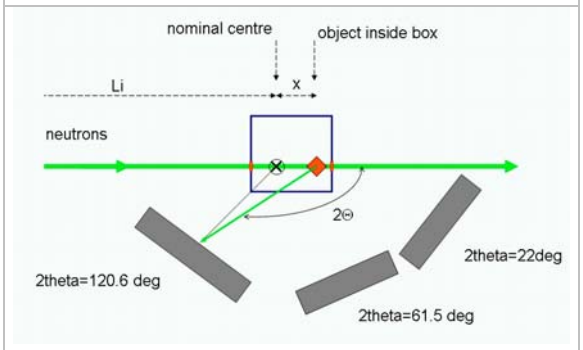

There are, however, some common characteristics for all the measurements: the boxes were mounted on a platform or moving table inside a sample chamber to change the point of impact of the neutron beam and its direction relative to the boxes own coordinate system. The data were collected at standard ambient temperature conditions. Only for some boxes, the sample chamber was evacuated; otherwise measurements were performed in air. The air scattering turned out to be irrelevant. Neutron and X-ray radiographies were used as guides to select the most interesting 'shots' for TOF-ND analyses. The beam size was typically 10 x10 mm^2 except for INES where a beam of 40 x 40 mm^2 was used. Alignments were performed by eye, data collection times lasted between minutes and two hours at most, and data were collected with all available detectors of the instrument.

Correspondingly, in the analyses, all data were taken into account, even though in the following, only selected portions of the diffraction patterns are shown.

Figure 4 shows a photo of one of the boxes on a moving table inside the ROTAX sample chamber. The schematic highlights the following features of the experiment:

- The beam size was typically 10x10 mm^2.
- The detectors collect data from a neutron 'chord' through the whole of the sample.
- If a scattering volume element inside the box is laterally displaced from the nominal centre of the diffractometer, then Bragg peak positions of that material are shifted to different d-values in the pattern. In Fig. 4, the displacement 'x' translates into different d-spacing shifts for the different detector banks. Hence, also the Bragg peaks from the walls of the cubes are shifted with respect to the nominal Al or Fe (database) positions, respectively. Then, in case of a weak neutron-absorbing material inside the box one observes double patterns at backscattering and forward scattering angles. Is, however, the material strong neutron-absorbing, only single Al or Fe Bragg peaks are observed at backscattering angles.
- On one hand, the d-spacing shifts hamper the identification of a phase. On the other hand, these 'x'-shifts can also be used to reconstruct the spatial distribution of the material in an extended object (Gutmann et al. 2006):

  $\Delta d/d = x * \cos(\theta) / L_2$, where Δd is the distance between the observed and the nominal peak position, d is the d-spacing, in Å, L_2 is the distance between sample position and detector, and θ is half the scattering angle.
- Because of the peak shifts for horizontal displacements, accurate lateral positioning of the box in the sample chamber is important in order to obtain signals from the material at the focus. However, without secondary collimation, scattering contributions from other sample parts in the beam cannot be avoided. A vertical shift of the material or sample does not affect the position of the diffraction peaks.

Figure 5 shows for one of the Black Boxes a section of a neutron diffraction pattern collected on ROTAX.

The art of analysing a neutron diffraction pattern obtained from a multi-component sample is to disentangle the different patterns generated by the constituent 'phases', minerals, metals or other crystalline compounds. In the case of the Black Box analyses, the crystalline phases were generally identified by pattern comparison with a database of mineral and metal phases. Semi-quantitative analysis was performed by Rietveld fitting with GSAS (Larsen & von Dreele 1986; Young 1993).

HU ISSN 1786-271X; urn:nbn:hu-4106

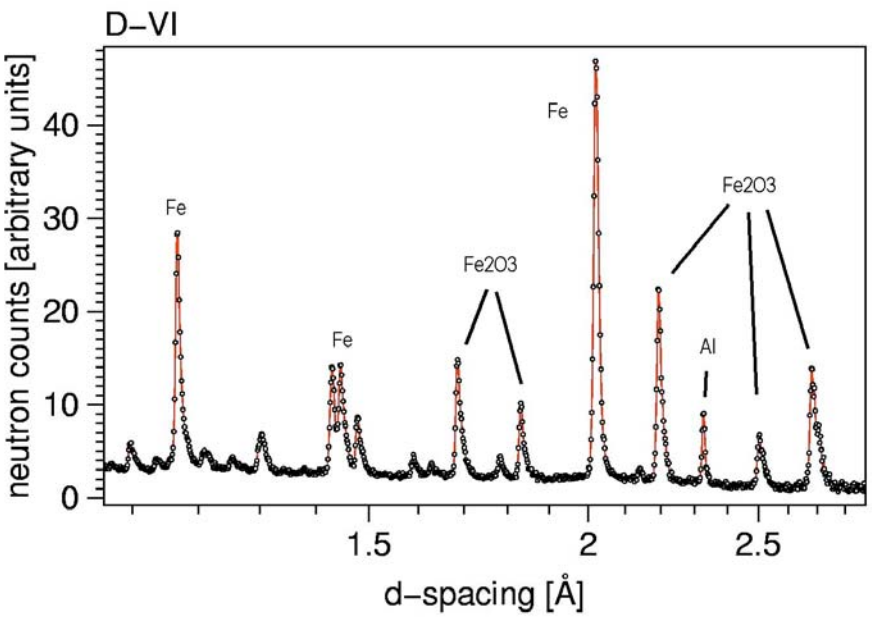

Figure 5.

A TOF-ND pattern of Black Box D-VI

The GSAS analysis suite is used to check the measured neutron patterns against theoretical single phase database patterns, and thus to confirm or reject the presence of an assumed phase. A full quantitative analysis is difficult and actually impractical due to the above described peak shifts caused by off-focus scattering because Rietveld programs cannot account for different off-centre displacements of different phases in the same data set.

Comments on some experimental and crystallographic aspects of the Black Box analysis

Figure 5 shows a typical neutron diffraction pattern, here of box D-VI, which contains iron and hematite, Fe_2O_3. The neutron diffractogramm is characterised by Bragg peaks, which are quantitatively analysed in terms of peak-intensities, -positions and -widths. The data contain information on the crystal structures and magnetic structures (hematite is magnetic at ambient temperatures) as well as on texture, i.e. the orientation distribution of the crystallites in the material. Each crystalline component yields a characteristic pattern, a 'fingerprint'. For a multi-component sample, the respective single-phase patterns superpose. Non-crystalline components or amorphous materials (typically organic materials) do not give rise to Bragg peaks and are therefore not taken into account in the diffraction analysis. However, both inorganic and organic hydrogenous materials are noticeable in the diffraction data by a typical 'hydrogen background' of often large intensity originating from the incoherent (i.e. non-Bragg) scattering of hydrogen atoms.

Neutron diffraction can differentiate between different phases and modifications of a compound, as well as its corrosion products. Structural differentiation is a strength compared to elemental analysis methods. Different phases in a phase diagram of materials are distinguished, for instance, the face centred cubic (fcc) structure of alpha-brass and the body centred cubic (bcc) structure of the beta-brass phase. For many metal structures, which crystallise in the fcc-lattice, the diffraction patterns appear very similar, because the structures are isotypic and scattering is usually not measured on an absolute scale. Then, the differences between diffraction patterns are only recognisable from slightly different peak positions due to different lattice parameters. Usually, with an optimised geometry, the unit cell parameters (lattice parameters, given in Angstrom) of compounds can be determined by TOF-ND with high accuracy, for example, the fcc structures of steel (a= 3.608 Å) and copper (a=3.6145 Å), or the structures of Al (a=4.048 Å), Ag (a= 4.086 Å), and Au (a= 4.078 Å). It is obvious that for the discrimination of silver and gold, a high-resolution instrument is required. However, as mentioned above, the neutron data peaks recorded from the Black Boxes are affected by peak shifts, if the scattering happens off the diffractometer centre. This makes the measurements of lattice parameters less accurate, and differentiation between some fcc structures becomes difficult. In the case of the Black Box analysis this applies, for example, to the above-mentioned structures of copper (Cu) and steel (Fe), or to Al, Ag and Au. In such situations, it is crucial to have results from other techniques such as PGAA in order to determine the correct metal phase(s).

HU ISSN 1786-271X; urn:nbn:hu-4106

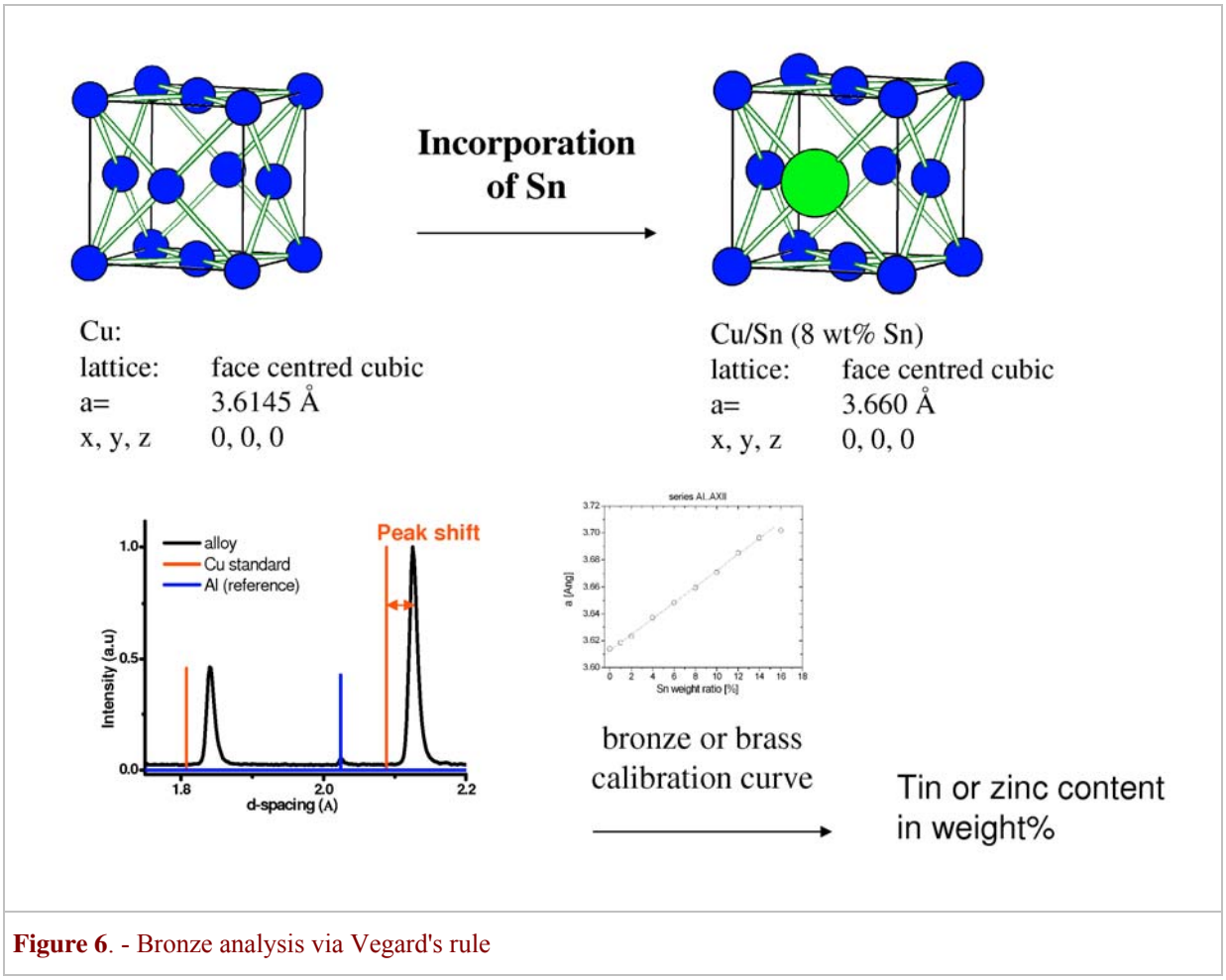

Figure 6. - Bronze analysis via Vegard's rule

The lattice parameter of the fcc cell determined ('refined') with GSAS from the Black Box data gives a first indication of the composition of the lattice. Incorporation of an element, such as tin or zinc, into the copper lattice expands the unit cell according to the size of the guest atoms (Sn is larger than Zn). Phases with fcc- lattice parameters significantly exceeding that of copper (a=3.6145 Å), are then evaluated as copper alloys Cu/Sn (bronze) or Cu/Zn (brass). The amount of Sn or Zn can be estimated from calibration curves for copper alloy standards (Siano 2002) as soon as the type of guest element is known from PGAA (**Figure 6**).

There are well established procedures in crystallography to study single-phase samples (powders or single crystals) and also multi-phase samples in case of well defined diffraction geometry. In comparison, the analyses of the Black Boxes data present a much higher degree of complexity due to:

- Interference of different materials, crystalline and amorphous, inside a box; powders, single crystals, textured materials, compounds of high and low symmetries
- scattering contributions from sample parts off-set from the instrument centre i.e. the neutron data depend on which material is in front or in the rear of the box
- materials with different absorption properties

The fact that the materials to be analysed are inside containers that themselves give rise to significant Bragg diffraction has further consequences. Al inside an Al-box, and Fe inside a Fe-box are obviously difficult to analyse, even though the Bragg peaks from the box walls are shifted in the patterns: the overlap of peaks is too high to disentangle the patterns. Since silver has a similar lattice parameter as aluminium, it is difficult to detect and quantify silver objects inside an aluminium box. Furthermore, for most of the cases, there are double-peaks of Fe or Al from the box walls. These wall-double-peaks can, however, not be satisfactorily fitted in a standard GSAS refinement which is the main reason why a full quantitative analysis of Black Boxes data may fail to work well and why the weight fractions given in this paper must be considered as semi-quantitative estimates only.

HU ISSN 1786-271X; urn:nbn:hu-4106

TOF-ND results

The tables in the appendix summarise the neutron diffraction results on seventeen Black Boxes. For most of them, radiographies were available at the time of the ROTAX and GEM experiments, and they were used to guide the TOF-ND measurements. Also, PGAA results were available for the TOF-ND analyses, and they helped to identify some of the components inside the boxes. The layouts and the material compositions of the boxes disclosed after the analyses could be compared to the diffraction analyses results. The first part of each table (a) in the appendix presents the results of the neutron diffraction analyses; the second part (b) compares the results from TOF-ND and PGAA with the actual composition of a box (reality check).

In many cases, the TOF-ND analysis succeeded in correctly and completely identifying the materials inside the boxes. In other cases, only partial information could be obtained. In a few cases, TOF-ND could not provide useful information on the contents of boxes, because data remained unexplained, were too complex or could not be analysed due to poor counting statistics. All in all, TOF-ND was relatively straightforward to provide results of metals with their generally highly symmetric structures, but TOF-ND struggled with mixtures of multi-phase 'low symmetry' components, e.g. combinations of ceramics, as in H-VIII (Dúzs 2008) .

The INES data were collected with a large neutron beam of approximately 40 x 40 mm^2, at a time when X-ray or neutron radiographies were not yet available. Hence, the entire box was illuminated during an analysis, and consequently, the data contained Bragg peaks from all components of the box. It turned out, that these data could not be analysed because of the complexity of the diffraction patterns. The INES data are therefore not taken into account and omitted from the appendix.

Discussion

Radiographic and tomographic data have proven to be essential in guiding the diffraction experiments, and saving valuable neutron beam time. In some cases, 2D X-ray radiographies were fully sufficient for the location of the features inside a box. In many other cases, 3D tomographic data were required, i.e. views from different angles. Vice versa, for a proper physical and structural interpretation of the radiographic features, TOF-ND and PGAA data were essential. In some cases, TOF-ND and PGAA yielded valuable complementary information, for example for copper alloys, where TOF-ND cannot determine the alloying elements.

It turned out that the definition of a unique object coordinate system ensuring reproducible orientation at different facilities is a very important issue if radiography, PGAA and TOF-ND data are to be combined. Objects and radiographies of them need to be provided with such a reference system, as well as with information on the incident beam direction in the radiography. This was not always the case in the current study.

Alignment of the samples on the TOF-ND instruments was not always adequate, because carried out by eye only. An accurate sample positioning device is required. Also an in-situ collection of a radiographic image, as alignment aid (like demonstrated at NIPS for PGAA in Budapest), would be highly desirable for TOF-ND. Moreover, secondary collimation would allow for selecting individual scattering volumes along the incident beam direction (see double-chord set-up Budapest, (Kis et al. 2008) in spite of intensity reduction).

Finally, the analyses should become more quantitative, rather than semi-quantitative as in the present study. This is, however, not possible without an extensive revision of the analysis software, for instance with respect to allowing for different sample offset corrections for different phases in one and the same dataset.

In summary, related to the complexity of the samples, TOF- ND analyses were hampered by a number of circumstances:

- too large beam sizes (e.g. 10 x 10 mm^2 or 10 x 20 mm^2)
- missing secondary collimation
- inaccurate positioning and alignment of samples in the beam
- Bragg peak shifts
- errors in coordinate assignments to radiographies
- neutron absorption
- H-containing materials
- difficulties to identify complex materials and single crystals (gems, jewellery) at backscattering angles when the box is filled with a highly absorbing material

In a number of cases, TOF-ND performed well and added complementary information to radiographies and PGAA data. Some illustrating examples are:

- For box D-II, TOF-ND discovered a beta-brass alloy inside one of the copper alloy spirals. This result could only be achieved by neutrons which penetrate into the core of the wire. X-ray diffraction detected the beta-phase in the wire's interior only after grinding a piece of wire. Still, the neutron diffraction cannot tell if the beta-brass phase is in the core or in the surface of the wire

HU ISSN 1786-271X; urn:nbn:hu-4106

owing to the insufficient spatial resolution. Since, however, an initial X-ray analysis of the intact wire had 'seen' only copper, one can infer that the additional phase must stem from the wire's interior.

- Extra cementite (Fe_3C) peaks were identified in the iron rods of box D-IV. The corresponding carbon content is estimated to 0.7 wt%.
- Different iron modifications (ferrite, steel) and iron oxides (FeO, Fe_2O_3, Fe_3O_4) are differentiated, as demonstrated for D-VI and H-VI.
- TOF-ND, in combination with PGAA, distinguishes between copper alloys and copper phases

All these examples demonstrate the need for diffraction experiments for the full characterisation of a material/object. At the same time, the fruitful combination of element analysis methods (PGAA) and phase analysis method (TOF-ND) is illustrated.

In many cases, the diffraction analysis was hindered by the complexity of the diffraction data, originating from the superposition of patterns from different parts of a box, when the neutron beam had been crossing several components. This shows that the beam size and the contributing irradiated volume are too big. An improved set-up would need to use a secondary collimator on the scattered beam side, following the example of the double-chord set-up at NIPS. Such a set-up is actually used at ISIS for structure and phase mapping on the engineering instrument ENGIN-X. On this instrument, a spatial resolution, of for instance 2 x 2 x 2 mm^3, is achieved by tight collimation of both incident and scattered radiation, which define the gauge volume (Kockelmann & Kirfel 2006). This set-up avoids recording sample-offset scattering and the accompanying peak shifts. The method appears ideal for the analysis of metals, but would also struggle to provide useful information for ceramics and clay minerals, mainly due to too low intensity emitted from the gauge volume.

Limited by the neutron flux, the recording of complete three dimensional maps with TOF-ND is very slow. Data collection times would be in the order of many hours up to days, which must be considered un-economical. More appropriate are linear depths scans, as for box D-VI, and profile scans on parts of the sample that have been beforehand surveyed by neutron or X-ray tomography.

The Black Boxes results highlight some aspects for analyses of archaeological objects with neutrons. Neutron analyses are non-destructive and provide information from the interior of the boxes. However, relatively low spatial resolutions compared to those of other methods such as X-ray methods need to be kept in mind when thinking about neutron projects. Even the spatial resolution of NT of typically 0.1 mm is still not good enough for many applications. Neutrons have high penetration in materials, but much depending on the material. Even for materials like Fe or copper, absorption is substantial and noticeable so that absorption corrections would have to be applied for a quantitative analysis. For hydrogen-containing minerals or water-soaked samples, the penetration depths are even as small as in the order of millimetres. Thus, for such materials, neutron attenuation plays an even more destructive role. Since the attenuation is not known before the experiment, attenuation measurements by NT are useful prior a TOF-ND experiment is performed.

Neutron diffraction provides information about the crystalline components. However, for multi-phase mixtures, e.g. a mixture of different types of pottery, the complexity of diffraction patterns can be overwhelming.

Conclusions

We have used time-of-flight neutron diffraction at ISIS to analyse components inside closed 'Black Boxes'. TOF-ND is necessary to characterise the features in radiographic data in terms of their phases and structures, information which is not available from other methods. For instance, cementite in iron is identified, which can be used to determine carbon contents. Different copper alloy phases can be identified and quantified, such as a beta-brass core inside an alpha-brass coating of a brass wire.

TOF-ND and PGAA are standard non-destructive techniques for phase or bulk elemental analysis, respectively. They both provide information averaged over the irradiated volume, which is primarily determined by the neutron beam cross section, and the extension of the object in the incident beam direction. Both methods are relatively fast with a wide beam spot, but the spatial resolution is often not sufficient to reveal fine details inside the objects. Reducing the beam size is at the expense of valuable neutron beam time, and as such often impractical. In many cases the combination of results from NT, XT, TOF-ND and PGAA can sufficiently reveal the properties of the materials. However, also in many other cases, the spatial resolution of TOF-ND is not sufficient, when scanning on a micro-meter scale is required.

The analysis of the Black Boxes suggests a best procedure for non-destructive analyses of objects:

- A conventional surface analysis technique (walls in the case of the boxes) characterises the outside of the objects as good as possible.
- X-ray radiography or neutron tomography produce high-resolution 2D/3D images that show

HU ISSN 1786-271X; urn:nbn:hu-4106 © by the author(s)

the internal geometrical structure and attenuation features in quantitative terms. Radiographic data prior to the diffraction experiments are absolutely essential to guide the TOF-ND structure analysis. In many cases, X-ray radiographies will be sufficient. In-situ neutron radiography to guide the experiments would be useful.

- Collection of 1D or 2D diffraction data (3D diffraction imaging is rather lengthy and un-economical). Analyses have to be performed using a unique object coordinate system, ensuring reproducible orientation.
- Collection of elemental data by PGAA and/or NRCA is essential for a proper identification of materials.

Acknowledgements

We acknowledge the support of ANCIENT CHARM EU FP6 NEST Contract No. 15311. The contributions of the ANTARES group at FRM-II, Garching, Germany, and the Centre for X-ray tomography at the University of Ghent on tomography experiments are much appreciated. We thank S. Imberti, ISIS Facility, for the support during the INES measurements.

References

DAY, P., ENDERBY, J.E., WILLIAMS, W.G., CHAPON, L.C., HANNON, A.C., RADAELLI, P.G. & SOPER, A.K. (2004): GEM: The general materials diffractometer at ISIS - multibank capabilities for studying crystalline and disordered materials. *Neutron News* **15(1)** 19-23.

DÚZS K. (2008): Realisation of the planned 'Black Boxes' in the Hungarian National Museum. *Archeometriai Műhely / Archaeometry Workshop* **2008/1** 7-20.

GORINI, G. (2007): Ancient Charm: A research project for neutron-based investigation of cultural-heritage objects. *Il Nuovo Cimento* **30C(1)** 47-58.

GUTMANN M.J., KOCKELMANN W, CHAPON L.C., RADAELLI P.G. (2006): Imaging crystallographic phases using time-of-flight neutron diffraction, *Physica B* **385** 1203-1205.

HAJNAL Zs. (2008): Test objects for developing 3D material analysis on Cultural Heritage objects: Plans for the 'Black Boxes' to be analysed in the Ancient Charm Project. *Archeometriai Műhely / Archaeometry Workshop* **2008/1** 3-6.

IMBERTI, S. et al., (2008): Neutron diffractometer INES for quantitative phase analysis of archaeological objects, *Meas. Sci. Technol.* **19** 034003 8 pp.

KIRFEL, A. (2008): Construction and description of the UNIBONN 'Black Boxes'. *Archeometriai Műhely / Archaeometry Workshop* **2008/1** 21-34.

KIS, Z., et al. (2008): Prompt Gamma Activation Imaging on 'Black Boxes' in the 'Ancient Charm' Project. *Archeometriai Műhely / Archaeometry Workshop* **2008/1** 41-60.

KOCKELMANN, W. & KIRFEL, A. (2006): Neutron diffraction imaging of cultural heritage objects. *Archeometriai Műhely / Archaeometry Workshop* **2006/2** 1-15.

KOCKELMANN, W., KIRFEL, A., HAEHNEL, E. (2001): Non-destructive Phase Analysis of Archaeological Ceramics using TOF Neutron Diffraction. *J. Archaeol. Sci*. **28** 213-222.

KOCKELMANN, W., WEISSER, M., HEINEN, H., KIRFEL, A. & SCHAFER, W. (2000): Application spectrum and data quality of the Time-to-Flight Neutron Diffractometer ROTAX at ISIS. *Materials Science Forum* **321-324 I** 332-337.

KUDEJOVA, P. (2008): Neutron and X-Ray imaging of the 'Black Boxes' for the Ancient Charm project. *Archeometriai Műhely / Archaeometry Workshop* **2008/1** 35-40.

KUDEJOVA, P., CIZEK, J., SCHULZE, R., JOLIE, J., SCHILLINGER, B., LORENZ, K., MÜHLBAUER, M., MASSCHAELE, B., DIERICK, M. & VLASSENBROECK, J. (2007): A marker-free 3D image registration for the ANCIENT CHARM project. Case study with neutron and X-ray tomography datasets. *Notiziario Neutroni e Luce di Sincrotrone* **12(2)** 6-13.

LARSON, A.C., VAN DREELE, R.B (1986): General Structure Analysis System (GSAS), *Los Alamos National Laboratory Report LAUR **86-748,*** 1-231.

POSTMA, H., SCHILLEBEECKX, P., HALBERTSMA, R.B. (2004): *Archaeometry* **46** 635-646.

SIANO S., KOCKELMANN W., BAFILE U., CELLI M., IOZZO M., MICCIO M., MOZE O., PINI, R., SALIMBENI R., ZOPPI M., (2002): Quantitative multiphase analysis of archaeological bronzes by neutron diffraction, *Applied Physics A* **74 (Suppl.)** S1139-S1142.

YOUNG R.A (ed.) (1993): *The Rietveld Method, International Union of Crystallography*. Oxford, University Press. 1-38.

HU ISSN 1786-271X; urn:nbn:hu-4106

KÖZLEMÉNYEK

Ahol októberben mindnyájunknak ott kellene lennünk: Róma, Re.Se.A.R.C.H. Workshop

SZÉKELY BALÁZS[1,2]

[1] Bécsi Műszaki Egyetem, Fotogrammetriai és Távérzékelési Intézet, Ausztria
[2] ELTE Geofizikai és Űrtudományi Tanszék, Budapest

Email: balazs.szekely@ipf.tuwien.ac.at

*Az archeometriai körökben talán kevésbé ismert EARSeL 2008. október 1-4. között első alkalommal rendezi meg a "**Advances in Remote Sensing for Archaeology and Cultural Heritage Management**" (Re.Se.ARCH) című nemzetközi műhelytalálkozót, mely a régészeti és kulturális örökségvédelmi célú távérzékelés legújabb technológiáit bemutató seregszemléje. Az alábbiakban egy rövid kedvcsinálót igyekszem nyújtani az aktív részvételhez.*

Az EARSeL (*European Association of Remote Sensing Laboratories*) a távérzékeléssel foglalkozó európai intézmények és cégek egyik fontos fóruma, mely 1977-ben alakult az Európai Űrügynökség (ESA), az Európa Tanács és az Európai Bizottság támogatásával. A jelenleg mintegy 250 tagot számláló szervezet célja többek között a távérzékelés legmodernebb technológiáinak a döntéshozókkal való megismertetése, az oktatásba való integrálása, és a gyakorlatban való elterjesztése. Annak érdekében, hogy távérzékelés igen széles területét minél hatékonyabban átfoghassa a szervezet, szakmai érdekcsoportokat (*Special Interest Groups*, SIG) alakítanak ki az egyes szakterületek. Van például radar-távérzékelési, a szárazföldi hó- és jégtakaróval foglalkozó, és városi távérzékelési csoport is. Az egyik legújabb SIG a régészeti és kulturális örökségvédelmi területen 2007 júniusában alakult, és az angol nevéből (*Remote Sensing for Archeology and Cultural Heritage*) igen ötletesen Re.Se.Ar.C.H.-nak rövidítik. A római konferenciát ez a szakterület részvételével szervezi a *Consiglio Nazionale delle Richerche* (CNR; Olasz Tudományos Kutatási Tanács) két szakintézete számos támogató intézmény és szponzor segítségével.

A *konferencia témakörei* láttán az archeometriával foglalkozó szakembernek azonnal önkéntelenül is a gyors októberi repülőjegy-foglalás vágya jut az eszébe:

- légi régészet: az archív légifotóktól a multi-spektrális és hiperspektrális leképzésig;
- aktív légi távérzékelés (LiDAR, SAR): adat-feldolgozási kérdések és alkalmazások;
- űrfelvételek a régészetben: adatfeldolgozási módszerek és esettanulmányok;
- a felszínalatti viszonyok leképezése földradarral, mágneses és elektromos tomográfiával régészeti célra;
- a felszínalatti érzékelés inverziós problémái;
- régészeti és a kulturális örökségvédelemi célú légi- és űrtávérzékelési adatok integrá-ciója földi távérzékelt adatokkal;
- háromdimenziós vizualizáció és virtuális valóság a táj- és lelőhely-rekonstrukcióban;
- távérzékelésre, térinformatikára és információ-technológiára alapuló tájrégészet és ős-környezeti rekonstrukció;
- a természeti és kulturális örökségvédelem menedzselése: távérzékelési, térinformatikai és információtechnológiai alkalmazások;
- régészeti leletmentés;
- a nemzetközi régészeti kampányok mint a régé-szettudomány kiemelkedő laboratóriumai;
- a távérzékelési és a földi tényadatok integrációja.

A szokásos előadásokon, posztereken kívül terepi kirándulás is tarkítja a programot. A résztvevők által előadott anyagok konferenciakötetben jelennek meg, ehhez a kész cikkeket júniusig várják az előzőleg elfogadott absztraktok alapján. A cikkek egy része az EARSeL on-line referált szakújságjában, az *EARSeL eProceedings* is megjelenik.

Ugyan a 275 eurós (EARSeL tagoknak 250 eurós, diákoknak 150 eurós) regisztrációs díj nem kevés, mégis azt gondolom, érdemes elővenni a jegyzeteinket, hogy hol is tudnánk pályázni a részvételi díjra és az egyéb költségekre, mert a fent vázolt témák valóban a szakma legizgalmasabb területeit fedik le, és minden bizonnyal rengeteg

HU ISSN 1786-271X; urn:nbn:hu-4106

érdekes előadást és posztert lehet majd látni. Csak bíztatni tudom a hazai szakma képviselőit az előadással, poszterrel való részvételre, hiszen hazánkban a fenti területek közül szinte mind tényleg jelentősen képviselve van. Kár lenne, ha az általános pénzhiány és szervezeti problémák megakadályoznának minket abban, hogy kiváló ötleteink és gondos, alapos munkánk eredménye az őt megillető teret megkapja ezen a minden bizonnyal színvonalas konferencián, ahol véleményem szerint új kezdeményezések, projektek magjainak kialakulása is várható.

A végére maradt, ami talán a legfontosabb, a konferencia honlapja:

http://www.ibam.cnr.it/earsel/workshop/Workshop.htm

HU ISSN 1786-271X; urn:nbn:hu-4106

Appendix:

Tables of TOF-ND results.

The radiographic images were taken at the Center for X-ray tomography at the University of Ghent.

In the section “complementary information” results are reported as far as they contribute to the clarification of TOF-ND results. A full description of the PGAA data is given in [Kis et al. 2008].

“Box Alignment” in the set-up section refers to the positioning of the box in the sample chamber with respect to (wrt) the nominal diffractometer centre.

- “no offset”: centre of box coincides with centre of diffractometer;

In the section “Reality check” some details of the actual construction are given. A full description of the PGAA data is given in [Kirfel et al. 2008].

Table 1 (a). *TOF Neutron Diffraction results on D-II*

Box no.	X-ray radiograph	Set-Up	Diffraction patterns	ND results
D-II	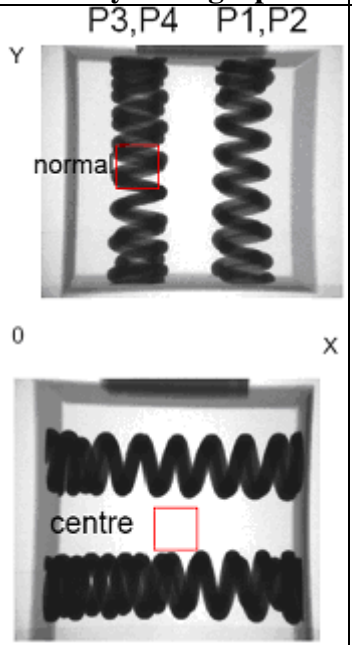	**Instrument: ROTAX** beam size 10x10 mm; beam along y Central box alignment: no offset; P1-P4: aligned with incident beam. "normal": incident beam normal to the spiral. Beam traverses two spirals P3-P4. no offset "centre": incident neutron beam aimed at box centre to determine filling. no offset	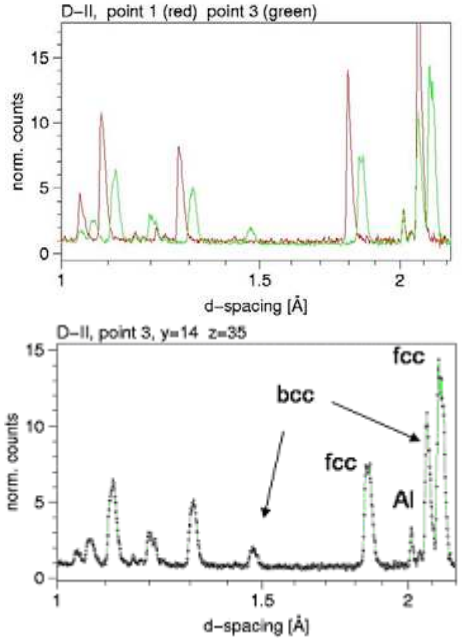	**Point 1**: fcc a=3.60 Å (Cu-type); **Point 2**: fcc a=3.601 Å (Cu-type) **Point 3**: fcc a=3.69 Å (Cu-type) (80wt%); bcc-phase (20wt%), a=2.94 Å **Point 4**: fcc a=3.686 Å (Cu-type) (85wt%), bcc-phase (15wt%), a=2.95 Å **Centre**: beam along z, empty (only Al peaks) **Normal** to the spiral, beam along z: fcc a=3.690 Å (Cu-type) (85wt%), bcc-phase (15wt%) a=2.94Å

Table 1 (b). *Comments on TOF-ND results on D-II*

Box no.	Box content from TOF-ND	Complementary info	Reality Check
D-II	- Springs made of different materials but combination of two phases (fcc+bcc) - The lattice parameter indicates a **copper alloy** (bronze/brass) for the fcc metal, and beta-brass for the bcc-phase. The peak shift of the copper alloy (fcc phase) compared to 1+2 is clearly visible in the diffraction patterns. The 'normal shot' went through 3+4, and confirms results on point P3+P4 Lattice parameter of bronze/brass: a=3.686 Å. This value can be interpreted as $Cu_{0.7}Zn_{0.3}$ brass (= 40wt% Zn) or a bronze $Cu_{0.93}Sn_{0.07}$ (= 12wt% Sn). These cases are indistinguishable. - no filling materials	none	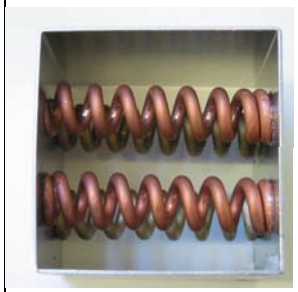 - The springs are made of Cu and brass. The brass consists of $Cu_{64}Zn_{36}$, with alpha-brass on the surface and beta-brass in there wire core. TOF-ND identifies the different phases of the two types of springs: two Cu-type phases with different lattice parameters. - TOF-ND also **identifies** the beta-brass component (*bcc*-phase) which is consistent with the Cu-Zn phase diagram for a $Cu_{60}Zn_{40}$ brass.

Table 2 (a). *TOF Neutron Diffraction results on D-IV*

Box no.	X-ray radiograph	Set-Up	Diffraction patterns	ND results
D-IV	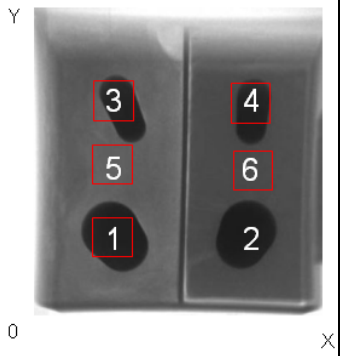	**Instrument: ROTAX** beam size 10x10 mm; beam along z box alignment: P1-P6 aligned with incident beam; no offset	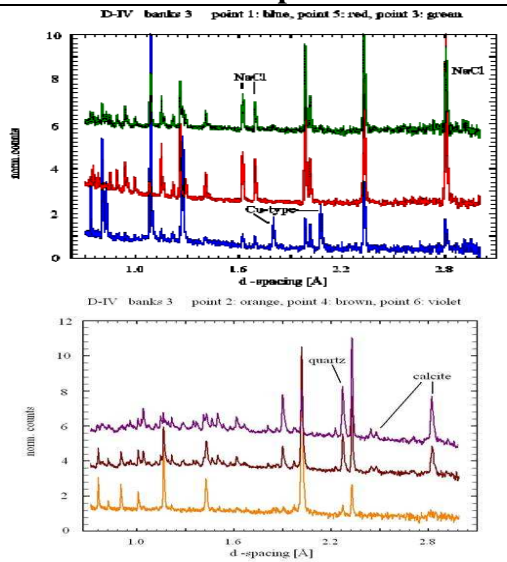	**Point 1**: NaCl, Cu-type (fcc) a=3.592 Å, steel (Fe) or copper (Cu) **Point 2**: bcc a=2.845 Å, ferrite (Fe) + cementite (Fe_3C), in clay=calcite+quartz **Point 3**: NaCl, small fcc peaks a=3.6 Å, steel (Fe) or copper (Cu) **Point 4**: calcite, quartz, bcc a=2.845 Å, ferrite (Fe) **Point 5**: NaCl **Point 6**: calcite (75wt%), quartz (25 wt%)

Table 2 (b). *Comments on TOF-ND results on D-IV*

Box no.	Box content from TOF-ND	Complementary info	Reality Check
D-IV	- Two compartments with different filling materials: salt (NaCl) and clay consisting of quartz (25 wt% SiO_2) and calcite (75wt% $CaCO_3$). - The **objects** in the two chambers are made of different materials: **1**: fcc-structure, Cu-type (fcc structure); lattice parameter (a=3.592 Å) is closer to steel (3.594 A) than to copper (3.615 A) **2**: Bcc lattice, ferrite (Fe); extra cementite (Fe_3C) peaks; clay peaks are small compared to the Fe peaks; **3**: fcc-structure, Cu-type (fcc structure); lattice parameter (a=3.592 Å) indicates steel **4**: The rod material is bcc-Fe (ferrite)	- **PGAA** identifies fcc-metal as **Cu** for points (1) and (3) - **PGAA** identifies **Al** as separator material. 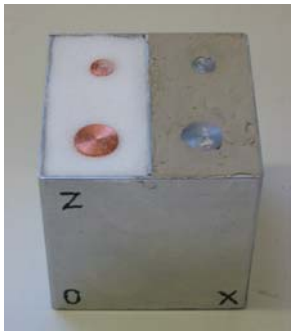	Cu and Iron rods, embedded in halite (NaCl) and clay (51% calcite, 20% quartz, 12% muscovite, 17% kaolinite) - The main components are identified by TOF-ND. - PGAA is required to decide on the fcc-material: copper. - For the clay the two main components were identified with approximately the correct proportions. - After disclosure of the content, kaolinite is identified in the pattern. - Muscovite was not detected by TOF-ND. - The lattice parameters of Cu and Fe are systematically shifted towards lower values. This is probably due to absorption (i.e. apparent shift of the material towards the neutron source.) - **Extra phase**: Cementite is observed in the ferrite. - The second wall of the box is not visible for both filling materials. The Cu rod in position 3 was almost missed by the neutron beam due to misalignment of the box on the instrument.

Table 3 (a). *TOF Neutron Diffraction results on D-V*

Box no.	X-ray radiograph	Set-Up	Diffraction patterns	ND results
D-V	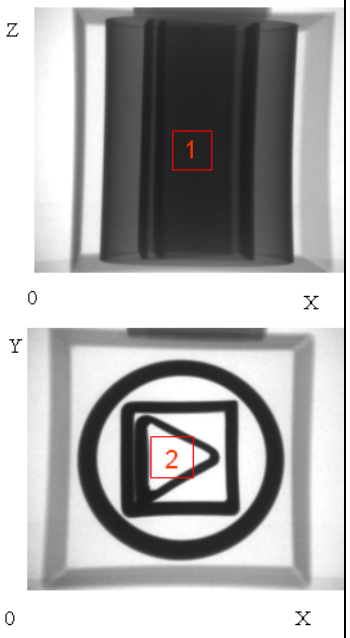	**Instrument: ROTAX** Point 1: beam size 10x10 mm; beam along y Point 2: beam size 10x10 mm; beam along z box alignment: P1-2 aligned with incident beam; no offset	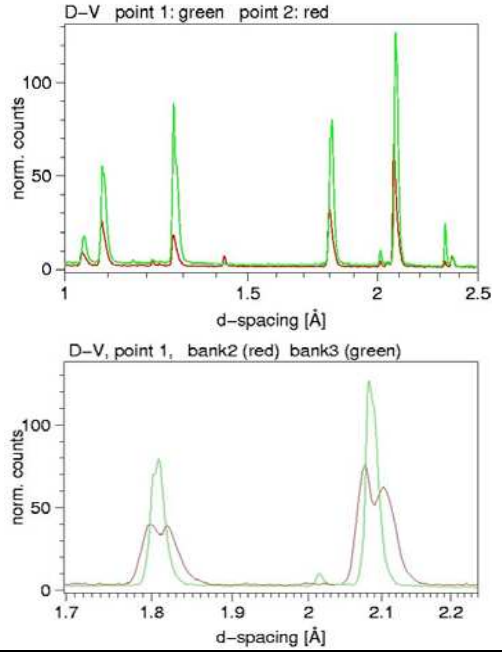	**Point 1**: Cu-type (*fcc*), a=3.608 Å **Point 2**: Cu-type (*fcc*), a=3.598 Å

Table 3 (b). *Comments on TOF-ND results on D-V*

Box no.	Box content from TOF-ND	Complementary info	Reality Check
D-V	- The two analysis points show the **same set of peaks**, i.e. all the parts of the internal object are made of the **same material**; - The object is made of an fcc material with **Cu type structure**; the lattice parameters point to steel rather than copper but peaks can be shifted due to displacement of the object inside the box. - The rest of the **box** is **empty**. - Inspection of the diffraction patterns shows the following features: **1.** Fcc Cu-type material is textured (preferred orientation of grains) **2.** The aluminium peak intensities are different for point 1 and point 2 due to absorption of neutrons in the copper **3.** Splitting of peaks in bank-2 (double pattern) indicates transition of beam through two walls.	- **PGAA** identifies fcc-metal as **Cu**.	 - The **objects** consist of **pure copper**. - The main phase is identified by TOF-ND. PGAA differentiates between steel and Cu.

Table 4 (a). *TOF Neutron Diffraction results on D-VI*

Box no.	X-ray radiograph	Set-Up	Diffraction patterns	ND results
D-VI	**(a)** 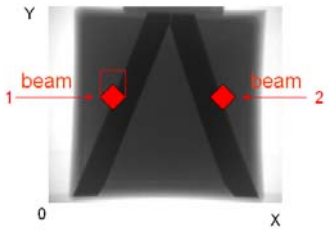 **(b)** 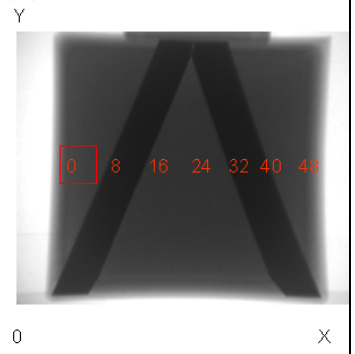 	**Instrument: ROTAX** **(a)** Point 1: beam size 10x10 mm; beam along x Point 2: beam size 10x10 mm; beam along minus x **(b)** Scan along x [mm]; beam size 10x10 mm; beam along z box alignment: no offset	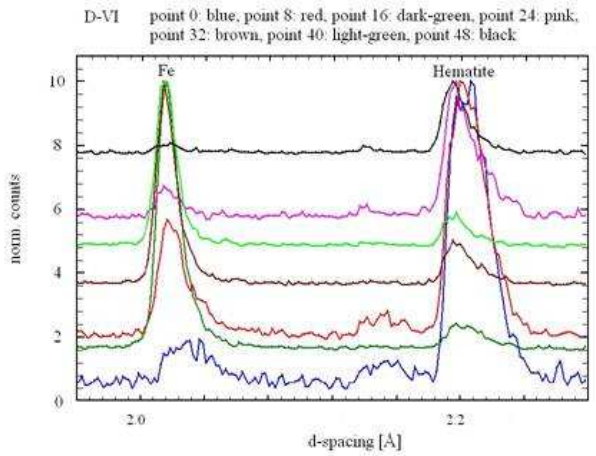 	**(a)** **Point 1**: Hematite (Fe_2O_3), bcc type structure, a=2.86 Å, ferrite (Fe) **Point 2**: Hematite (Fe_2O_3) , bcc type structure, a=2.85 Å, ferrite (Fe) **(b)** **Point 0**: Fe_2O_3 (Hematite), wall **Point 8**: Fe_2O_3 (17wt%), ferrite (83wt%) **Point 16**: Fe_2O_3 (86 wt%), ferrite (14 wt%) **Point 24**: Fe_2O_3 (94 wt%), ferrite (6 wt%) **Point 32**: Fe_2O_3 (38wt%), ferrite (62wt%) **Point 40**: Fe_2O_3 (37wt%), ferrite (63wt%) **Point 48**: Fe_2O_3 (100wt%) ferrite (0 wt%)

Table 4 (b). *Comments on TOF-ND results on D-VI*

Box no.	Box content from TOF-ND	Complementary info	Reality Check	
D-VI	- The two inclined '**plates**' are of the **same material**: ferrite (bcc-Fe); - The x-scan shows that the V-shape object is **ferrite** and that the box is **filled with hematite** (not the other way round).	- **PGAA** confirms presence of **Fe** and absence of other elements;	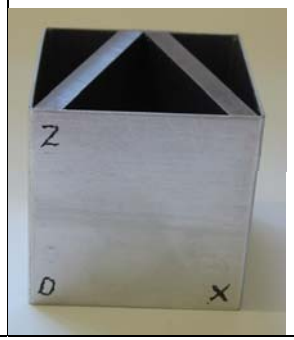 	- The main components (ferrite and hematite) are identified. - This box highlights the **advantage** of **TOF-ND** compared to element-sensitive methods: oxides, corrosion phases, secondary alteration phases can be distinguished from alloys.

Table 5 (a). *TOF Neutron Diffraction results on D-VII*

Box no.	X-ray radiograph	Set-Up	Diffraction patterns	ND results
D-VII	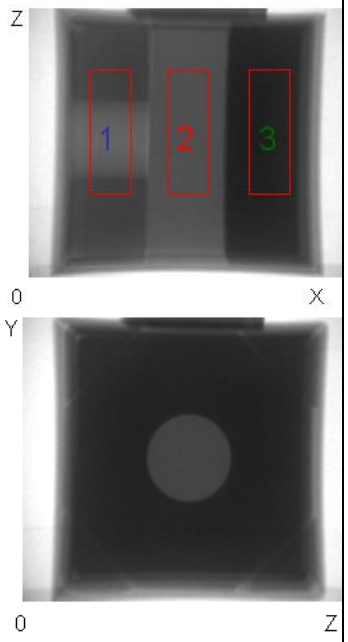	**Instrument: ROTAX** beam size 10x30 mm; beam along y box alignment: no offset	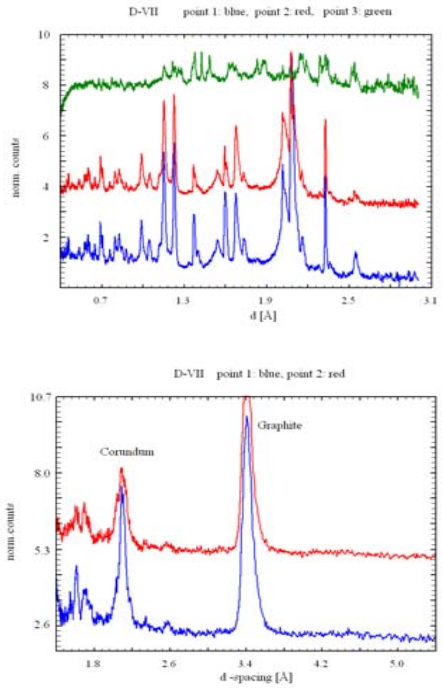	**Point 1**: graphite (C) + corundum (Al_2O_3) in equal parts **Point 2**: graphite (C) + corundum (Al_2O_3) in almost equal parts **Point 3**: phase not identified

Table 5 (b). *Comments on TOF-ND results on D-VII*

Box no.	Box content from TOF-ND	Complementary info	Reality Check
D-VII	- Analysis **points 1** and **2** are made of the **same material**: graphite and corundum. - Analysis point 3 shows a rich spectrum of diffraction peaks. The pattern could not be unravelled, or assigned to a single phase.	- **PGAA** identifies **Na** which may come from diaoyudaoite ($Al_{10.35}$ $Mg_{0.65}O_{16}$)($Na_{1.65}O$) - **PGAA** identifies **Si** and **H** which comes from pyrophyllite	 - **Graphite** and **corundum** were **identified**. - The peaks of diaoyudaoite ($Al_{10.35}$ $Mg_{0.65}O_{16}$)($Na_{1.65}O$) at 11.2 and 5.7 Å were observed but the compounds was not identified. - The peak-rich pattern of pyrophyllite was recognised, but the mineral was not identified. - The simultaneous observation of graphite and corundum in equal amounts for point 1 and point 2 indicates a substantial **misalignment** of the box on the diffractometer, or wrong axes description on the radiographies.

Table 6 (a). *TOF Neutron Diffraction results on D-VIII*

Box no.	X-ray radiograph	Set-Up	Diffraction patterns	ND results
D-VIII	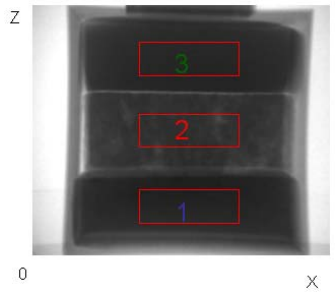	**Instrument: ROTAX** beam size 30x10 mm; beam along y box alignment: no offset	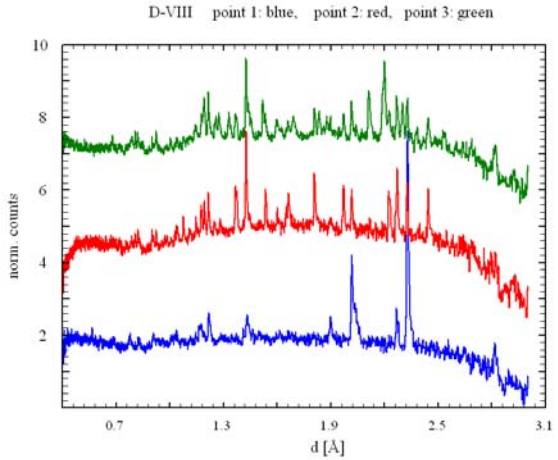	**Point 1**: calcite ($CaCO_3$), high background **Point 2**: quartz (SiO_2), on high amorphous background **Point 3**: quartz (SiO_2)(25wt%), mullite $3Al_2O_3$ $2SiO_2$ (55wt%), cordierite $Mg_2Al_4Si_5O_{18}$ (10wt%), cristobalite (SiO_2) (5wt%), identified in the data after box content is revealed; other un-indexed peaks on high background level

Table 6 (b). *Comments on TOF-ND results on D-VIII*

Box no.	Box content from TOF-ND	Complementary info	Reality Check
D-VIII	- **Point 1** shows a very high hydrogen background indicating mineral with H-content; the beam is stopped in the box, there are no Al-peaks from the back aluminium wall of the box; there are practically no peaks in forward scattering. The main component is calcite. - In **Point 2** quartz is identified. - **Point 3** has a large amorphous background, most likely due to H-containing substance/mineral, or glassy component. The patterns contain Bragg peaks from quartz, mullite, cordierite and cristobalite. A large peak at 2.84 A is unidentified.	- **PGAA** identifies **hydrogen** on all points, in agreement with the neutron background, in contrast to x-ray analysis.	 - **P1** is on a slab of clay. TOF-ND sees the main component, calcite. The clay seems to be more hydrogenous than in D-IV. - **P2** is on a slab of brick stone (quartz, albite, muscovite, hematite). TOF-ND sees only main component, quartz. - **P3** is on a slab of fire brick (schamotte) (mullite, quartz, cordierite). The phases mullite, cordierite were not identified from the observed peak-rich spectrum because the peaks were only from backscattering. (Mineral phases are best identified in forward scattering). Once the box content was revealed, the phase fractions from TOF-ND are in the right order of magnitude.

Table 7 (a). TOF Neutron Diffraction results on D-IX

Box no.	X-ray radiograph	Set-Up	Diffraction patterns	ND results
D-IX	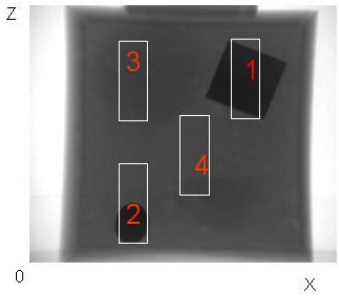	**Instrument: ROTAX** beam size 10x30 mm; beam along y box alignment: P1-P4 aligned with incident beam; offset on diffractometer according to radiography	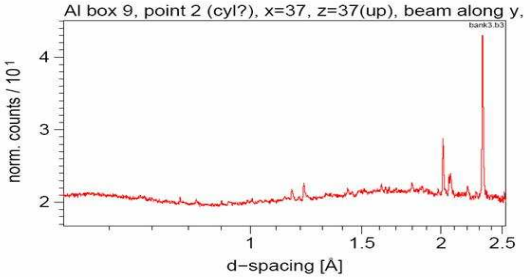 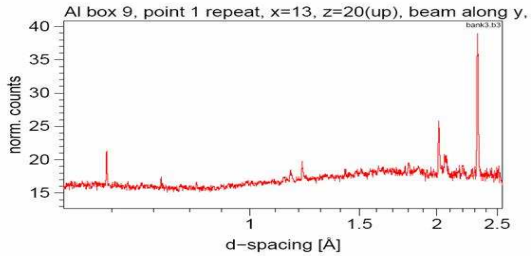	**Point 1-4**: gypsum, high amorphous background

Table 7 (b). Comments on TOF-ND results on D-IX

Box no.	Box content from TOF-ND	Complementary info	Reality Check
D-IX	- All patterns exhibit a very **high** (hydrogen) **background**, i.e. indicate compounds with hydrogen. - The patterns only show the front wall of the Al-cube, i.e. the beam is stopped within the box. - There are **weak peaks** in the patterns from the filling material (they are in all patterns). The filling material is not identified. - **P1** has extra single crystal peaks in backscattering at low d-spacing; not possible to index with low d-value lines;	- **NRCA** analysis on INES identifies the Ag rod on point 2. 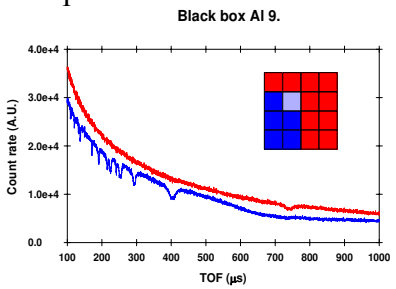 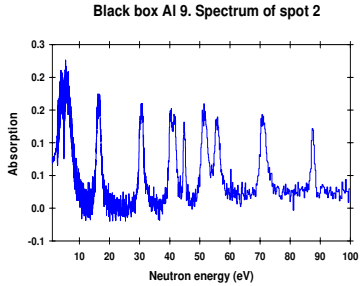	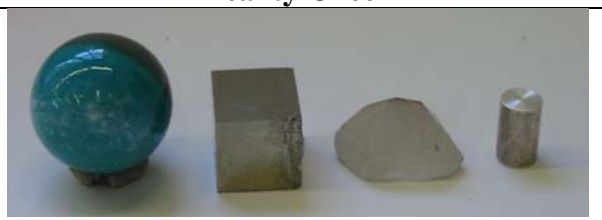 - Box is filled with gypsum ($CaSO_4$ $(H_2O)_2$). - Embedded are: **1.** pyrite single crystal (FeS2) in point 1 **2.** Silver rod in point 2 **3.** Glass sphere in point 3 **4.** Quartz crystal in point 4 - The extra peaks of the filling material are only identified after disclosure of the box fillings. - The single crystal peaks of FeS_2 are visible in the data but were not identified. - no identifiable signals from the other objects in the box. The glassy signal from the glass object is covered by the gypsum scattering. Ag-peaks in TOF-ND data are hidden under the Al peaks.

Table 8 (a). *TOF Neutron Diffraction results on D-X*

Box no.	X-ray radiograph	Set-Up	Diffraction patterns	ND results
D-X	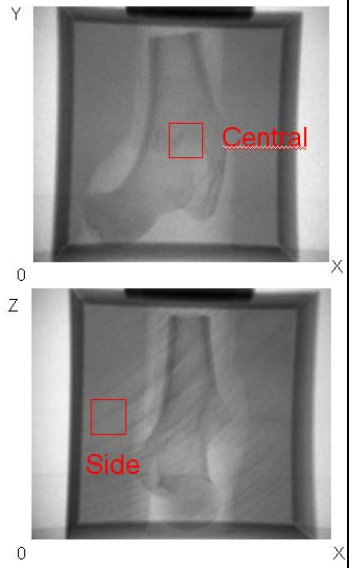	**Instrument: ROTAX** beam size 10x10 mm; box alignment: no offset	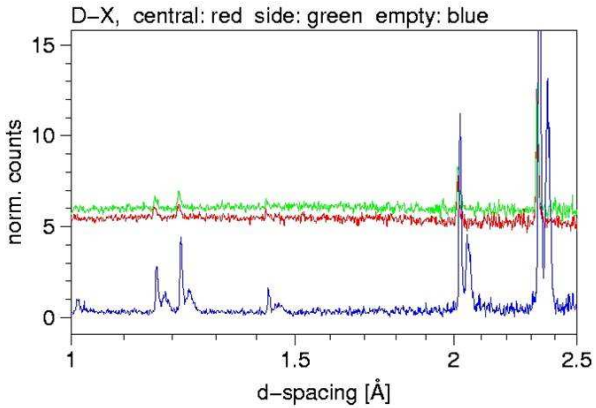	**Central**: beam along z, high background scattering **Side**: beam along y, high background scattering

Table 8 (b). *Comments on TOF-ND results on D-X*

Box no.	Box content from TOF-ND	Complementary info	Reality Check
D-X	- The diffraction patterns do show Al peaks from the box wall, but only from one wall. - - The aluminium peaks are only in backscattering; - Therefore the box cannot be empty. There are no peaks of bone material. - The high neutron background indicates scattering by hydrogen; the hydrogen can be in the bone (visible in x-ray radiography) but there may also be filling material around the bone;	none	- Badger bone, inside beech wood, lower part of bone wrapped in leather; - TOF-ND cannot provide information due to missing crystallinity of the material.

Table 9 (a). *TOF Neutron Diffraction results on D-XI*

Box no.	X-ray radiograph	Set-Up	Diffraction patterns	ND results
D-XI		**Instrument: ROTAX** beam size 10x30 mm; box alignment: no offset	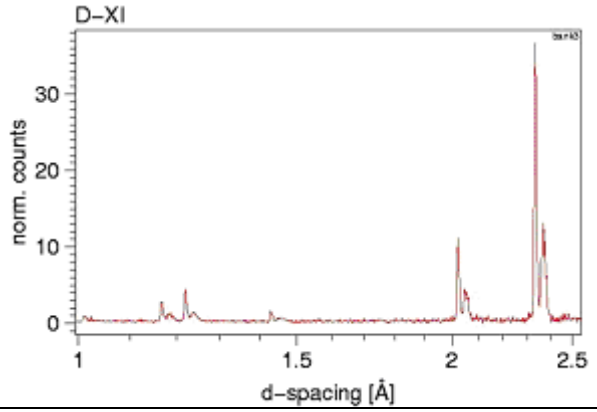	Doublets of Al peaks from front and back-wall scattering

Table 9 (b). *Comments on TOF-ND results on D-XI*

Box no.	Box content from TOF-ND	Complementary info	Reality Check
D-XI	- We observe diffraction patterns from the **front wall** and from the **back wall**. The patterns show the fcc structure of aluminium. Moreover, the patterns show a drastic texture (preferred grain orientation of the Al grains). - The **distance** between the **double peaks** is related to the distance between front and back wall of the box (x): $\Delta d/d = x * \cos(\theta) / L_2$ where Δd is the distance between two peaks in Å, L_2 the distance between sample position and detector, and where θ is ½ the detector angle. - The **intensities** of the **peaks** from the back wall are much reduced compared to the peak intensities from the front wall due to absorption.	none	- **Empty box**, made of aluminium. The front and back walls are x=50 mm apart. Wall thickness 1 mm.

Table 10 (a). *TOF Neutron Diffraction results on H-I*

Box no.	X-ray radiograph	Set-Up	Diffraction patterns
H-I	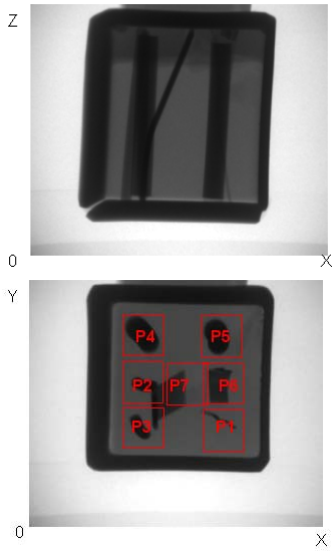	**Instrument: GEM** beam size10x10 mm; beam along z (top side towards beam, side with number "I" facing down) box alignment: no offset	**P1**: copper or steel (small peaks) **P2**: copper a=3.62 Å, small copper alloy component a=3.7 Å, Al/Ag **P3**: copper alloy a=3.69 Å **P4**: fcc-phase a=3.7 Å: bronze or brass; Al/Ag **P5**: copper alloy, a=3.62 Å, Al/Ag, maybe Zn **P6**: fcc a=3.60 Å (copper or steel), Al/Ag **P7**: fcc a=3.60 Å (small peaks) All diffraction patterns contains gypsum ($CaSO_4(H_2O)_2$) peaks.

Table 10 (b). *Comments on TOF- ND results on H-I*

Box no.	Box content from TOF-ND	Complementary info	Reality Check
H-I	The analysis points P1-7 reveal the following main materials (in addition to gypsum): **P1:** copper (Cu) or steel (Fe) **P2:** copper **P3:** brass or bronze **P4:** brass or brass **P5:** copper, indications of Zn; **P6:** copper or steel; strong Al/Ag peaks **P7**: indications of copper/steel peaks - All patterns show Al/Ag peaks, apart from P1, P6	- **PGAA** observed **Cu**, **Zn** and **Fe**, i.e. no Sn. This means, the copper alloy is most likely brass (Cu-Zn). - **PGAA** does not find Al or Ag.	 **1** - copper wire **2** - brass wire **3** - copper wire **4** - brass rod **5** - copper rod **6** - zinc plate **7** - iron plate on gypsum plate - Copper on **P1** was first overlooked, but peaks are present in data. **P1**, **P4**, **P5** were assigned correctly. - **P2**, **P3** analyses are wrong. **P2** was analysed as copper; small brass component is correct. **P3** was analysed as brass, but it is copper. Since copper and brass are easy to distinguish there seems to be an alignment error. Zinc on **P6** is not identified (Zn: peaks at 2.09, 2.31, 2.47 Å). There are small Zn peaks in **P2**. - **P7** shows fcc-phase, in agreement with steel. Pb peaks, identified in the first analysis, are from gypsum. - Ag/Al was identified but is not present.

Table 11 (a). *TOF Neutron Diffraction results on H-II*

Box no.	X-ray radiograph	Set-Up	Diffraction patterns	ND results
H-II	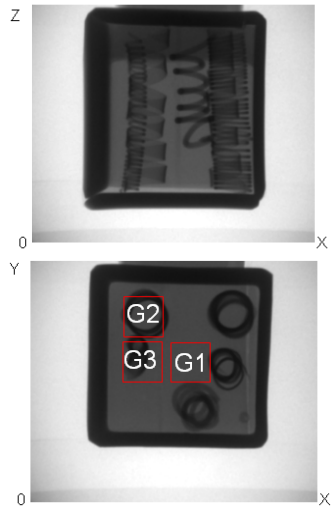	**Instrument: GEM** beam size10x10 mm; beam along z box alignment: no offset	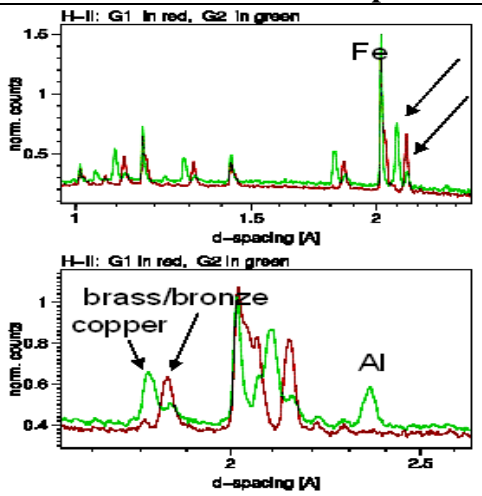 copper brass/bronze	"**Filling**" peaks gypsum: $CaSO_4(H_2O)_2$ **G1:** gypsum, strong copper alloy peaks (a=3.70 Å) **G2**: gypsum, strong copper/steel (a=3.62 Å), + weak copper alloy (a=3.70 Å) peaks; **G3**: gypsum, Al, copper alloy/steel phase (a=3.59 Å), strong Al/Ag

Table 11 (b). *Comments on ND results (Black Box H-II)*

Box no.	Box content from TOF-ND	Complementary info	Reality Check
H-II	- The **filling material** is gypsum. The box contains metallic springs, made of different materials: copper/steel and bronze/brass. - **G1** in the centre shows strong copper alloy peaks (bronze or brass), presumably from one of the springs. - **G2** shows a copper/steel fcc-phase, next to a much weaker bronze/brass phase. Extra strong peaks indicate Al/Ag. - **G3** shows a weak copper/steel phase. Extra strong peaks indicate Al/Ag. - The Cu/Al phases are not present in the forward scattering banks.	none	 **1** - brass spring **2** - brass spring **3** - copper spring **4** - brass spring **5** - copper spring - The springs were correctly identified as metal (bronze or brass) springs. - The points **G1** was intended as a shot in the centre to determine the filling material. The presence of copper in the data indicates a "failed shot". - **G2** (brass) is wrongly assigned as copper. **G3** (Cu) is correct. - Beta brass components are not detected. - Gypsum was not identified as a plate, but as a powder filling. This could have been detected by comparing the patterns to the ones of other gypsum-filled boxes. There could be a mis-orientation of the box on the instrument.

Table 12 (a). TOF Neutron Diffraction results on H-III

Box no.	X-ray radiograph	Set-Up	Diffraction patterns	ND results
H-III	**(a)**  **(b)** 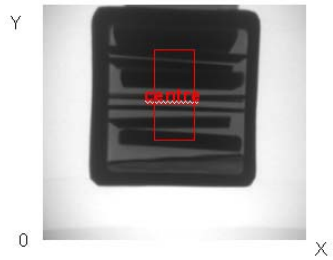 	**Instrument: GEM** **(a)** beam size 5x20 mm; beam along y (side with number H-III facing incoming beam) **(b)** Beam size 10x20 mm; beam along z box alignment: no offset	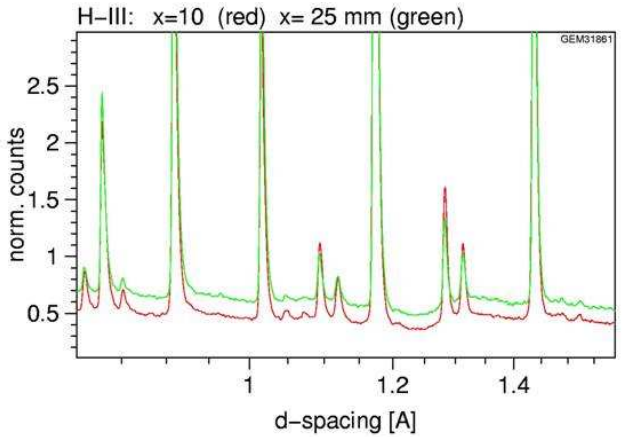 	**(a)** **Point 1**: x=5, copper alloy 1 (a=3.618 Å), copper alloy 2 (a=3.70 Å) **Point 2**: x=10, copper alloy 1 (a=3.614 Å), copper alloy 2 (a=3.70 Å) **Point 3**: x=15, copper alloy 1 (a=3.613 Å), copper alloy 2 (a=3.70 Å) **Point 4**: x=20, copper alloy 1 (a=3.613 Å), copper alloy 2 (a=3.70 Å) **Point 5**: x=22.5, copper alloy 1 (a=3.613 Å), copper alloy 2 (a=3.70 Å) **Point 6**: x=25, copper alloy 1 (a=3.613 Å), copper alloy 2 (a=3.70 Å) **Point 7**: x=30, copper alloy 1 (a=3.613 Å), copper alloy 2 (a=3.70 Å) **Point 8**: x=32.5, copper alloy 1 (a=3.613 Å), copper alloy 2 (a=3.70 Å) **(b)** **Point Centre**: copper alloy 1 (a=3.615 Å), copper alloy 2 (a=3.70 Å)

Table 12 (b). Comments on TOF-ND results on H-III

Box no.	Box content from TOF-ND	Complementary info	Reality Check
H-III	- The data show the same phases (copper-type phase, copper alloy phase) for all points, in similar phase ratios. - The **copper-type phase** (a=3.613 Å) can be steel or copper. - The copper alloy (a=3.7 Å) can be bronze or brass. - There is **no filling material** identified.	- **PGAA** data show copper and iron as elements. The PGAA scan identifies the copper-type phase as copper. No filling material is detected. - **PGAA** identifies the copper alloy with the larger lattice parameter as brass.	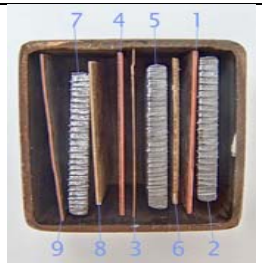 **1** - copper sheet **2** - iron sheet **3** - brass sheet **4** - copper sheet **5** - iron sheet **6** - brass sheet **7** - iron sheet **8** - brass sheet **9** - steel sheet - All TOF-data show the same pattern. It has to be assumed that the scan was not, as planned, across the different plates. Maybe the incoming beam was impinging on the flat side of the sheets. - TOF-ND does not (easily) recognise an iron object in an iron box, although it is principally possible to separate the inside-objects via peak shift analysis. - TOF-ND failed to identify the steel sheet (9).

Table 13 (a). *TOF Neutron Diffraction results on H-IV*

Box no.	X-ray radiograph	Set-Up	Diffraction patterns
H-IV	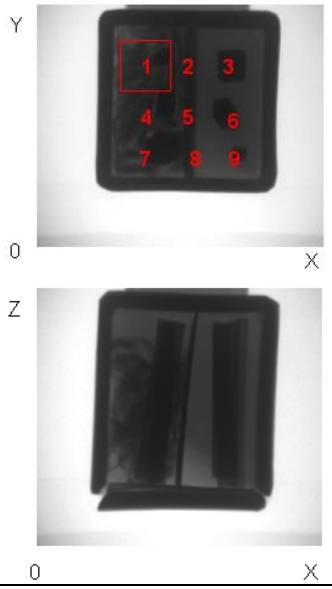	**Instrument: GEM** beam size 10x10 mm; beam along z (top side facing incoming beam, side with numbers down) box alignment: no offset	All patterns exhibit: quartz (SiO_2), gypsum $CaSO_4(H_2O)_2$, copper alloy (a=3.654 Å), **Point 1**: Quartz (12%), gypsum (7%), copper alloy (3%), Al/Ag (1%), FeO (3%), Fe_3O_4 **Point 4**: Quartz (17%), gypsum (5%), copper alloy (2%), FeO (2%), Fe_3O_4 **Point 7**: Quartz (11%), gypsum (6%), copper alloy (2%), FeO (2%) **Point 2**: Quartz (26%), gypsum (7%), copper alloy (3%), Al/Ag (5%), FeO (1%) **Point 5**: Quartz (27%), gypsum (7%), copper alloy (3%), Al/Ag (2%) **Point 8**: Quartz (17%), gypsum (7%), copper alloy (3%) **Point 3**: Quartz (31%), gypsum (6%), copper alloy (3%), Al/Ag (13%) **Point 6**: Quartz (27%), gypsum (6%), copper alloy (2%), Al/Ag (12%) **Point 9**: Quartz (20%), gypsum (5%), copper alloy (3%))

Table 13 (b). *Comments on TOF-ND results on H-IV*

Box no.	Box content from TOF-ND	Complementary info	Reality Check
H-IV	- The box is divided into **two parts**. All data show quartz and gypsum. However, P3, P6, P9 contains much more quartz. - The **copper alloy** can be brass (17wt% Zn) or bronze (5 wt% Sn). This component is high for P2,5,8, and low otherwise, indication that the separating sheet is made out of copper alloy. - **Copper alloy** contents are small.	- **PGAA** idenfies Fe and Mn, with the latter probably in the ferrite. - **PGAA** identifies Al, rather than Ag. - One filling material contains Si and B (?) as main component (SiO_2). The other filling material contains Fe as main component. - **PGAA** identifies Cu, in agreement with the TOF-data.	 **1**, **2**, **3** - iron **4** - thin steel plate **5** - fill grit **6** - fill sand - TOF-ND does not easily recognise a ferrite object in a box made of ferritic iron, although it is principally possible to separate the inside-objects via peak shift analysis from the wall material. - The gypsum was not identified as a plate, but as a powder filling. Has quartz spilled into left side of the box? Where is Al and Cu in the box? The nominal elemental composition is: Fe, Mn, C, B, Al, Si, K, Ti

Table 14 (a). TOF Neutron Diffraction results on H-V

Box no.	X-ray radiograph	Set-Up	Diffraction patterns	Box no.
H-V	**(a)** 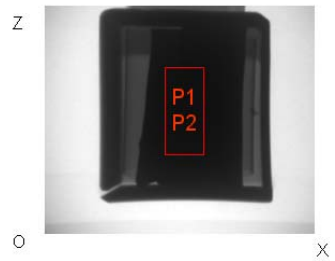 **(b)** 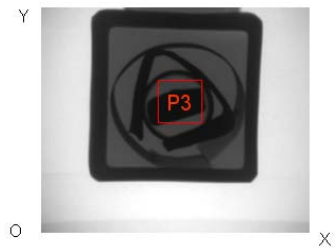	**Instrument: GEM** **(a)** beam size 10x20 mm; beam along y **(b)** beam size 10x10mm; beam along z box alignment: no offset	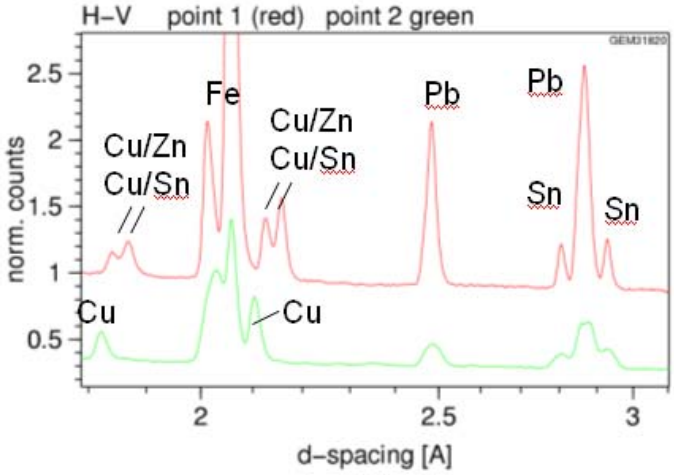	**(a)** **P1+2**: gypsum $CaSO_4$ $(H_2O)_2$ (small peaks), Pb, Sn, copper alloy (a=3.7 Å) **(b)** **P3**: gypsum CaSO4 (H2O)2 (strong peaks), Pb, Sn, copper alloy (a=3.63 Å), Al/Ag (small)

Table 14 (b). Comments on TOF-ND results on H-V

Box no.	Box content from TOF-ND	Complementary info	Reality Check
H-V	- The box contains gypsum (filling). - There is a combination of metals: Pb, Sn, copper alloy, Al/Ag. - **P1** shows split bronze/brass peaks, but **P3** not. Therefore the bronze/brass might be the outermost ring; the copper alloy peaks are different for P1 and P3. - The Pb peaks are split in P2. Therefore Pb could be the second-outermost metal in the box. The Sn could be part of a Pb/Sn solder. - There is a **peak** at **2.34 Å** in P3 which indicates a fcc metal such as Al or Ag/Au. Pb and Sn are present in the center as well. - **P3** shows the 2.34 Å peak while it is hardly visible in P1. Therefore is can be assumed that Al/Ag/Au is the innermost metal in the box.	none	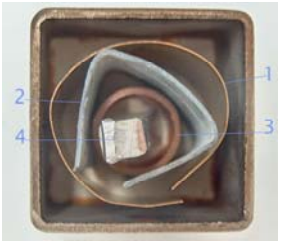 **1** - brass plate **2** - lead plate **3** - copper tube **4** - thin lead solider Mounted on a gypsum plate - The outer ring was correctly identified as copper alloy. Cu/Sn and Cu/Zn cannot be distinguished by TOF-ND. - The Pb ring was correctly identified. - The different copper alloy for P3 corresponds to the (short) copper ring which is out of sight in P1. The Cu lattice constant from TOF-ND is too large. - The inner metal is Pb/Sn eutectic which gives separate Pb and Sn peaks. Pb/Sn inside a Pb-sheet is difficult to see. - Al/Ag was wrongly identified as the centre object. Is there a top Al plate? - The gypsum peaks are smaller in P1+2 compared to P3 because there is just the bottom gypsum plate. Gypsum peaks in P3 remain unexplained

Table 15 (a). *TOF Neutron Diffraction results on H-VI*

Box no.	X-ray radiograph	Set-Up	Diffraction patterns	Box no.
H-VI	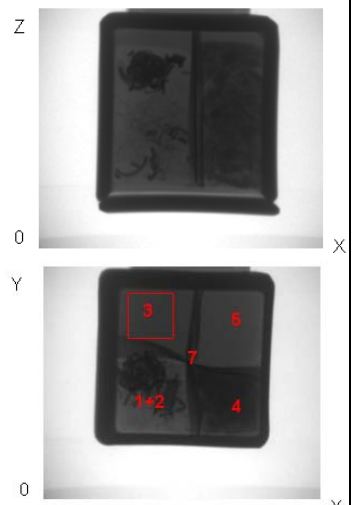	**Instrument: GEM** beam size 10x10 mm; beam along z box alignment: no offset	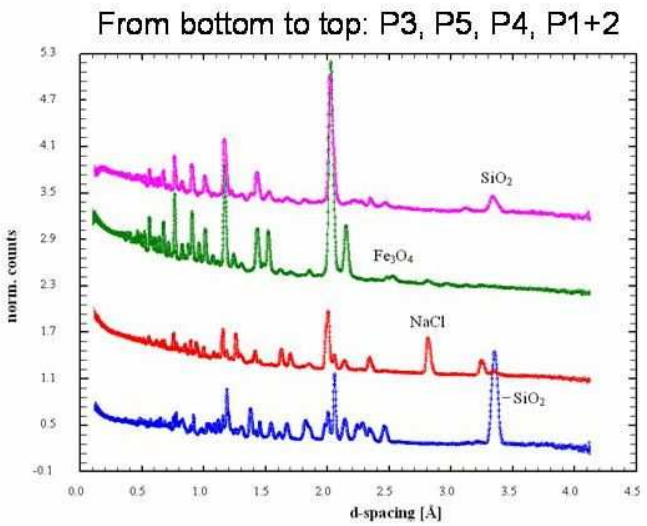	**P1+2:** quartz (SiO_2), gypsum ($CaSO_4(H_2O)_2$), talc ($Mg_3(OH)_2(Si_4O_{10})$), Al or Ag **P3:** quartz, gypsum, talc, Al/Ag, fcc-Cu-type (a=3.7 Å) **P4:** gypsum, talc, fcc-Cu-type (a=3.7 Å), Magnetite (Fe_3O_4), maybe FeO; **P5:** quartz, gypsum, halite (NaCl), gypsum, talc, fcc Cu-type (a=3.7 Å) **P7:** gypsum, halite, talc, fcc Cu-type (a=3.7 Å), Al/Ag, FeO

Table 15 (b). *Comments on TOF-ND results on H-VI*

Box no.	Box content from TOF-ND	Complementary info	Reality Check
H-VI	- The radiography shows that the box is divided into 4 sectors. - There are a number of peaks that are common to **all sectors**, either because it is a filling material or a wall material: gypsum, Al, talc (peaks at 9.6, 4.56 3.13 Å). - There is the following additional material in the *4 chambers*: • Main phase in **P1+2**: Al/Ag • Main phase in **P3**: quartz • Main phase in **P5**: halite (NaCl) • Main phases in **P4**: iron oxides (FeO, Fe_3O_4)	- **PGAA** identifies Ag rather than Al. - **PGAA** confirms the presence of a copper alloy as the fcc-phase. - The presence of Zn indicates brass rather than bronze.	 **1** - silver wire **2** - fill talcum **3** - fill sand **4** - fill grit iron **5** - fill salt (NaCl) **6** – copper sheets **7** –aluminium sheet - The main components in the compartments were identified. - The fcc-copper phase has a lattice parameter that rather indicates brass than pure copper, confirmed by PGAA. - The brass sheets are visible in all data except for point 1+2 (larger sector) which indicates a slight problem with the alignment of the box. - TOF-ND shows talc in all sectors. This result may indicate a misalignment or it may indicate that talc powder leaked from 1+2 into other compartments

Table 16 (a). *TOF Neutron Diffraction results on H-VIII*

Box no.	X-ray radiograph	Set-Up	Diffraction patterns	Box no.
H-VIII	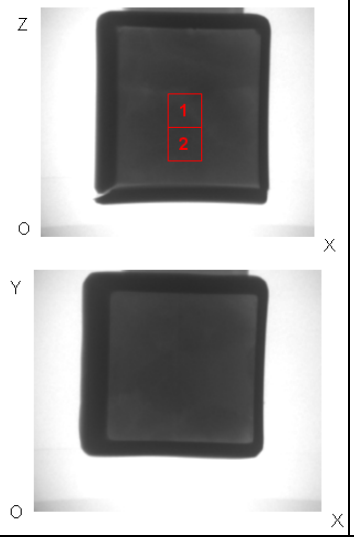	**Instrument: GEM** Beam along y; side with number "VIII" facing incoming beam box alignment: no offset	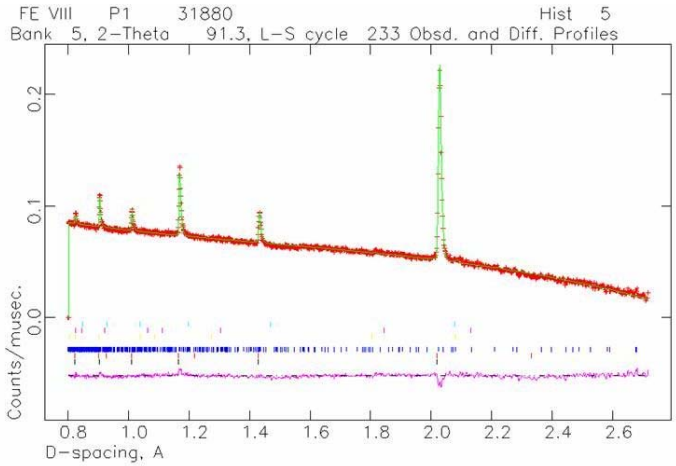	All diffraction patterns show single Fe peaks from the box walls. **Point 1**: moderate background **Point 2**: moderate background

Table 16 (b). *Comments on TOF-ND results on H-VIII*

Box no.	Box content from TOF-ND	Complementary info	Reality Check
H-VIII	- Only Bragg peaks of ferrite (front wall) are observed. - The beam does not pass through the box. - The box is filled with a neutron-stopping material. - TOF-ND "sees" no crystalline material. - The backgrounds in the neutron diffraction patterns are decreasing with increasing d-spacing (i.e. with increasing wavelengths). This is typical for absorbing or self-absorbing material (e.g. hydrogen-containing compounds).	- **PGAA** data suggest gypsum as main material (Ca, S, H). - Other elements from **PGAA** are Al, Si, K, Ti. .	  - Neolitic chaff tempered pottery; filling material is gypsum - The material inside the box is not identified. There are slight hints of gypsum peaks in the TOF-ND data. - The gypsum filler is impenetrable for the thermal neutron beam.

Table 17 (a). *TOF Neutron Diffraction results on H-IX*

Box no.	X-ray radiograph	Set-Up	Diffraction patterns	Box no.
H-IX	**(a)** 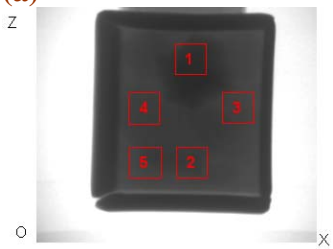 **(b)** 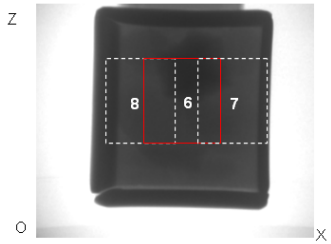 	**Instrument: GEM** Beam along y (side with number "IX" facing incoming beam) **(a)** Beam size: 10x10 mm **(b)** Beam size: 20x40 mm box alignment: no offset	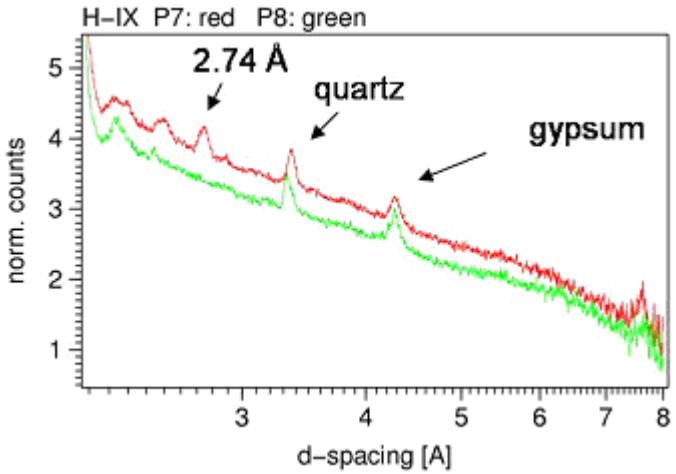 	Diffraction patterns show strong Fe peaks from front wall and weak peaks from back wall of the box. All points P1-P8 show gypsum $CaSO_4(H_2O)_2$ and quartz (SiO_2). **(a)** **P1**: extra characteristic peaks at 2.33, 3.31 Å **P2**: extra characteristic peaks at 2.50, 2.73 Å **P3**: extra characteristic peaks at 2.33, 2.73 Å **P4**: extra characteristic peak at 2.33 Å **(b)** **P6**: extra characteristic peaks at 2.44, 2.73, 3.31 Å **P7**: extra characteristic peak at 2.73 Å

Table 17 (b). *Comments on TOF-ND results on H-IX*

Box no.	Box content from TOF-ND	Complementary info	Reality Check
H-IX	- Apart from Fe peaks, there is a confusing pattern of Bragg peaks. All points show quartz and gypsum peaks (mixture of the two as filler). - **Gypsum** peaks are observed in forward scattering. This means that the neutrons are able to penetrate the box, in contrast to H-VIII. - The background in the neutron diffraction patterns is decreasing with increasing d-spacing (i.e. with increasing wavelengths). This is typical for a hydrogen-containing material, such as the gypsum filler). - 2.33 Å peaks in P1,3,4 indicate presence of Al/Ag.	none	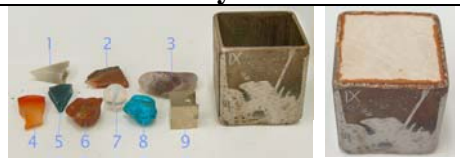 ***1, 2*** *– achat* ***3*** *- amethyst* ***4, 6*** *– cornean* ***5*** *- blue glass* ***7****-achat globular bead* ***8****–turqoise* ***9*** *-pyrite* **Filler material**: gypsum - **Gypsum** and **quartz** are identified. Gypsum is the filling material, quartz is present in form of several localized objects rather than a filler. A finer scan would have revealed this. - **Achat** and **amethyst** are different varieties of quartz (SiO_2). - What's cornean? - The glass bead was not detected. - P2,3,6,7 show pyrite (2.74 Å peak). This does not agree with the cube-feature in the radiography. (orientation problem?) - Al/Ag is not present. The peaks at 2.33, 2.44, 3.31 Å are unexplained. - Quartz in P5 is polycrystalline, while quartz in P1 is a single crystal. - It is surprising that this box is more transparent than H-VIII.